



Ecole doctorale du Département de Géologie

THÈSE EN COTUELLE

présentée à l'Université de Liège

par

Jacques Richard MACHE

En vue de l'obtention du titre de

Docteur en Sciences

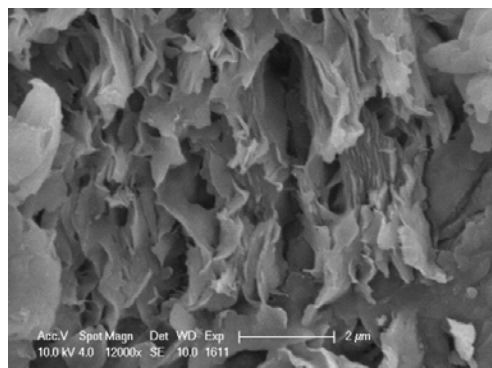
LPCM₂

**MINERALOGIE ET PROPRIETES PHYSICO-CHIMIQUES
DES SMECTITES DE BANA ET SABGA (CAMEROUN).**

Utilisation dans la décoloration d'une huile végétale alimentaire

Promoteurs: Dr. Nathalie FAGEL

Pr. Daniel NJOPWOUO



Année académique: 2012-2013



Ecole doctorale du Département de Géologie

THÈSE EN COTUTELLE

présentée à l'Université de Liège

par

Jacques Richard MACHE

En vue de l'obtention du titre de

Docteur en Sciences

LPCM₂

**MINERALOGIE ET PROPRIETES PHYSICO-CHIMIQUES
DES SMECTITES DE BANA ET SABGA (CAMEROUN).**

Utilisation dans la décoloration d'une huile végétale alimentaire

soutenue publiquement le 24 Juin 2013 devant le jury composé:

Mme. JAVAUX Emmanuelle	Professeur	Université de Liège
M. YVON Jacques	Professeur	Université de Lorraine
Mme. PETIT Sabine	Directeur de recherche	Université de Poitiers
M. PIRARD Eric	Professeur	Université de Liège
M. HATERT Frédéric	Chargé de cours	Université de Liège
Mme. FAGEL Nathalie	Chargé de cours	Université de Liège
M. NJOPWOUO Daniel	Professeur	Université de Yaoundé I

Je dédie cette thèse

A Alice ma tendre épouse

A Gyavira Thérèse,

Arthur Nathan

et

Dominique Audrey

mes chers enfants

REMERCIEMENTS

La présente étude a été réalisée au sein de l'Unité de Recherche Argiles, Géochimie et Environnement Sédimentaires (AGEs) de l'Université de Liège et au Laboratoire de Physico-chimie des Matériaux Minéraux (LPCM₂) de l'Université de Yaoundé I. Cette thèse s'inscrit dans le cadre d'une convention de cotutelle entre l'Université de Liège et l'Université de Yaoundé I.

A l'issue de ces six années de recherche, je tiens à exprimer ma vive reconnaissance aux nombreuses personnes qui ont participées, de près ou de loin, à l'élaboration de cette thèse.

Je profite de cette occasion pour exprimer ma profonde gratitude à Madame Nathalie Fagel pour l'opportunité et l'honneur qu'elle m'a accordés en m'accueillant au sein de son unité de recherche. Je lui adresse également ma profonde reconnaissance pour l'intérêt qu'elle a constamment consacré à mes travaux de thèse et pour son précieux soutien.

Mes sincères remerciements s'adressent également à Monsieur Daniel Njopwouo pour l'encadrement et les discussions enrichissantes et encourageantes qu'il m'a accordés au cours de la réalisation de mes travaux de recherche.

J'exprime aussi toute ma reconnaissance envers Monsieur Pierre Signing pour l'intérêt qu'il a toujours accordé pour mes travaux depuis le DEA. Ses conseils avisés et ses connaissances m'ont permis d'avancer dans les moments les plus difficiles.

Je tiens à remercier Madame Emmanuelle Javaux pour m'avoir honoré de présider le jury de cette thèse.

Merci tout particulièrement à Messieurs Jacques Yvon, Eric Pirard et Frédéric Hatert qui ont accepté de juger ce travail.

J'exprime ici toute ma reconnaissance envers Madame Sabine Petit pour avoir accepté de participer au jury de cette thèse.

Je suis très reconnaissant à Monsieur Fabien Thomas, Directeur du Laboratoire Interdisciplinaire des Environnements Continentaux (LIEC) de l'Université de Lorraine (Nancy, France), pour m'avoir accueilli au sein de son laboratoire et facilité les analyses au cours de mes séjours de recherche.

J'adresse également mes vifs remerciements à tous les membres du Département de Géologie de la Faculté des Sciences de l'Université de Liège, particulièrement à Mariella Guadagnano, Joëlle Schmetz et Marcella Giraldo pour leurs multiples attentions à mon égard.

Qu'il me soit permis de témoigner ma reconnaissance à tous les membres de l'Unité de Recherche Argiles, Géochimie et Environnement Sédimentaires (AGES) pour ces riches moments passés ensemble.

Mes sincères remerciements à la coordonatrice d'Erasmus Mundus ACP de l'ULg Madame Anne Villemot pour toute sa disponibilité et son aide précieuses tout au long de mon séjour.

Je voudrais remercier la Commission Européenne qui, par le programme Erasmus Mundus ACP m'a donné l'opportunité d'effectuer ces travaux de recherche à travers une bourse doctorale de vingt mois à l'Université de Liège.

Mes sincères remerciements à mes amis et camarades en particulier à Jean Aimé Mbey, Achille Balo, Cyrill Ngally, Zoila Epossi, Emmanuel Sobgwi, Luc Titti, Stéphanie Ketep, Aurélie Djoumessi, Moise Jojo Ngapna et Yacouba Mefire pour leurs encouragements durant ces années.

Je tiens à remercier des doctorants stagiaires algériens Bachir Lamouri et Mechati pour les discussions quasi-quotidiennes sur les minéraux argileux et leurs applications.

Je suis très reconnaissant envers mes parents, mes frères et sœurs pour m'avoir soutenu tout le long de mon parcours académique et pour avoir cru en moi.

Je tiens à remercier particulièrement du fond de cœur Josselin Mefire, Adamou Njoumansie, Arnaud Maffo, Aubin Nzeukou, Nicole Nana, Gil Herman Poupie et Jean-Marcelin Manga pour les bons moments passés ensemble.

Je voudrais dire ma reconnaissance à Virginie Renson, Arnaud Comblin, Nancy Claes, Jean Yves De Vleeschouwer et Nadia Anoun pour tout ce qu'ils ont fait pour moi durant mon séjour liégeois.

Je voudrais dire ma reconnaissance à mes amis collègues de la Mission de Promotion de Matériaux Locaux (MIPROMALO) qui, tout au long de ces années, m'ont soutenu et encouragé, qu'ils trouvent ici l'accomplissement de leurs attentes.

Mes sincères remerciements à tous ceux qui, de près ou de loin, ont contribué à l'élaboration de cette thèse.

Gloire soit rendue à l'Eternel, le Dieu des Armées pour tout ce qu'il a fait pour moi durant ce parcours. Louange, Honneur et Adoration lui appartient.

J.R MACHE

Résumé

Dans cette étude, des échantillons d'argiles ont été collectés dans les localités de Bana et Sabga, respectivement dans les régions de l'Ouest et Nord-ouest Cameroun. Le but de cette étude était de déterminer leurs compositions minéralogiques, leurs propriétés physico-chimiques et d'évaluer leur potentielle utilisation dans la décoloration de l'huile de palme, qui représente la principale huile végétale comestible produite et raffinée au Cameroun.

Les résultats obtenus à partir des analyses classiques (DRX, FTIR, ATD/ATG et MEB) ont révélé que la montmorillonite est le minéral de base dans ces matériaux. Elle est associée à la kaolinite et au mica. Sont aussi identifiés en quantités variable les minéraux non-argileux tels que le quartz, l'anatase, la cristobalite, les feldspaths potassiques et l'heulandite. Les analyses chimiques des éléments majeurs montrent que les argiles de Bana et Sabga sont constituées principalement des oxydes SiO_2 , Al_2O_3 et Fe_2O_3 . Les argiles de Bana possèdent une capacité d'échange cationique (CEC) variant entre 50 et 60 méq/100 g et une surface spécifique comprise entre 50 et 60 m^2/g . Les argiles de Sabga présentent une capacité d'échange cationique plus faible (38 à 46 méq/100g) et une plus large gamme de surface spécifique (33 à 90 m^2/g). Le bilan minéralogique des argiles étudiées a permis de sélectionner dans chaque localité un échantillon pour un traitement à l'acide sulfurique.

Le traitement acide de ces matériaux a conduit à des modifications structurales, morphologiques et texturales. Les analyses par la diffraction de rayon X montrent une diminution progressive de l'intensité de la réfection (001) de la montmorillonite et un déplacement de sa distance basale (d_{001}). Le traitement par des acides de plus en plus concentrés provoque une augmentation de la surface spécifique des produits obtenus et une diminution de leur capacité d'échange cationique.

L'évaluation du pouvoir décolorant de l'argile de Bana riche en smectite et présentant une évolution significative en termes de propriétés physiques et texturales suite à l'activation montre que l'argile activée présente une forte capacité de décoloration (~87 %) par rapport à l'argile naturelle (~55 %). La décoloration de l'huile de palme par ces matériaux, activés ou non, ne provoque aucune dégradation à l'huile traitée. Ces matériaux peuvent donc être valorisés comme terres décolorantes dans le processus de raffinage des huiles.

Mots-clés: Argiles naturelles, smectites, minéralogie, propriétés physico-chimiques, activation acide, huile de palme, décoloration

Abstract

In this study, clay samples were collected in the localities of Bana and Sabga, in the regions of the west and north-west Cameroon, respectively. The purpose of this study was to determine their mineralogical composition, their physico-chemical properties and to assess their potential use in the bleaching process of palm oil, which is the main edible vegetable oil produced and refined in Cameroon.

The results obtained from the analyses (XRD, FTIR, DTA / TGA and SEM) revealed that montmorillonite is the main clay mineral in these materials. It is associated with kaolinite and mica. Non-clay minerals such as quartz, anatase, cristobalite, K-feldspar and heulandite are also identified in variable quantities. Chemical analyses of the major elements show that the clays from Bana and Sabga consist mainly of the follow oxides such as SiO_2 , Al_2O_3 and Fe_2O_3 . Bana clays have a cation exchange capacity (CEC) between 50 and 60 meq/100 g and a specific surface area between 50 and 60 m^2/g . Sabga clays have a lower capacity cation exchange (38- 46 meq/100 g) and a wider range of specific surface area (33-90 m^2/g). The characterization of the natural clays allowed to select of one sample by locality for sulfuric acid treatment.

The acid treatment of these materials led to structural, morphological and textural changes. Analysis by X-ray diffraction showed a progressive decrease in the intensity of the (001) reflection of montmorillonite and a shift of its basal d_{001} -value. Treatment with more acid concentration causes an increase in the surface area of the obtained products and a decrease in cation exchange capacity.

The assessment of the bleaching power of natural and acid-activated Bana clay in palm oil decolorization shows that the activated clay has a high bleaching capacity (~ 87%) compared to the natural clay (~ 55%). palm oil Bleaching by these clay materials does not deteriorate the bleached oil. These materials can thus be used as bleaching earths in the refining oil process.

Keywords: Natural clays, smectites, mineralogy, physico-chemical properties, acid-activation, palm oil, decolorization

Table des matières

INTRODUCTION GÉNÉRALE.....	1
<i>Références bibliographiques.....</i>	<i>6</i>
CHAPITRE I: SYNTHÈSE BIBLIOGRAPHIQUE.....	11
I. Minéraux argileux.....	11
I.1. Définition.....	11
I.2. Structure et classification des minéraux argileux.....	11
I.2.1 Structure des minéraux argileux.....	11
I.2.2 Classification des minéraux argileux	13
I.2.2.1. Les minéraux phylliteux.....	14
I.2.2.1.1. Les minéraux 1:1.....	15
I.2.2.1.2. Les minéraux 2:1 et 2:1:1.....	16
I.2.2.2. Les minéraux fibreux.....	22
I.2.2.3. Les minéraux interstratifiés.....	23
I.3. Applications des minéraux argileux dans la décoloration des huiles végétales.....	24
Conclusion.....	27
<i>Références bibliographiques.....</i>	<i>28</i>
CHAPITRE II: CARACTERISATIONS DES ARGILES DE SABGA ET BANA (CAMEROUN).....	31
Introduction.....	31
II.1. Résumé des articles.....	31
II.2. Smectite clay from Sabga deposit (Cameroon): Mineralogical and Physicochemical properties (J.R. MACHE, P. SIGNING, A. NJOYA, F. KUNYU, J.A. MBEY, D. NJOPWOUO AND N. FAGEL, <i>accepted for publication in Clay Minerals</i>).	33
<i>References.....</i>	<i>55</i>
II.3. Mineralogical, Physicochemical Properties of Smectite Clay from Bana (Western- Cameroon) and Preliminary test as Potential oil bleaching earth (J.R. Mache, P. Signing, J.A. Mbey, F. Thomas, D. Njopwouo AND N. Fagel, <i>Submitted for Applied Clay Science</i>).....	59
<i>References.....</i>	<i>80</i>

CHAPITRE III: INFLUENCE DU TRAITEMENT ACIDE SUR LES PROPRIETES PHYSICO-CHIMIQUES, MINERALOGIQUES ET TEXTURALES DES ARGILES DE BANA ET SABGA.....	86
Introduction.....	86
III.1. Résumé de l'article.....	87
III.2. Acid activation of smectite clays from Cameroon: Effect on mineralogical and physico-chemical properties (J. R. Mache, P. Signing, J. A. Mbey, A. Razafitianamaharavo, D. Njopwouo, N. Fagel, Submitted for <i>Colloids and Surfaces A: Physicochemical and Engineering Aspects</i>).....	88
References.....	110
CHAPITRE IV: EVALUATION DU POUVOIR DECOLORANT DES ARGILES MODIFIEES.....	113
Introduction.....	113
IV.1. Résumé de l'article.....	113
IV.2. Bleaching Performance of acid-activated smectite clays from Bana (West Region of Cameroon). (J.R. Mache, P. Signing, J.A. Mbey, F. Thomas, D. Njopwouo, N. Fagel, <i>In preparation</i>)	115
References.....	131
CONCLUSION GÉNÉRALE ET PERSPECTIVES.....	133-135

INTRODUCTION GENERALE

Les minéraux argileux, principalement détritiques sont issus de l'altération physique ou chimique des roches préexistantes (Millot, 1964). Riches en aluminium et en silicium, les minéraux argileux constituent l'essentiel de l'écorce terrestre (90% en masse) (Rontenberg, 2007). Ils sont caractérisés par une structure en feuillets et des dimensions de l'ordre du micromètre. Ce qui leur confère une grande surface par unité de masse et, pour certains d'entre eux, des propriétés de gonflements en présence d'eau et d'échange ionique. Une fois dispersés dans l'eau, les minéraux argileux acquièrent des propriétés colloïdales.

Ces différentes propriétés minéralogiques, physico-chimiques et texturales ont conduit l'homme, dans la recherche de son bien être, à utiliser les minéraux argileux comme principales matières premières pour des applications très variées: élaboration de briques, tuiles, terre cuite, faïence, porcelaine, utilisation comme agent de texture dans les peintures, agent de blanchiment du papier, ou agent de renforcement des matériaux plastiques à base de polymères (Brunet, 1986; Prasad et al., 1991; Konta, 1995; Harvey & Murray, 1997; Ekosse, 2000; Carretero, 2002). On trouve également les minéraux argileux comme catalyseurs, notamment dans l'industrie pharmaceutique, ou comme membranes pour des procédés de filtration dans l'industrie agro-alimentaire (Murray, 2000). Les smectites dites « argiles gonflantes » sont utilisées pour les boues de forages dans l'industrie pétrolière mais aussi comme adsorbant pour la décoloration des huiles (Konta, 1995; Murray, 1999).

Pour ces raisons, la recherche de nouveaux gisements, la caractérisation et la valorisation des matériaux argileux restent toujours d'actualité. Highley (1994) et Harvey (1995) suggèrent que la production des matériaux géologiques tels que les minéraux argileux peut être utilisée comme un indice de la maturité économique de pays en développement, ces matériaux pouvant jouer un rôle déterminant dans la croissance économique des industries locales.

Depuis près de trois décennies de nombreux travaux de recherches ont été menés par plusieurs chercheurs sur les matériaux argileux du Cameroun et leur potentielle valorisation. Ces travaux ont notamment portés sur le talc (Nkoumbou et al., 2006, 2008), l'halloysite (Njopwouo et Wandji, 1982) et les argiles kaoliniques qui, jusqu'ici représentent le dépôt argileux le plus important dont dispose le Cameroun (Njopwouo et Wandji, 1985 ; Elimbi et al., 2003 ; Njoya et al., 2006 ; Njoya et al., 2007 ; Pialy et al., 2008 ; Nkoumbou et al., 2009; Ekosse, 2010). Les applications recherchées pour l'utilisation de ces matériaux argileux ont

portés sur l'élaboration des produits cuits (briques, tuiles, réfractaires, céramiques fines et porcelaines) (Diko et al., 2011 ; Djangang et al., 2007, 2008a, 2008b, 2010, 2011; Elimbi et al., 2001, 2002, 2004, 2011; Kamseu et al., 2007, 2008, 2009, 2011 ; Leonelli et al., 2008 ; Melo et al., 2003 ; Pialy et al., 2009), la formulation des ciments géopolymères à base des argiles riches en kaolinites (Kamseu et al., 2010 ; Lemougna et al., 2011; Obonyo et al., 2011; Tchakounté et al., 2012; 2013), la charge minérale dans le renforcement du caoutchouc et comme catalyseur dans la polymérisation du styrène (Njopwouo, 1984 ; Njopwouo et al., 1987, 1988a, 1988b) et, tout récemment, dans l'élaboration des films composites à partir d'amidon de manioc et de kaolin (Mbey et al., 2012). Les résultats significatifs enregistrés jusqu'ici et le développement des activités de la Mission de promotion des Matériaux Locaux du Cameroun (MIPROMALO)¹ mise en place par le gouvernement du Cameroun en 1990 et ayant pour mission principale la vulgarisation des résultats sur les matériaux locaux, sont des indicateurs qui témoignent de l'intérêt porté sur les ressources naturelles telles que les matériaux argileux.

Toutefois, la valorisation des ressources locales dans les pays en voie de développement, comme le Cameroun, passe par l'identification d'autres types des matériaux argileux à valeurs économiques tels que les smectites, qui offriront des applications industrielles autres que celles données jusqu'ici par les argiles kaolinitiques. Ces nouvelles voies, qui partent de la recherche d'autres nouveaux gisements de matériaux argileux et de leur potentielle utilisation, doivent tenir compte d'une triple approche alliant à la fois, la disponibilité de la matière première, l'impact socio-économique (à long ou moins terme), et l'environnement du marché tant local que sous-régional.

Ces dernières années, le marché camerounais des terres décolorantes (terme désignant les minéraux argileux à usage industriels essentiellement composés de montmorillonite naturels ou activés) est principalement desservi par des importations des pays suivants: Chine, Allemagne, France et Angleterre (Statistiques pour l'importation de Chine 2004-2005: ~320.000 Kg)². Destinées au raffinage dans lequel elles servent à la décoloration des huiles, ces terres, en industrie de raffinage des huiles végétales, constituent le principal secteur d'utilisation de ces matériaux argileux au Cameroun, secteur en plein développement. En effet, dans tout type de procédé de raffinage des huiles végétales, qu'il soit chimique ou

¹ : www.mipromalo.cm (consulté le 27/02/2013)

² : <http://www.izf.net/menu/base-de-donnees-des-statistiques> (Base des données statistiques d'importation et d'exportation des pays de la Zone Franc) (consulté le 01/03/2013)

physique comporte une étape critique et déterminante qui est la décoloration. Cette étape consiste à fixer les pigments, chlorophylles et autres impuretés (métaux lourds, principalement le fer et cuivre) contenus dans les huiles sur un support solide. Les matériaux adsorbants généralement utilisés pour l'étape de décoloration dans les huileries sont des matériaux argileux constitués de montmorillonite activée à l'acide sulfurique ou chlorhydrique (Christidi et al., 1997; Falaras et al., 1999 ; Taha et al., 2011). Ces adsorbants introduits dans la chaîne de raffinage des huiles constituent l'un des intrants coûteux importés par ces industries.

Afin de tenter de réduire ces importations et de trouver des matériaux argileux de rechanges, les travaux de Djoufac et al. (2007) et Nguetnkam (2008) ont porté sur la caractérisation des vertisols du Nord-Cameroun. Les premiers tests d'aptitude aux usages industriels se sont révélés encourageants pour l'utilisation, en décoloration, des huiles végétales (coton, maïs et palme). Il apparaît donc impératif de mener des recherches de prospections des potentiels gisements de minéraux argileux de type smectites (en particulier de type montmorillonite) dans d'autres régions du Cameroun. Dans l'optique de préciser le ou les domaines d'utilisation potentielle des argiles prélevées dans les régions de l'Ouest et Nord-ouest du Cameroun, nous avons voulu :

- identifier et collecter les échantillons d'argiles dans les localités de Bana et Sabga, respectivement dans les régions de l'Ouest et Nord-ouest;
- caractériser ces matériaux argileux sur les plans minéralogiques, physico-chimiques et texturales;
- tester leur pouvoir décolorant naturel vis-à-vis de l'huile de palme brute;
- proposer un traitement nécessaire en vue de l'optimisation de leur pouvoir décolorant naturel;
- évaluer les capacités décolorantes des argiles modifiées.

Le sujet de cette thèse « **Minéralogies et propriétés physico-chimiques des smectites de Bana et Sabga. Utilisation dans la décoloration d'une huile végétale** » est une contribution au programme de recherche intitulé : *Valorisation des Matériaux Argileux du Cameroun*, coordonné par le Professeur Daniel Njopwou, Directeur du Laboratoire de Physico-chimie des Matériaux Minéraux de l'Université de Yaoundé I. Cette voie de valorisation pourra en outre apporter une solution dans la recherche des matériaux argileux locaux de substitution aux importations.

S'agissant des phases minérales qui lui sont constitutives, de leurs propriétés et en vue d'enrichir la base de données des argiles au Cameroun, sur le plan scientifique, nous avons procédé à l'identification, la caractérisation minéralogique, physico-chimique et texturale des matériaux argileux collectés sur les sites de Bana et de Sabga. Ces deux zones sont localisées respectivement dans les régions de l'Ouest et du Nord-Ouest du Cameroun. Elles sont situées sur la ligne volcanique du Cameroun (CLV). Une étude d'optimisation de leurs propriétés physico-chimiques et texturales a été menée, grâce au traitement des matériaux par activation à l'acide sulfurique à diverses concentrations, à température constante et à un temps fixe.

L'enjeu technologique de ce travail réside sur l'évaluation du pouvoir décolorant des smectites ainsi collectées dans leur état naturel et lorsqu'elles sont traitées à l'acide sulfurique.

La présente thèse comporte 4 chapitres. Le premier présente une synthèse bibliographique. Il y est question de procéder à un rappel succinct de connaissances spécifiques sur les minéraux argileux, leur structure et classification ainsi que leurs applications dans la décoloration des huiles végétales. Le deuxième comporte deux articles. Un premier, accepté à *Clay Minerals* et, un deuxième, soumis et en cours de reviewing dans la revue *Applied Clay Science*. Dans ces deux articles, il s'agit de caractériser les différents échantillons de matériaux collectés à Bana et Sabga qui sont les localités sur lesquelles porte cette étude. Pour cela, nous avons utilisé les méthodes de caractérisation classiques telles que : la diffraction des rayons X, la spectroscopie infrarouge, les analyses thermiques (DSC, ATD et ATG), les analyses chimiques (ICP-AES, ICP-MS), les mesures des surfaces spécifiques (adsorption azote à 77K), les mesures de capacité d'échange cationique, la microscopie électronique à balayage et la mobilité électrophorétique. L'association de ces techniques analytiques a permis de préciser la nature et l'abondance des différentes phases minérales de nos matériaux argileux. En particulier, nous avons testé le pouvoir décolorant à l'état naturel d'un de nos matériaux à la décoloration de l'huile de palme. Dans le troisième chapitre, nous étudions l'activation, à l'acide sulfurique, sous diverses concentrations des argiles, à température et durée d'activation constantes (80°C, 2 heures). Il y est également question d'analyser les produits obtenus à l'issu de ce traitement par des techniques telles que : la diffraction des rayons X, la spectroscopie infrarouge, les analyses thermiques, les mesures de surfaces spécifiques (adsorption d'azote), les mesures des capacités d'échanges cationiques, les analyses chimiques (éléments majeurs), les analyses par absorption atomique et analyse capillaires (cations dissous), l'analyse granulométrique laser et la microscopie

électronique à balayage. L'association de ces techniques nous a permis de montrer comment le traitement acide apportait des modifications structurales sur certains minéraux argileux et la variation de leurs paramètres physico-chimiques. Cette section est présentée sous la forme d'un article, lui aussi, soumis à la revue *Colloids and Surfaces A: Physicochemical and Engineering Aspects* et actuellement en cours d'évaluation. Enfin, dans le quatrième chapitre, nous présentons, sous la forme d'un article en préparation, les résultats des tests de décoloration des argiles activées sur une huile végétale (huile de palme). Pour atteindre ce but, nous avons fait appel à la spectroscopie U.V qui permettra de suivre l'évolution de la coloration de l'huile de palme par la mesure de l'absorbance du pigment (béta-carotène) responsable de la coloration. L'étude de la qualité de l'huile avant et après décoloration a été suivie dans cette même section par l'apport de la spectroscopie infrarouge et de la chromatographie gazeuse couplée à la spectroscopie de masse (CG-MS).

Une conclusion générale vient rappeler les résultats originaux et les principaux apports de cette étude. Elle souligne notamment la contribution de ce travail dans la valorisation des matériaux argileux du Cameroun. Afin de poursuivre les études sur les smectites de Bana et Sabga, des perspectives à court, moyen et long terme seront développées pour leur meilleure valorisation.

Références bibliographiques

- Brunet F. (1986) Thèse de Docteur en Pharmacie de l'Université de Paris XI, France.
- Carretero M.I. (2002) Clays minerals and their beneficial effects upon human health. *Applied Clay Science*, **21**(21), 155-163.
- Christidis G.E., Scott P.W. & Dunham A.C. (1997) Acid activation and bleaching capacity of bentonites from the islands of Milos and Chios, Aegean, Greece. *Applied Clay Science*, **12**(4), 329-347.
- Diko M.L., Ekosse G.E., Ayonghe S.N., Ntasin E.B. (2011) Physical characterization of clayey materials from tertiary volcanic cones in Limbe (Cameroon) for ceramic applications. *Applied Clay Science*, **51**(3), 380-384.
- Djangang C.N., Elimbi A., Melo U.C., Nkoumbou C., Lecomte G., Yvon J., Bonnet J.P. & Njopwouo D. (2007) Characteristics and Ceramic Properties of Clays from Mayouom deposit (west Cameroon). *Industrial Ceramics*, **27**(2), 79-88.
- Djangang C. N., Elimbi A., Lecomte G. L., Nkoumbou C., Soro J., Blanchart P., Bonnet J. P. & Njopwouo D. (2008a) Sintering of clay-chamotte ceramic composites for refractory bricks. *Ceramics International*, **34**(5), 1207-1213.
- Djangang C.N., Elimbi A., Lecomte G.L., Soro J., Nkoumbou C., Yvon J., Blanchart P. & Njopwouo D. (2008b) Refractory ceramics from clays of Mayouom and Mvan in Cameroon. *Applied Clay Science*, **39**(1-2), 10 -18.
- Djangang C.N., Lecomte G., Soro J., Elimbi A., Blanchart P., Njopwouo D. (2010) Elaboration de Céramiques Poreuses à base de Sciure de Bois et de deux Argiles du Cameroun. *Annales de Chimie Science des Matériaux*, **34**(1), 1-16.
- Djangang C.N., Kamseu E., Ndikontar M.K., Lecomte G.L., Soro J., Melo U.C., Elimbi A., Blanchart P. & Njopwouo D. (2011) Sintering Behaviour of Porous Ceramic Kaolin-Corundum Composites: Phase Evolution and Densification. *Materials Science & Engineering A*, **528**, 8311-8318.
- Djoufac Woumfo., Kamga R., Figueras F. & Njopwouo D. (2007) Acid activation and bleaching capacity of some Cameroonian smectite soil clays. *Applied Clay Science*, **37**, 149-156.
- Ekosse G.E. (2000) The Mokoro kaolin deposit, south eastern Botswana: Its genesis and possible industrial applications. *Applied Clay Science*, **16**, 301-320.

- Ekosse G.E. (2010) Kaolin deposits and occurrences in Africa: Geology, mineralogy and utilization. *Applied Clay Science*, **50**(2), 212-236.
- Elimbi A., Njopwouo D., Pialy P. & R. Wandji. (2001) Propriétés des Produits de cuisson de deux argiles kaolinitiques de l’Ouest du Cameroun. *Silicates Industriels*, **66** (9-10), 121-125.
- Elimbi A. & Njopwouo D. (2002) Firing characteristics of ceramics from the Bomkoul kaolinitic clay deposit (Cameroun). *Tile & brick International*, **18**(6), 364-369.
- Elimbi A., Yeugouo E., Nenwa J, Liboum. & Njopwouo D. (2003) Caractérisations chimiques et minéralogiques de deux matériaux du gisement argileux de Bakong (Cameroun). *African Journal of Material and Minerals*, **06**(1), 13-19.
- Elimbi A., Founyapté S. & Njopwouo D. (2004) Effets de la température de cuisson sur la composition minéralogique et les propriétés physiques et mécaniques de deux matériaux argileux de Bakong (Cameroun). *Annales de Chimie Science des Matériaux*, **29**(2), 67-77.
- Elimbi A., Piakue J.C., Djangang C.N. & Njopwouo D. (2011) Etude Dilatométrique et Thermique des Produits Crus et Cuits de trois nuances d’Argiles Kaolinitiques. *Annales de la Faculté des Sciences, Université de Yaoundé I, Série Chimie*, **38**(1), 1-19.
- Fagel N. (2010) Géologie des argiles. Les Editions de l’Université de Liège. Pp 68-99
- Falaras P., Kovanis I., Lezou F. & Seiragakis G. (1999) Cottonseed oil bleaching by acid-activated montmorillonite. *Clay Minerals*, **34**, 221–232.
- Harvey C.C. (1995) Industrial kaolin and market growth on the Pacific Rim. Proceeding of the Focus on British Columbia Industrial Minerals, Vancouver, Canada, 29-38.
- Harvey C.C. & Murray H.H. (1997) Industrial clays in the 21st century: A perspective of exploration, technology and utilization. *Applied Clay Science*, **11**, 285-310.
- Highley D.E. (1994) The role of industrial minerals in the economies developing countries. In: Industrial minerals in developing countries. AGID Report Series. Geoscience in International Development, **18**, 1-12.
- Kamseu E., Leonelli C., Boccaccini D.N., Veronesi P., Miselli P., Pellacani G., Melo U.C. (2007). Characterization of Porcelain Compositions using two china Clays from Cameroon. *Ceramics International* **33**(5), 851-857.

- Kamseu E., Braccini S., Corradi A. & Leonelli C. (2008) Microstructural Evolution during Thermal Treatment of three Kaolinitic Clays from Cameroon. *Advances in Applied Ceramics*, **108**(6), 338-346.
- Kamseu E., Rizzuti A., Miselli P., Veronesi P. & Leonelli C. (2009) Use of noncontact Dilatometry for the Assessment of the Sintering Kinetics during Mullitization of three Kaolinitic Clays from Cameroon. *Journal of thermal analysis and calorimetry*, **3**(98), 757-763.
- Kamseu E., Rizzuti A., Leonelli C. & Perera D. (2010) Enhanced Thermal Stability in K₂O-metakaolin-based Geopolymer concretes by Al₂O₃ and SiO₂ Fillers Addition. *Journal of Materials Science*, **7**(45), 1715-1724.
- Kamseu E., Leonelli C. & Obonyo E. (2011) Evolution of Fired Clay Products: from Origin to Sustainable Building Ceramics. *International Ceramic*, **3**(4), 221-225.
- Konta J. (1995) Clay and man: Clay raw materials in the service of man. *Applied Clay Science*, **10**, 275-335.
- Lemougna P.N., Mackenzie J.D.K. & Melo U.C. (2011) Synthesis and Thermal Properties of Inorganic Polymers (geopolymers) for Structural and Refractory Applications from Volcanic Ash. *Ceramics International*, **37**, 3011-3018.
- Leonelli C., Kamseu E., Melo U.C., Corradi A. & Pellacani G.C. (2008) Mullitisation Behavior during Thermal Treatment of three Kaolinitic Clays from Cameroon: Densification, Sintering Kinetic and Microstructure. *International Ceramic*, **57**(6), 396-401.
- Mbey J.A., Hoppe S. & Thomas F. (2012) Cassava starch-kaolinite composite film. Effect of clay content and clay modification on film properties. *Carbohydrate Polymers*, **88**(1), 213-222.
- Melo U.C., Kamseu E. & Djangang C. (2003) Effects of fluxes on the fired properties between 950-1050°C of some Cameroonian clays. *Tile & Bricks International*, **19**(6), 384-390.
- Millot G. (1964) Géologie des argiles: Altérations, Sédimentologie, Géochimie. Masson et Cie, Paris, P.35.
- Murray H.H. (1999) Applied clay mineralogy today and tomorrow. *Clay Minerals*, **34**, 39-49.
- Murray H.H. (2000) Traditional and new application for kaolin, smectite and palygorskite. A general overview. *Applied Clay Science*, **7**, 207-221.

- Nguetnkam J.P., Kamga R., Villiéras F., Ekodeck G.E. & Yvon J. (2008) Assessing the bleaching capacity of some Cameroonian clays on vegetable oils. *Applied Clay Science*, **39**, 113-121.
- Njopwouo D. & Wandji R. (1982) Un gisement d'halloysite à Balengou (Ouest-Cameroun). *Revue Scientifique et Technique, Série Science de la Terre*, **2**, 41-54.
- Njopwouo. (1984) Thèse de doctorat de l'Université de Yaoundé, Cameroun.
- Njopwouo D. & Wandji R. (1985) Minéralogie de l'argile kaolinitique Bomkoul (Cameroun). *Revue Scientifique et Technique, Série Science de la Terre*, **1**(3-4), 71-81.
- Njopwouo D., Roques G. & Wandji R. (1987) A contribution to the study of the catalytic action of clays on the polymerisation of styrene: I-Charaterization of polystyrenes. *Clay Minerals*, **22**(1), 145-156.
- Njopwouo D. & Wandji R. (1988a) Minéralogie et comportement de quelques argiles camerounaises au renforcement du caoutchouc naturel par voie humide. *Annales de la Faculté des Sciences, Université de Yaoundé I, Série Chimie*, **2**(1-2), 187-199.
- Njopwouo D., Roques G. & Wandji R. (1988b) A contribution to the study of the catalytic action of clays on the polymerisation of styrene: Reaction mechanism. *Clay Minerals*, **23**(1), 35-43.
- Njoya A., Nkoumbou C., Grosbois C., Njopwouo D., Njoya D., Courtin A.N, Yvon J. & Martin F. (2006) Genesis of Mayouom kaolin deposit (Western Cameroon). *Applied Clay Science*, **32**(1-2), 125-140.
- Njoya D., Elimbi A., Nkoumbou C., Njoya A., Njopwouo D., Lecomte G. & Yvon J. (2007) Contribution à l'Etude Physico-Chimique et Minéralogique de quelques Echantillons d'Argiles de Mayouom (Cameroun). *Annales de Chimie Science des Matériaux*, **32**(1), 55-688.
- Nkoumbou C., Njopwouo D., Villiéras F., Njoya A., Yonta G.C., Ngo Njock L., Yvon J. & Tchoua F.M. (2006) Geological study and physico-chemical Characteristics of Talc of Boumnyebel (Centre-Cameroun). *Journal of African Earth Sciences*, **54**, 61-73.
- Nkoumbou C., Villiéras F., Barres O., Bihannic I., Pelletier M., Razafitianamaharavo A., Metang V., Yonta Ngoune C., Njopwouo D. & Yvon J. (2008) Physicochemical properties of talc ore from Pout-kelle and Memel deposits (central Cameroon). *Clay Minerals*, **43**(2), 317-337.

- Nkoumbou C., Njoya A., Grosbois C., Njoya D., Njopwouo D., Yvon J., Martin F. (2009) Kaolin from Mayouom (Western Cameroon): Industrial Suitability Evaluation. *Applied Clay Science*, **43**(1), 118-124.
- Obonyo E., Kamseu E., Melo U.C. & Leonelli C. (2011) Advancing the Use of Secondary Inputs in Geopolymer Binders for Sustainable Cementitious Composites. *A Review Sustainability*, **2**(3), 410-423.
- Pialy P., Nkoumbou C., Villiéras F., Razafitianamaharavo A., Barres O., Pelletier M., Ollivier G., Bihannic I., Njopwouo D., Yvon J. & Bonnet J.P. (2008) Characterization for industrial applications of clays from Lembo deposit, Mount Bana (Cameroon). *Clay Minerals*, **3**(43), 415-436.
- Pialy P., Tessier-Doyen N., Njopwouo D. & Bonnet J.P. (2009) Effects of densification and mullitization on the evolution of the elastic properties of a clay-based material during firing. *Journal of the European Ceramic Society*, **29**(9), 1579-1586.
- Prasad M.S., Reid K.J. & Murray H.H. (1991) Kaolin: processing, properties and applications. *Applied Clay Science*, **6**(2), 87-119.
- Rontenberg. (2007) Thèse de doctorat de l'Université Pierre et Marie Curie, Paris 6, France.
- Taha K.K., Suleiman T.M. & Musa M.A. (2011) Performance of Sudanese activated bentonite in bleaching cottonseed oil. *Journal of Bangladesh Chemical Society*, **24**(2), 191-201.
- Tchakoute H. K., Elimbi A., Mbey J.A., Ngally Sabouang C.J. & Njopwouo D. (2012) The effect of adding alumina-oxide to metakaolin and volcanic ash on geopolymers products: A comparative study. *Construction and Building Materials*, **35**, 960-969.
- Tchakoute H. K., Elimbi A., Diffo Kenne B.B., Mbey J.A. & Njopwouo D. (2013) Synthesis of geopolymers from volcanic ash via alkaline fusion method: Effect of $\text{Al}_2\text{O}_3/\text{Na}_2\text{O}$ molar ratio of soda – volcanic ash. *Ceramics International*, **39** (1), 269-276.

CHAPITRE I

SYNTHESE BIBLIOGRAPHIQUE

Minéraux argileux et application dans la décoloration des huiles végétales

Dans ce chapitre, seront présentées les généralités sur les minéraux argileux et, plus particulièrement, les applications des smectites. Un accent sera mis sur l'utilisation des smectites dans la décoloration des huiles végétales, étape critique et déterminante dans tout processus de raffinage physique ou chimique des huiles végétales, minérales et animales.

I. Minéraux Argileux

Cette section s'organise autour de trois rubriques. Dans un premier temps, nous allons définir ce que sont les minéraux argileux (§I.1). Puis, après les avoir défini, nous ferons ressortir leur structure et leur classification (§I.2), pour enfin aborder les aspects relatifs à leurs applications dans la décoloration des huiles végétales (§I.3).

I.1. Définition

Le terme « minéraux argileux » se réfère à des phyllosilicates ou minéraux qui confèrent à l'argile une plasticité et qui durcissent à la cuisson ou au séchage ([Guggenheim et al., 2006](#)). Cette définition élargit celle de Brindley et Pedro (1972) en mettant en relation les minéraux argileux aux propriétés des argiles. Cependant, les minéraux argileux ne sont pas définis à priori comme de grains fins, car l'argile désigne tout matériau naturel, composé de grains fins. Les minéraux argileux peuvent être de n'importe quelle taille de cristallite de sorte que le terme « minéraux argileux » soit conforme à la définition du « minéral », qui n'est pas lié à la taille des cristallites.

I.2. Structure et classification des minéraux argileux

Dans cette séquence, sera présenté en premier lieu les différentes structures des minéraux argileux (§I.2.1) et par la suite leur classification en grands groupes ou familles (§I.2.2).

I.2.1. Structure des minéraux argileux

Les minéraux argileux sont structuralement constitués d'un agencement de tétraèdres siliciques (SiO_4^{4-}) et/ou éventuellement AlO_4^{5-} , et d'octaèdres aluminiques et/ou magnésiques. Ces tétraèdres et ces octaèdres résultent de la superposition de trois types de

plans anioniques disposés parallèlement et contenant des anions oxygène et des groupements hydroxyle. Ces plans dénommés X, Y et Z sont séparés par un espace dit « inter-feuillet » qui peut être occupé par des cations hydratés.

Le plan anionique X (Figure I.1), non compact, est constitué uniquement d'anions oxygène dans lequel un anion O^{2-} sur deux est manquant tous les deux rangs, définissant ainsi une cavité hexagonale (rayon ionique $O^{2-} = 1,30 \text{ \AA}$; dimensions des hexagones : côté, $2,60 \text{ \AA}$ et diagonale, $5,20 \text{ \AA}$). Cette cavité a un diamètre de $2,6 \text{ \AA}$, chaque anion a quatre voisins dans le plan (coordonnance 4).

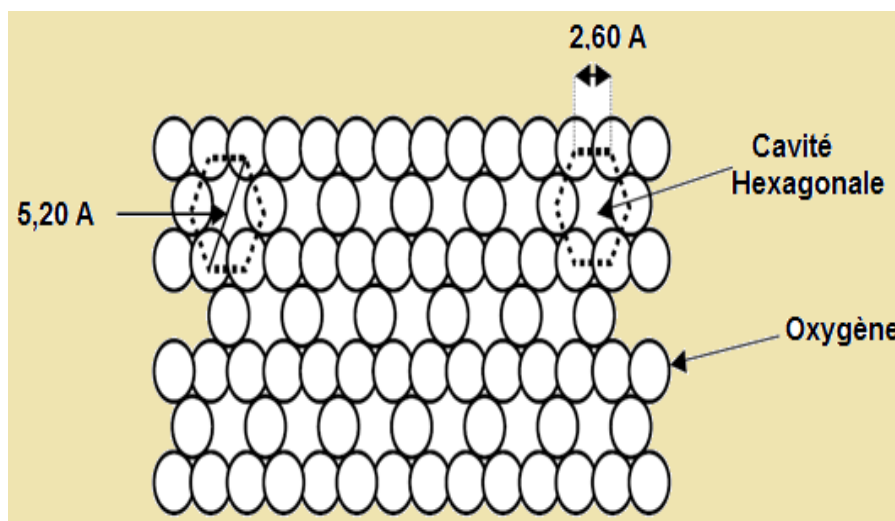


Figure I.1: Représentation schématique du plan anionique X ([Konan, 2006](#))

Le plan anionique Y (Figure I.2), compact comprend à la fois des atomes d'oxygène et des groupements hydroxyles (OH^-). Sur chaque ligne, un anion oxygène sur trois est remplacé par un groupement OH^- . Ainsi, chaque groupement OH^- est entouré de six anions oxygène O^{2-} .

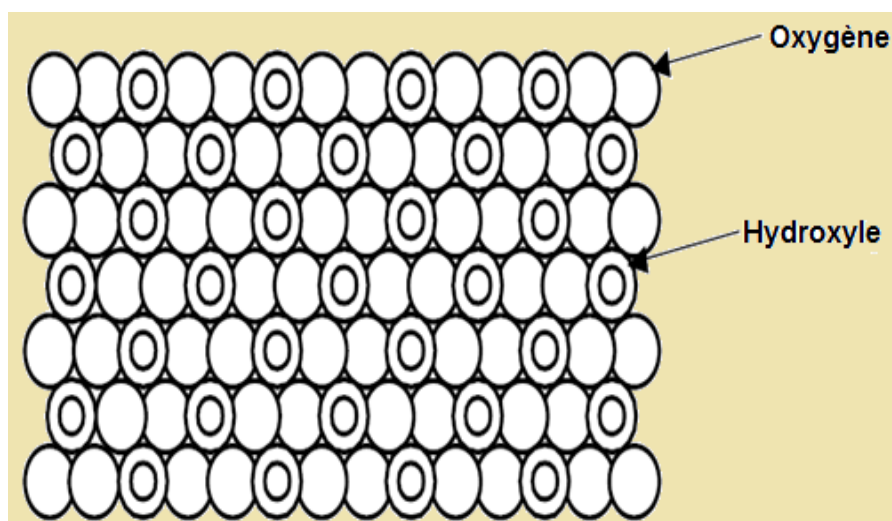


Figure I.2: Représentation schématique du plan anionique Y ([Konan, 2006](#)).

Le plan anionique Z (Figure I.3) est un plan compact formé uniquement des groupements hydroxyles (OH^-). Les groupements hydroxyles de deux rangs contigus sont décalés d'un rayon si bien que les centres de deux groupements hydroxyles d'une même ligne et celui placé sur une ligne voisine sont situés au sommet d'un triangle équilatéral.

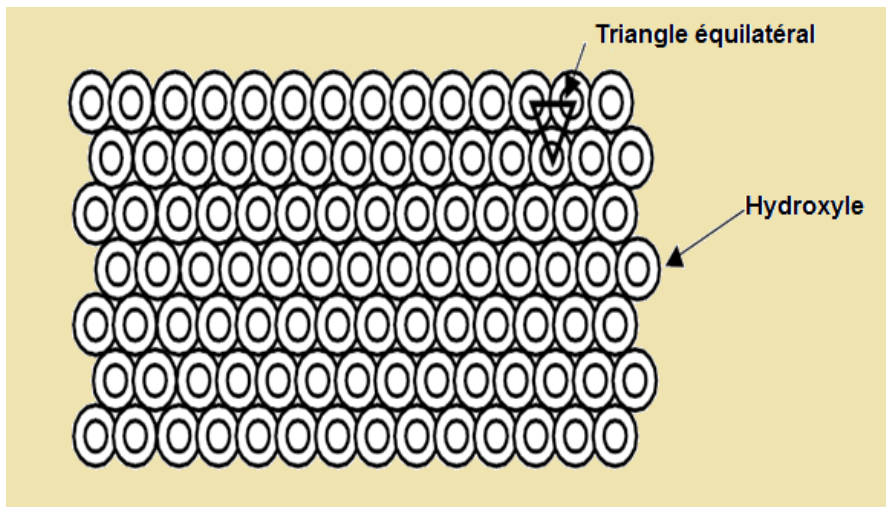


Figure I.3: *Représentation schématique du plan anionique Z (Konan, 2006).*

L'ensemble feuillets-espace inter-feuillet est appelée « *unité structurale* » et l'épaisseur de celle-ci, nommée « *distance basale* », constitue une caractéristique essentielle des minéraux argileux (Bouchet et al., 2000; Pialy, 2009). Les lacunes laissées par ces plans anioniques constituent les environnements octaédriques et tétraédriques.

I.2.2. Classification des minéraux argileux

La classification et la nomenclature des minéraux argileux restent deux éléments assez délicats car les espèces microcristallines qui les constituent sont sujettes à des variations de composition dues aux nombreuses possibilités de substitution (Caillere, 1982). A cela, s'ajoutent deux autres contraintes : l'une, d'ordre structural, concerne les feuillets et leur mode d'agacement. L'autre, d'ordre technique, provient de la difficulté de séparer les cristallites des corps étrangers non cristallisés auxquels ils sont associés à l'état naturel. En outre, la nomenclature et la classification des minéraux argileux a connu au cours de ces années une évolution remarquable. La classification adoptée par le comité de nomenclature de l'*Association Internationale Pour l'Etude des Argiles* (AIPEA) s'appuie sur les grandes données structurales. Ainsi, sur la seule base du mode d'agencement des tétraèdres et des octaèdres, on distingue 3 grandes familles :

- les minéraux phylliteux ;
- les minéraux fibreux ;
- les minéraux interstratifiés.

I.2.2.1. Les minéraux phylliteux

Les minéraux phylliteux ou phyllosilicates sont les plus répandus et les plus étudiés. Ce sont des minéraux argileux qui présentent une structure en feuillets. Leur classification en grands groupes structuraux s'appuie, d'une part, sur le mode d'association des couches structurales (déficit de charge du feuillet) et, d'autre part, sur le taux d'occupation de la couche octaédrique (caractère di- ou tri-octaédrique) ([Konan, 2006; Pialy, 2009](#)). Le Tableau I.1 donne la classification des phyllosilicates.

Type de feuillet	Charge du feuillet (z) et nom du sous-groupe		Exemple de minéral	Nombre (n) de cations en couche octaédrique
Minéraux à 3 plans anioniques ou minéraux 1/1 (distance basale $\approx 7\text{ \AA}$)	z = 0	Kaolinite	Kaolinite	n = 4 : dioctaédrique
		Serpentine	Antigorite	n = 6 : trioctaédrique
Minéraux à 4 plans anioniques ou minéraux 2/1 (distance basale = 10 Å)	z = 0	Pyrophyllite	Pyrophyllite	n = 4 : dioctaédrique
		Talc	Talc	n = 6 : trioctaédrique
	0,25 < z < 0,6	Smectites	Montmorillonite	n = 4 : dioctaédrique n = 6 : trioctaédrique
		Vermiculites	Vermiculite	n = 4 : dioctaédrique n = 6 : trioctaédrique
	z ≈ 0,9	Illite. Glauconite	Illite	n = 4 : dioctaédrique n = 6 : trioctaédrique
		Micas ductiles	Muscovite	n = 4 : dioctaédrique n = 6 : trioctaédrique
	z ≈ 1	Micas	Biotite	n = 4 : dioctaédrique n = 6 : trioctaédrique
		rigides	Margarite	n = 4 : dioctaédrique n = 6 : trioctaédrique
Minéraux à 6 plans anioniques ou minéraux 2/1/1 (distance basale = 14 Å)	z variable	Chlorites	Sudoite	n = 4 : dioctaédrique n = 6 : trioctaédrique

Tableau I.1: Classification des phyllosilicates selon la charge z du feuillet ([Nibambin, 2003](#))

Selon la séquence d'empilement des plans anioniques X, Y et Z, cette famille peut se décomposer en trois sous groupes (Tableau I.1):

- Les minéraux à 3 plans anioniques (X, Y, Z), appelés minéraux 1:1 ;
- Les minéraux à 4 plans anioniques (X₁, Y₁, Y₂, X₂), appelés minéraux 2:1;
- Les minéraux à 6 plans anioniques (X₁, Y₁, Y₂, X₂, Z₁, Z₂), appelés minéraux 2:1:1.

I.2.2.1.1. Les minéraux 1:1

Les minéraux 1:1 notés encore T-O sont constitués de feuillets comprenant une couche tétraédrique (T) accolée à une couche octaédrique (O). La distance basale de ces minéraux est comprise entre 7,1 et 7,4 Å. Le motif élémentaire est formé par un empilement de 3 plans anioniques (X, Y et Z) et de 2 plans cationiques selon la séquence suivante:

- un plan non compact X d'atomes d'oxygène, qui forme la base des tétraèdres (SiO_4)⁴⁻
- un plan d'atomes de silicium ;
- un plan compact Y d'atomes d'oxygène et de groupements hydroxyle (hydroxyle interne) commun aux couches tétraédriques et octaédriques ;
- un plan d'atomes d'aluminium ;
- un plan compact Z de groupements hydroxyles (hydroxyles externes).

La Figure I.4 illustre une représentation des empilements des tétraèdres et octaèdres d'un minéral de type 1:1.

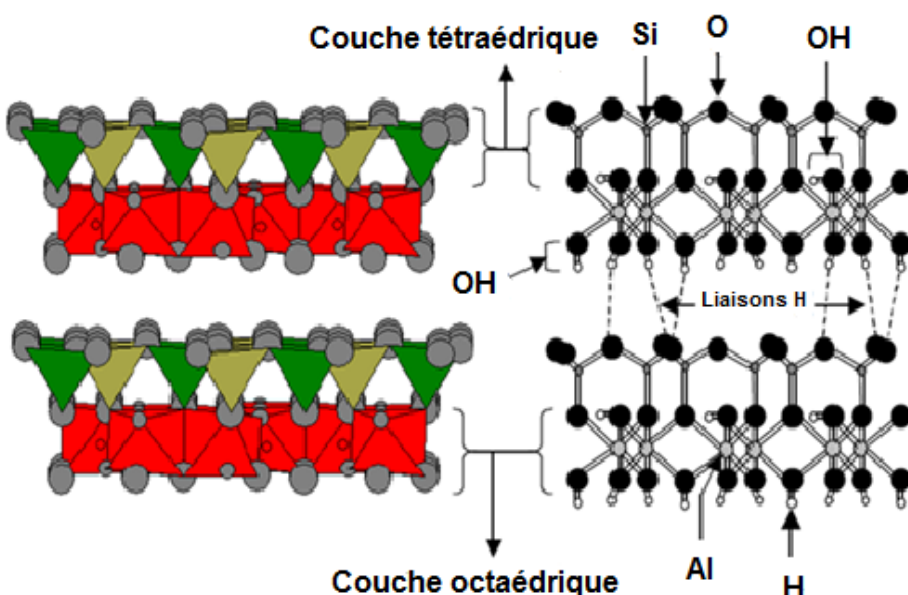


Figure I.4: Représentation des empilements de tétraèdres siliceux et d'octaèdre alumineux d'un minéral 1:1 (Konan, 2006).

Dans les couches tétraédriques, l'ion Si^{4+} peut être substitué par un autre ion de même taille, comme Al^{3+} . Les vides octaédriques peuvent eux aussi recevoir des ions tels que Al^{3+} , Fe^{3+} , Mg^{2+} et Fe^{2+} . Quand tous ces sites octaédriques sont occupés par des ions divalents (Mg^{2+} , Fe^{2+}), le minéral est dit *dioctaédrique*. Par contre si 2/3 de ces sites sont occupés par des ions trivalents on dit du minéral qu'il est *trioctaédrique*.

Les minéraux à couche *dioctaédrique* constituent la famille de la kaolinite de formule structurale $\text{Si}_2\text{O}_5\text{Al}_2(\text{OH})_4$ qui est le minéral argileux fondamental de la plus part des argiles et kaolin employé en céramique fine et pour les produits réfractaires. On subdivise la famille de kaolinite en minéraux hydraté et non hydraté.

- *Minéraux à couche dioctaédrique non hydraté* : Dans ces minéraux l'empilement des feuillets se fait sans possibilité d'intercalation de molécule d'eau, de molécule organique ou d'ion minéraux. Les minéraux de type kaolin dioctaédrique non hydraté comprennent quatre variété cristallographiques : la kaolinite, la nacrite, la dickite et le métahalloysite. Ils diffèrent par la disposition réciproque de leurs différents feuillets.
- *Minéraux à couche dioctaédrique hydraté* : Ces minéraux ont leurs feuillets séparés par une couche de molécules d'eau ou peuvent prendre place des ions minéraux ou des molécules organiques. Le minéral type est l'halloysite de formule :



La présence de molécules d'eau entre feuillets entraîne un écart réticulaire total de 10.1Å et une certaine indépendance des feuillets, qui permet leur enroulement en tubes (Brindley et al., 1950).

I.2.2.1.2. Les minéraux 2:1 et 2:1:1

Communément appelés aussi minéraux T-O-T car leurs feuillets sont constitués de deux couches tétraédriques contenant du silicium encadrant une couche octaédrique contenant de l'aluminium (Figure I.5).

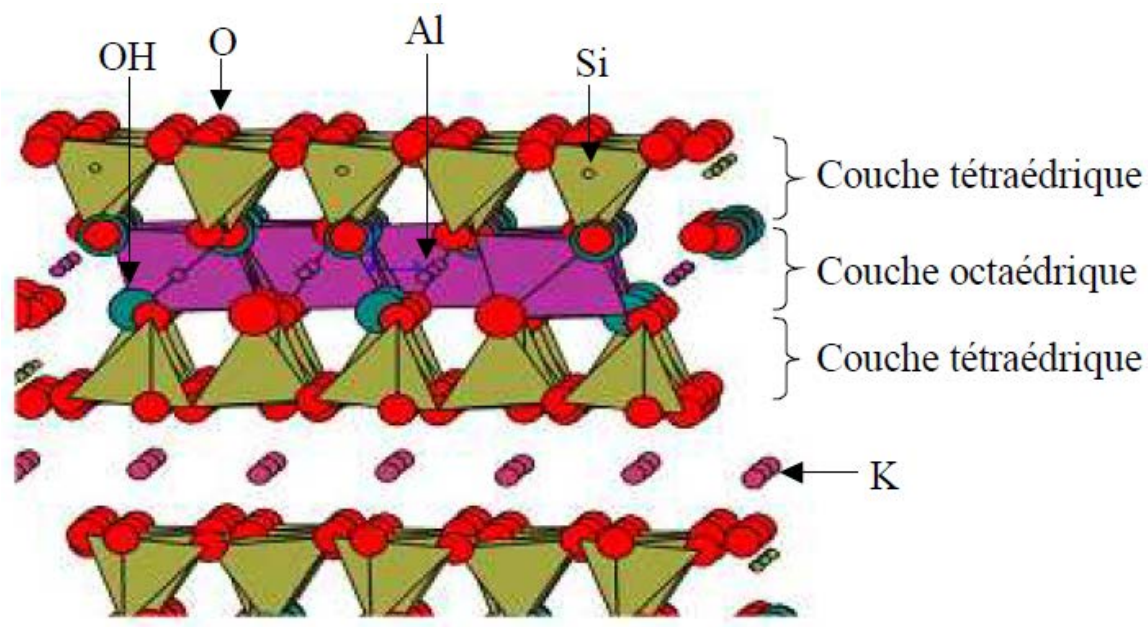
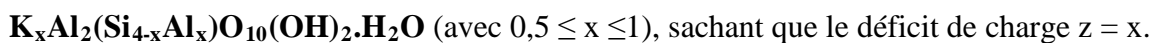


Figure I.5: Représentation schématique des empilements de tétraèdres siliceux et d'octaèdres alumineux d'un minéral idéal 2:1 ([Konan, 2006](#)).

Chaque couche tétraédrique forme un pavage bidimensionnel constitué d'anneaux pseudo-hexagonaux de 6 tétraèdres ayant chacun trois sommets en commun avec les tétraèdres voisins. Les ions oxygène situés sur ces sommets partagés sont appelés "oxygènes pontants". Le quatrième oxygène de chaque tétraèdre assure la liaison avec un cation de la couche octaédrique. Chaque octaèdre est constitué de deux groupements hydroxyles et de 4 atomes d'oxygène apicaux. Au sein des minéraux 2:1, des substitutions cationiques sont observées. Les ions Si^{4+} peuvent être remplacés par Al^{3+} et/ou Fe^{3+} dans les tétraèdres. Les ions Fe^{2+} , Mg^{2+} et Mn^{2+} peuvent se substituer aux ions Al^{3+} , ou Li^+ peut aussi remplacer Fe^{2+} ou Mg^{2+} dans les octaèdres. Ces substitutions engendrent un déficit de charge positive au niveau du feuillet. Ce déficit de charge du feuillet compris entre 0,2 et 0,9 peut être compensé par l'intercalation des cations (K^+ , Na^+ et Ca^{2+}) plus ou moins hydratés. Les eaux contenues dans ces cations pénètrent dans l'espace interfoliaire, induisant ainsi d'importantes modifications des propriétés de ces minéraux telle que le gonflement de la particule. Dans ce cas, la distance basale est fonction de la charge et du nombre de molécules d'eau associées à ces cations. En effet, les molécules d'eau font écran entre le cation compensateur et le feuillet, réduisant ainsi l'attraction cation compensateur-feuillet. Plus il y a de molécules d'eau, plus l'écran est important et plus la distance basale augmente. C'est le cas des smectites où chaque feuillet a une extension latérale très grande, de 0,1 à 1 μm , et est relativement flexible.

Le taux de substitution dans les différentes couches permet de distinguer les différents sous-groupes de minéraux 2:1.

- Lorsque le déficit de charge du feuillet est supérieur ou égal à 0,9, la compensation est assurée par la présence, dans l'espace interfoliaire, de cations non hydratés. La distance basale est voisine de 10 Å. C'est le cas de l'illite où le déficit de charge provient pour l'essentiel de substitutions dans les couches tétraédriques et où les cations compensateurs sont des ions K⁺ non hydratés (Carroll et al., 2005). Ces ions s'insèrent entre les feuillets et contribuent à rigidifier l'ensemble du minéral. La capacité de gonflement de l'illite par insertion d'eau entre les feuillets est inexisteante du fait de la faible distance interfeuillets. La formule des illites généralement admise est :



- Lorsque le déficit de charge varie entre 0,6 et 0,9 du fait de substitutions à la fois dans les couches tétraédriques et/ou octaédriques. La compensation électrique est assurée par l'insertion de cations plus ou moins hydratés dans l'espace interfoliaire. L'une des conséquences est que ce type de minéraux argileux peut accueillir des molécules d'eau dans l'espace interfoliaire et constituer ce qu'on appelle une « *argile gonflante* ». C'est le cas des smectites. Intéressons nous à ce cas qui fait l'objet de notre étude.

Les smectites sont des phyllosilicates constitués de deux couches tétraédriques encadrant une couche octaédrique (phyllosilicates 2:1) et qui présentent des propriétés de gonflement. Les minéraux les plus importants de cette famille sont la montmorillonite, la beidellite, l'hectorite et la saponite. La charge élevée de ces minéraux argileux est due, pour l'essentiel, à des substitutions isomorphiques. Cette charge est donc permanente, négative et dépendante du pH. Les cations compensateurs viennent se placer dans l'espace inter-foliaire pour combler le déficit de charge. Ces minéraux argileux ont une capacité d'échange cationique élevée. Des molécules d'eau sont susceptibles de s'intercaler dans l'espace interfoliaire et, ainsi, le degré d'hydratation dépend de la nature du cation et de l'humidité relative. Cette possibilité de « gonflement » des espaces interfoliaires conduit à désigner ces minéraux argileux par le terme « *argiles gonflantes* ». D'un point de vue textural, les smectites sont généralement constituées de feuillets de grande extension latérale, associés, les uns aux autres en nombre très variable selon l'humidité et la nature du cation échangeable. A titre d'exemple, La montmorillonite est la smectite la plus connue et la plus étudiée; sa structure est schématisée sur la Figure I.6. Dans sa structure, l'aluminium des couches octaédriques peut

être, en partie, remplacé par Mg, Fe, Zn, Ni, Li, etc. Il peut, d'autre part, remplacer au delà de 25 % du silicium dans la couche tétraédrique.

La formule générale de cette famille des minéraux argileux est :



Le déficit de charge est $Z=1-(x-y)$ et $0,2 < Z < 0,6$. Pour $x=1$ on a une montmorillonite.

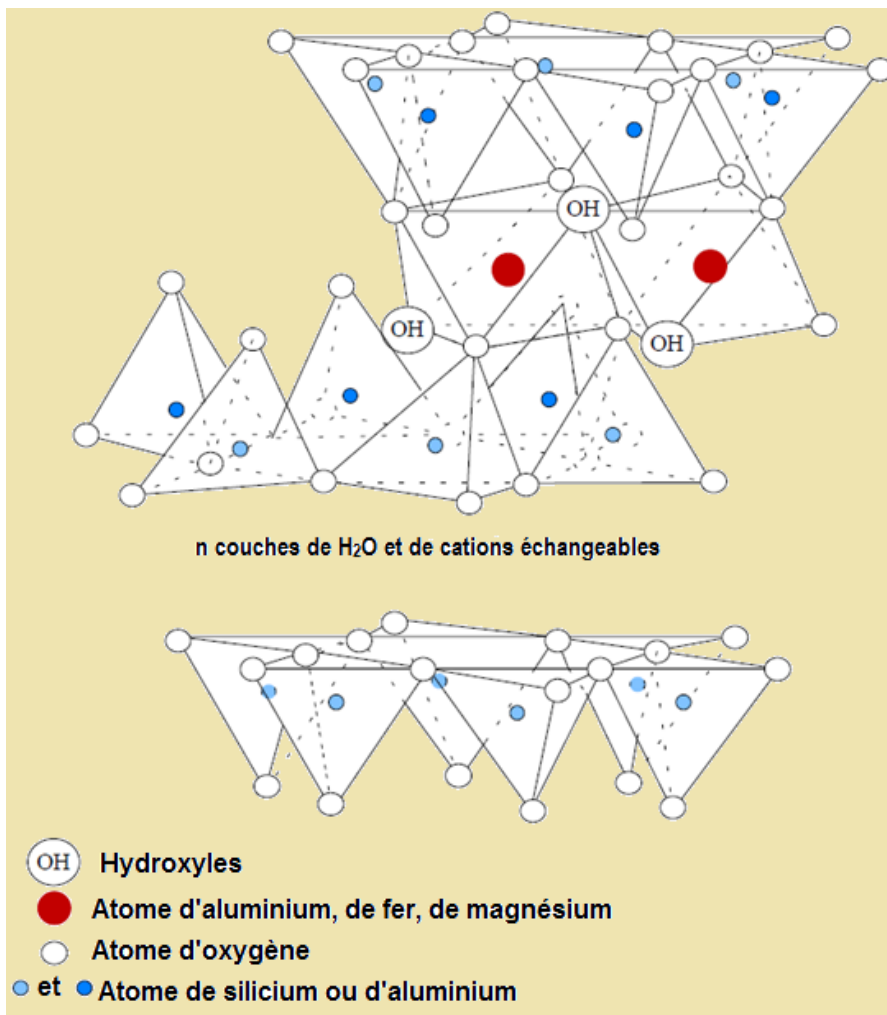


Figure I.6: Représentation schématique de la structure d'une montmorillonite (modifiée par Grim, 1962; Murray, 1999) (USGS Open-file report 01-041, Smectite Group, 2013)¹.

¹ : Smectite Group (2013 January11). In U. S. Geological Survey Open-file report 01-041, from http://pubs.usgs.gov/of/2001/of_01041/htmldocs/clays/smcl.htm

Le Tableau I.2 reporte la classification des différents minéraux argileux formant la classe des smectites.

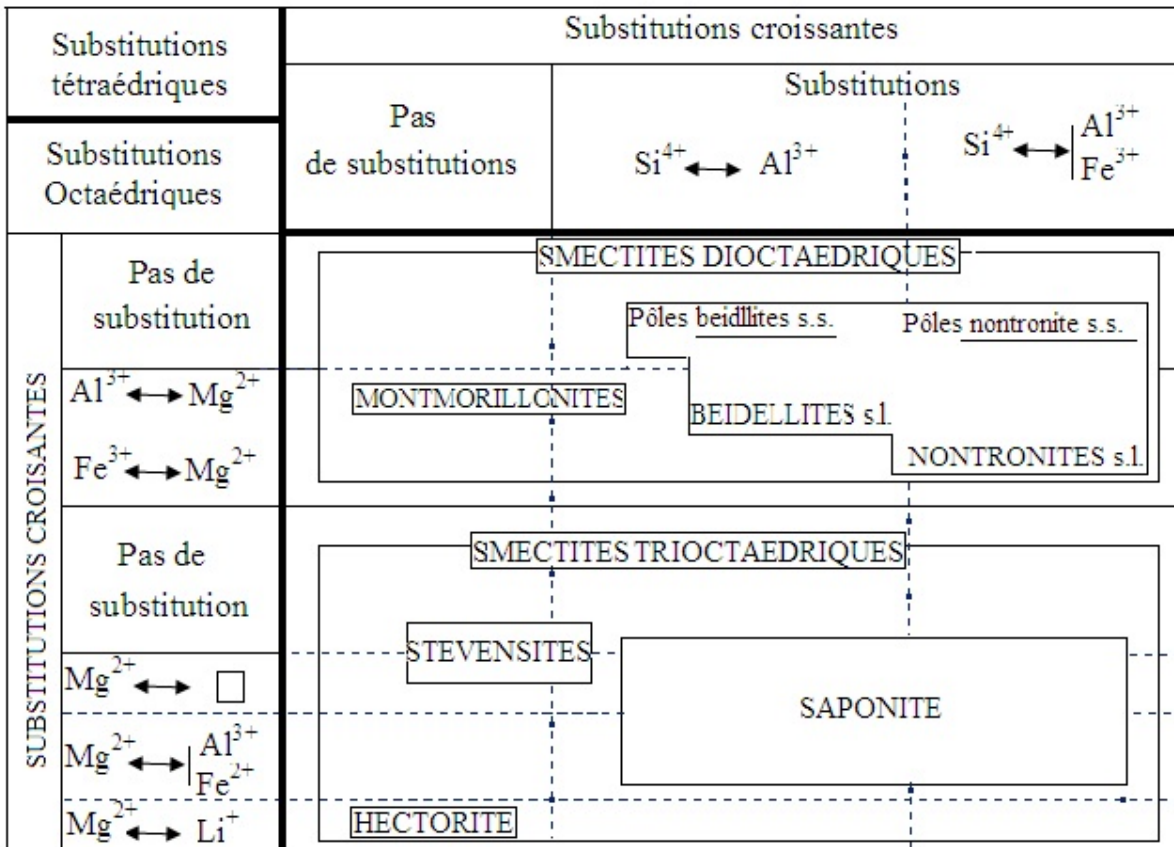


Tableau I.2: Les différents types de smectites ([Holtzapffel, 1985](#))

Les minéraux argileux 2:1 de type smectite se caractérisent par plusieurs propriétés dont les principales sont:

- surface spécifique;
 - capacité d'adsorption d'eau ;
 - charge de surfaces ;
 - microstructuration;
 - échanges ioniques ;
 - gonflement dans des milieux organiques ;
 - possibilité de greffage des molécules organosilanes.
- Lorsque le déficit de charge du feutre est compensé par une couche d'octaèdres à base d'hydroxyde de magnésium (brucite) ou d'hydroxyde d'aluminium (gibbsite) dans l'espace inter-foliaire, on parle de minéraux 2:1:1 (ou T-O-T-O). Ce groupe de minéraux

argileux exhibe une équidistance (distance basale du feuillets) d'environ 14 Å. Le minéral argileux cristallisant dans cette structure correspond à la famille des chlorites (Figure I.7). Ces minéraux ont pour formule générale :



les 2 sous-feuillets étant ici de charges respectives $z = -x$ et $z = +x$

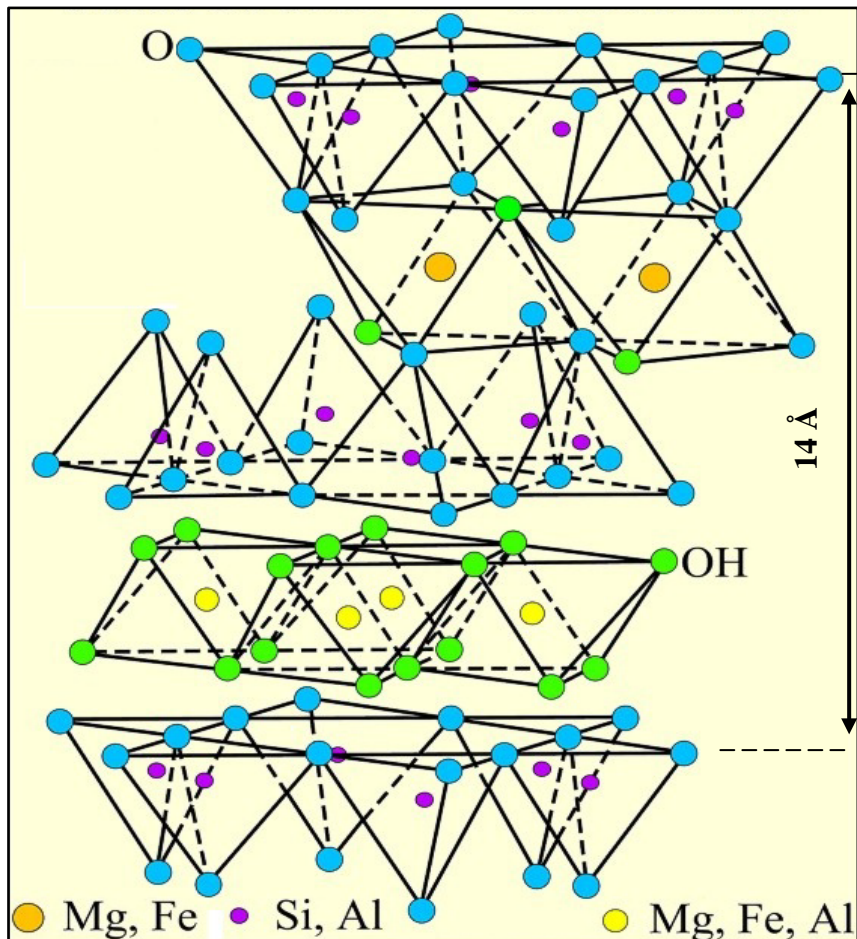


Figure I.7: Représentation des empilements de tétraèdres siliceux et d'octaèdre alumineux d'un minéral de type 2 :1 :1 cas de la chlorite (modifiée par Grim, 1962) (USGS Open-file report 01-041, Chlorite Group, 2013)².

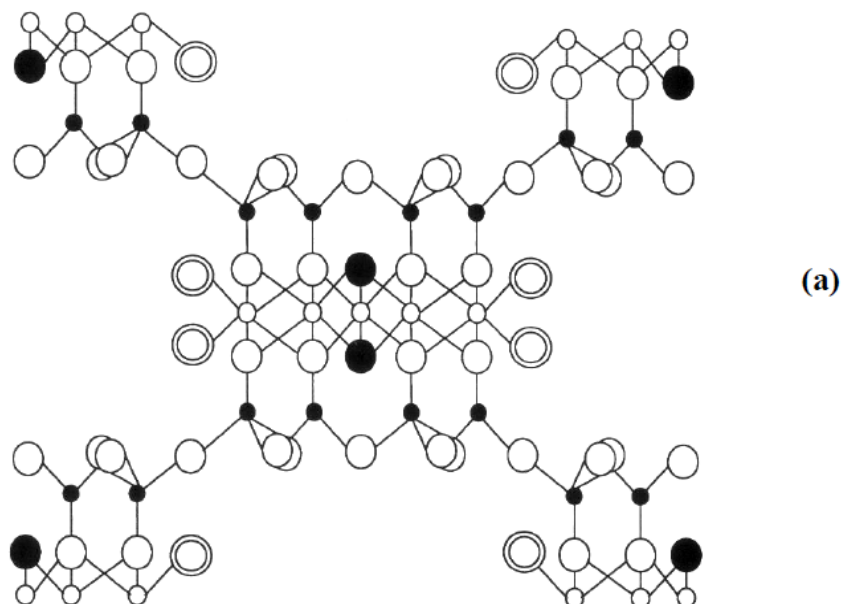
² : Smectite Group (2013 January 11). In U. S. Geological Survey Open-file report 01-041, from http://pubs.usgs.gov/of/2001/of_01041/htmldocs/clays/chlor.htm

I.2.2.2. Les minéraux fibreux

Ces minéraux appartiennent à deux principales familles (Figure I.8):

- La famille des palygorskites (encore appelées attapulgites) où l'empilement des deux plans discontinus fait apparaître un ruban à cinq octaèdres.
- La famille des sépiolites où l'empilement des deux plans discontinus fait apparaître un ruban à huit octaèdres.

Ils possèdent le caractère commun d'être constitués par des couches d'atomes d'oxygène hexagonales continues et séparées alternativement par deux couches d'oxygène à assemblage compact dont l'empilement forme des octaèdres, s'étendant en un long ruban dont la croissance est limitée à une dimension. La largeur du ruban caractérise chacune des familles. Les oxygènes du plan continu forment la base de tétraèdre dont la pointe est constituée par un oxygène du ruban. Ces tétraèdres sont occupés en leur centre par des ions Si^{4+} . Les lacunes octaédriques, quant à elles, sont occupées par les ions divalents (Mg^{2+}) ou les ions trivalents (Al^{3+}).



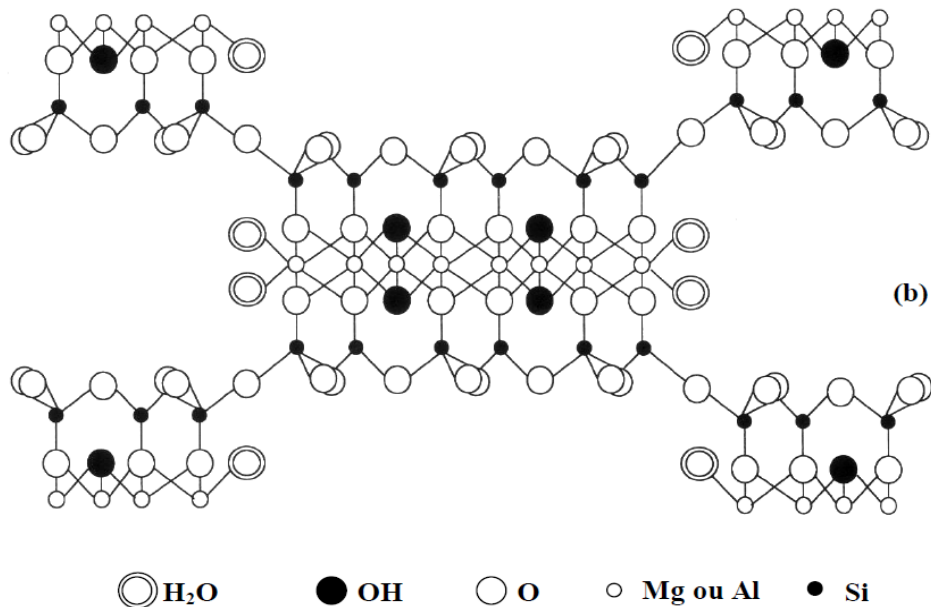


Figure I.8: *Structure des minéraux à pseudo-feuillets et à faciès fibreux :*

(a) Attapulgite; (b) Sépiolite ([Millot, 1964](#))

Ces rubans sont disposés alternativement au dessus ou au dessous de la couche continue d'oxygène à assemblage hexagonal, de sorte que la structure présente en coupe l'aspect d'une brique creuse. C'est cette disposition qui est à l'origine de l'expression « minéraux à pseudo-feuillets » ([Caillère et al., 1982; Chamayou & Legros, 1989](#)).

I.2.2.3. Les minéraux interstratifiés

Ce sont des minéraux argileux dans lesquels il y a alternance des feuillets de nature différente. Les édifices interstratifiés peuvent être de deux types :

- Les minéraux à interstratification régulière où l'empilement des différents types de feuillets (1 :1 et 2 :1) alternent selon des séquences répétitives (exemple d'empilement de minéraux interstratifiés à deux feuillets : 1:1/2:1, 2:1/2:1) (Figure I.9). Les récents développements des logiciels de modélisation des diffractogrammes de rayons X ont révélé que les interstratifiés à trois composants (2:1/2:1/2:1:1) (exemple : Illite/Smectite/Chlorite) ([Drits et al., 1997, 2004; Lanson et al., 2009; Hubert 2008](#)) étaient plus répandus qu'on ne le pensait.

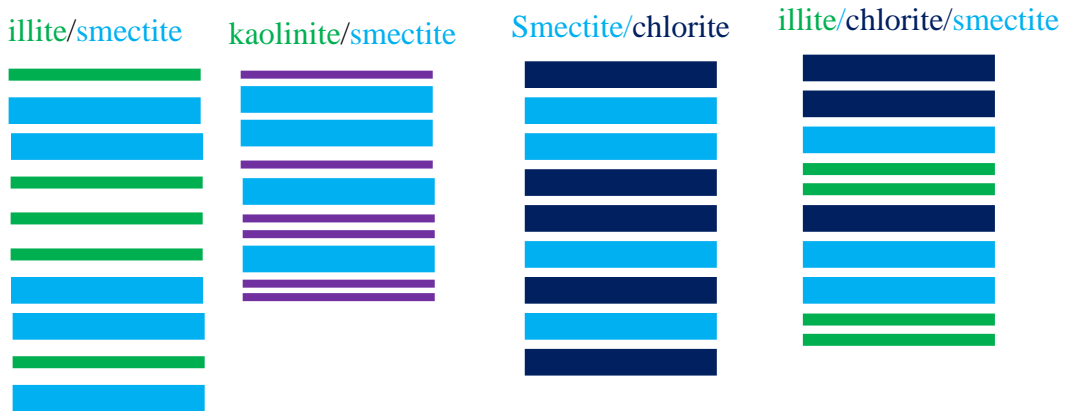


Figure I.9: *Différentes possibilités d'interstratification au sein des minéraux argileux avec deux ou trois composants*

- les minéraux à interstratification irrégulière ou l'empilement des différents types de feuillets (A et B) est aléatoire, c'est à dire aucune séquence répétitive ne régit l'alternance des feuillets (par exemple ABBAABAA...).

Les minéraux argileux interstratifiés à deux composants les plus couramment décrits dans les matériaux argileux sont :

- Illite/smectite (I/S) et kaolinite/smectite (K/S) qui correspondent à l'empilement de deux espèces dioctaédriques.
- Mica (biotite)/vermiculite ; chlorite/vermiculite et chlorite/smectite qui correspondent à des espèces trioctaédriques ou di/trioctaédriques. Les interstratifiés mica/vermiculite et chlorite/vermiculite sont en général ordonnés. Ils se forment par l'altération des phyllosilicates préexistants comme la biotite dans les roches cristallines (Meunier, 2005).

I.3. Minéraux Argileux et applications dans la décoloration des huiles végétales

Les minéraux argileux sont d'usage très ancien. De nos jours, ces utilisations deviennent de plus en plus croissantes au vue de nombreux résultats issus des récentes recherches. En fonction de leur minéralogie, de leurs propriétés physico-chimiques et même de la nature des minéraux non-argileux (impuretés) qui leur sont associées, les minéraux argileux sont utilisées seuls ou en additifs dans de nombreuses applications industrielles. Bon nombre de scientifiques ont écrit des revues exposant de façon exhaustive les différents usages des minéraux argileux, des applications traditionnelles aux usages les plus récents (Murray, 1991; Murray et al., 1993; Konta et al., 1995; Harvey et al., 1997; Murray, 2000). Ces applications sont liées aux propriétés des différentes classes des minéraux argileux. Dans

le cadre de cette thèse, nous ne donnerons que quelques-unes des applications des minéraux argileux de types « *smectites* ».

Les smectites décrites ci-dessus sont des minéraux argileux naturels très diversifiés dont les propriétés physico-chimiques, minéralogiques et texturales sont largement utilisées dans plusieurs domaines de l'activité humaine, depuis le simple concassage du matériau jusqu'à son traitement approfondi. Ces minéraux argileux, dits gonflants et possédant des propriétés adsorbantes ou absorbantes présentent, à cet effet, des grandes capacités d'échanges de l'ordre de 60 à 100 meq/100g ainsi que de grandes surfaces spécifiques pouvant atteindre 800 m²/g ([Caillère, 1989; Decarreau, 1990; Murray, 1999](#)). Ils trouvent leurs utilisations dans de nombreuses applications industrielles ([Murray, 1991; Bergaya et al., 2006](#)):

- Industrie chimique et pétrolière : Les smectites sont employées comme boues de forage dans le raffinage du pétrole et l'extraction du bitume. Ils servent aussi comme catalyseurs dans la pyrolyse et les réactions de cracking du pétrole, dans l'isomérisation conduisant à l'obtention d'hydrocarbures à haut indice d'octane ou dans la fabrication de parfums et essences ([Murray, 1999](#)). On peut également s'en servir dans l'alkylation des phénols. Ils sont également utilisés comme agents déshydratants, adsorbants pour les matériaux radioactifs ([Murray, 1999](#)).
- Industrie minière : ici la smectite notamment la montmorillonite, est utilisée pour favoriser la flottation des sulfures, oxydes et métaux lourds ([DeVaney, 1956](#)).
- Agriculture et horticulture : les smectites sont utilisées pour favoriser la rétention dans les sols de molécules potentiellement polluantes comme les pesticides et limitent leur dispersion dans le milieu naturel (cours d'eau ou les nappe phréatiques), ils participent aussi activement à la stabilisation de la matière organique des sols ([Dixon & Weed, 1989; Lagaly, 2001](#)). Leurs propriétés de sorption sont également exploitées pour l'adsorption des mycotoxines.
- Industrie pharmaceutique et cosmétique: Les minéraux argileux de type smectites ont une longue histoire d'utilisation comme excipient dans des formulations pharmaceutiques ([Hartwell, 1965; Murray, 1999](#)). Dans les liquides, ils sont principalement utilisés comme stabilisateurs de suspension et d'émulsion. Dans les pommades et suppositoires, ils sont utilisés pour contrôler la libération du médicament. Dans les formulations posologiques solides (comprimés), ils sont traditionnellement utilisées comme liants et agents de délitement, sous forme micronisée et de granulations humides pour la compression directe des comprimés. Les smectites sont également utilisées dans les formulations posologiques solides

comme composants du système de biodisponibilité de médicaments, cette application est d'intérêt croissant car ces excipients entièrement naturels offrent une combinaison unique de propriétés physico-chimiques (échange de cations, d'anions, liaison hydrogène, surface spécifique élevée) pour l'interaction médicament-argile. L'utilisation des minéraux argileux en cosmétologie est très ancienne (Murray, 1999). Ils y jouent un rôle essentiel comme charge minérale active. Ils ont un effet abrasif très doux. Leurs propriétés d'adsorption et d'échange autorisent leur association à de nombreux éléments actifs, notamment des colorants, des parfums, des huiles essentielles et des oligoéléments. Le fort pouvoir adsorbant des smectites est exploité pour la fabrication de nombreuses crèmes pour soins dermatologiques, onguents, poudres et shampoings (Hartwell, 1965; Gomes & Silva, 2007).

- Industrie agro-alimentaire : Les smectites sont utilisées dans le domaine agro-alimentaire comme agent de texture dans la fabrication de divers aliments pour animaux. Elles servent aussi pour la filtration des bières, la clarification des boissons (eaux, vins) ainsi que celle des huiles alimentaires d'origine végétales et minérales (Murray, 1999).

Pour ce qui est de la décoloration des huiles végétales, les minéraux argileux (smectites de type montmorillonites) sont utilisées dans leur état naturel (*Terre à foulon ou Fuller's Earth*), et surtout après une activation acide (Guo et Lua, 2000; Valenzuela et al., 2001; Wu Zhansheng et al, 2006; Okwara et al, 2006; Salawara et al., 2007; Siew Wai Lin et al, 2007). Dans tout procédé de raffinage d'huiles végétales, qu'il soit chimique ou physique, la décoloration est une étape critique et déterminante. Elle a pour but principal l'élimination des pigments tels que les carotènes, les chlorophylles et d'autres composés comme les phospholipides, les acides gras, les produits d'oxydation (peroxyde), les métaux en traces (fer, cuivre) et les composés phosphorés présents dans l'huile brute (Rossi et al, 2003; Woumfo et al., 2007; Nde-Aga et al., 2007; Nguetnkam et al., 2008). L'adsorption reste donc le procédé approprié d'élimination de ces impuretés dans lequel les smectites (montmorillonites) activées à diverses concentrations acides (acide sulfurique ou chlorhydrique) jouent le rôle d'adsorbants. Ce traitement augmente la charge sur les particules d'argile et les rend plus efficace dans la décoloration des huiles végétales, minérales et animales. L'utilisation industrielle de ces matériaux dans la décoloration est donc liée à leurs propriétés d'adsorption et de leur réactivité (Bergaya et al., 2006).

Conclusion

Les minéraux argileux de part leur diversité, leurs propriétés et leur disponibilité sont devenus au cours de ces deux derniers siècles, des matériaux d'intérêt dans la plupart des secteurs de production, comme matière première principale ou adjuvant. Les smectites en particulier et notamment les montmorillonites (calcique ou sodique), du fait de leur capacité à gonfler dans l'eau, leur capacité d'échange ionique, leur grande surface spécifique qu'elles développent et leurs propriétés adsorbantes et/ou absorbantes, constituent l'une des familles de minéraux argileux jouant un rôle important aussi bien dans les applications traditionnelles que industrielles modernes. Dans le cas de l'utilisation des minéraux argileux (smectites) pour la décoloration des huiles végétales, le recours à un traitement acide est parfois nécessaire afin d'améliorer leurs propriétés et, par conséquent, leur pouvoir décolorant lorsque ceux-ci ne sont pas doués de pouvoir décolorant à l'état naturel.

Dans le cadre de ce travail de thèse, nous avons identifié et collecté des échantillons dans la région de l'Ouest-Cameroun principalement dans les villages de Bana et Sabga. Pour parvenir à l'identification des phases minérales dans les matériaux ainsi collectés, et à la détermination de leurs propriétés physico-chimiques et texturales, nous avons fait appel aux techniques de caractérisations classiques et modernes décrites dans de nombreuses revues scientifiques. Dans l'optique d'une valorisation plus accrue des ces matériaux argileux dans la décoloration d'une huile végétale produite localement au Cameroun, nous avons procédé à une activation acide de ceux-ci afin d'optimiser leur pouvoir décolorant. Ces trois aspects, à savoir : caractérisation des matériaux argileux ; optimisation des propriétés par une activation acide et valorisation des dits matériaux dans la décoloration d'une huile végétale locale, constituent respectivement l'essentiel des trois chapitres qui seront développés dans la suite de ce travail.

Références bibliographiques

- Bergaya F., Theng B.K.G. & Lagaly G. (2006) Developments in Clay Science 1, Handbook of Clay Science, Chapter 10, Elsevier.
- Bouchet A., Meunier A. & Sardini P. (2000) Minéraux argileux: structure cristalline, identification par diffraction de rayons X", *Bulletin Elf Exploration Production*, Pau, Mémoire, 23, p.136.
- Brindley G. W., Oughton. & Robinson K. (1950) Polymorphism of the chlorites. I. Ordered structures. *Acta Crystallographica*, **3**, 408-416.
- Caillère S., Henin S. & Rautureau M. (1982) Minéralogie des argiles : Classification et nomenclature (Tome 2), Ed. Masson, Paris, pp. 9, 107 & 114.
- Caillère S., Hénin S. & Rautureau M. (1989) Les argiles Ed. SEPTIMA, 125p
- Carroll D. L., KempT.H., Bastow T.J. & Smith M.E. (2005) Solid-state NMR characterization of the thermal transformation of a Hungarian white illite. Solid State Nuclear Magnetic Resonance, **28**, p. 31-43.
- Chamayou H. & Legros J.P. (1989) Les bases physiques, chimiques et minéralogiques de la science du sol. Presses Universitaires de France, 593 P.
- Decarreau A. (1990) Matériaux argileux : Structure, propriétés et applications, Ed. SMFC-GFA, Paris, 587p.
- DeVaney F.D. (1956) U.S. Patent 2743172.
- Dixon J.B. & Weed S.B. (1989) Minerals in Soil Environments. no. 1. *Soil Science Society of America Inc.* USA, Madison, 1244 pp.
- Drits V.A., Sakharov B.A., Lindgreen H. & Salyn A. (1997) Sequential structure transformation of illite-smectite-vermiculite during diagenesis of Upper Jurassic shales from the North Sea and Denmark. *Clay Minerals*, **32**, 351-371.
- Drits V.A., Lindgreen H., Sakharov B.A., Jacobsen H.J. & Zviagina B.B. (2004) The detailed structure and origin of clay minerals at the Cretaceous/Tertiary boundary, Stevns Klint (Denmark). *Clay Minerals*, **39**, 367-390.
- Gomes C.S.F. & Silva J.B.P. (2007) Minerals and clay minerals in medical geology. *Applied Clay Science*, **36**, 4-21.
- Grim R. E. (1962) Applied clay mineralogy. McGraw Hill Book Co. Hong, Z. (1998). Effect of initial water content on compressibility of remoulded Ariake clays. Proc. Int. Symposium on Lowland Technology, Saga University, pp 69-74.

- Guggenheim S., Adams J.M., Bain D.C., Bergaya F., Brigatti M.F., Drits V.A., Formoso M.L.L., Galan' E., Kogure T. & Stanjek H. (2006) Summary of recommendations of nomenclature committees relevant to clay mineralogy: report of the association Internationale pour l'Etude des Argiles (AIPEA) Nomenclature Committee for 2006. *Clays and Clay Minerals*, **54**(6), 761-772.
- Guo J. & Lua A. C. (2000) Preparation and Characterization of Adsorbents from Palm Oil fruit solid wastes. *Journal of Oil Palm Research*. **12**(1), 64-70.
- Hartwell J. M. (1965) The diverse uses of montmorillonite, *Clay Minerals*, **6**, 111-118.
- Harvey C.C. & Murray H.H., (1997) Industrial clays in the 21st century: A perspective of exploration, technology and utilization. *Applied Clay Science*, **11**, 285-310.
- Holtzapffel T. (1985) Les minéraux argileux : préparation, analyse diffractométrique et détermination. *Société Géologique du Nord*, **12**, 15-43.
- Hubert F. (2008) Modélisation des diffractogrammes de minéraux argileux en assemblages complexes dans deux sols de climat tempéré. Implications minéralogique et pédologique. *Université de Poitiers*. 205p.
- Konan K. L. (2006) Thèse de l'Université de Limoges.
- Konta J. (1995) Clays and Man: Clay Raw Materials in the Service of Man. *Applied Clay Science*, **10**, 275-335.
- Lagaly G. (2001) Pesticide-clay interactions and formulations. *Applied Clay Science*, **18** (5-6), 205-209.
- Lanson B., Sakharov B.A., Claret F. & Drits V.A. (2009) Diagenetic smectite-to-illite transition in clay-rich sediments: A reappraisal of X-ray diffraction results using the multi-specimen method. *American Journal of Science*, **309**, 476-516.
- Meunier A. (2005) Clays. *Springer*, Heildeberg, 472 p.
- Millot G. (1964) Géologie des argiles: Altérations, Sédimentologie, Géochimie. Masson et Cie, Paris, P.35.
- Murray H.H. (1991) Overview-clay mineral applications. *Applied Clay Science*, **5**, 379-395.
- Murray H.H. & Keller W.D. (1993) Kaolins, kaolins and kaolins. In: Kaolin Genesis and Utilization, by Murray H.H., Bundy W and Harvey C eds. Special publication N° 1, The Clay Minerals Society, 1993.
- Murray H.H. (1999) Applied clay mineralogy today and tomorrow. *Clay Minerals*, **34**, 39M.9
- Murray H.H. (2000) Traditional and new application for kaolin, smectite and palygorskite. A general overview. *Applied Clay Science*, **7**, 207–221.

- Nde-Aga Binwie J., Kamga R. & Nguetnkam J. P. (2007) Adsorption of Palm Oil Carotene and free Fatty Acids onto Acid Activated Cameroonian Clays. *Journal of Applied Sciences*, **7**(17), 2462-2467.
- Nguetnkam J. P., Kamga R., Villiéras F., Ekodeck G. E. & Yvon J. (2008) Assessing the bleaching capacity of some Cameroonian clays on vegetable oils. *Applied Clay Science*, **39**, 113–121.
- Nibambin S.S. (2003) Thèse de l'Université de Limoges.
- Okwara C. A. & Osoka E.C. (2006) Caustic Activation of Local Clays Palm Oil Bleaching. *Journal of Engineering and Applied Sciences*, **1**(4), 526-529.
- Pialy P. (2009) Thèse de l'Université de Limoges.
- Rossi M., Gianazza M., Alamprese C. & Stanga F. (2003) The role of bleaching clays and synthetic silica in palm oil physical refining. *Food Chemistry*, **82**, 291–296.
- Salawara T.O., Dada E. O. & Alagbe S. O. (2007) Performance Evaluation of Acid Treated Clays for Palm Oil Bleaching. *Journal of Engineering and Applied Sciences*, **2**(11), 1677-1680.
- Siew Wai Lin. & Cheah Kien Yoo. (2007) Optimization of degumming with attapulgite and acid-activated clays in refining palm oil, *Journal of Oil Palm Research*, **19**, 373-380.
- Valenzuela D.F. & Souza Santos P. (2001) Studies on the acid activation of Brazilian smectitic clays. *Quimica Nova*, **24**, 345-353.
- Woumfo E.D., Kamga R., Figueras F. & Njopwouo D. (2007) Acid activation and bleaching capacity of some Cameroonian smectite soil clays. *Applied Clay Science*, **37**, 149-156.
- Wu Zhansheng., Li Chum., Sun Xifang., Xu Xiaolin., Dai Bin., Li jin'e. & Zhao Hongsheng. (2006) Characterization, Acid Activation and bleaching Performance of Bentonite from Xinjiang. *Chinese Journal of Chemical Engineering*, **14**(2), 253-258.

CHAPITRE II

CARACTERISATION DES ARGILES DE BANA ET SABGA

Introduction

Ce chapitre présente la caractérisation des différents échantillons de matériaux collectés lors de nos campagnes de terrain dans les zones de Sabga et Bana (objectif 1), et l'évaluation du pouvoir décolorant naturel de ces matériaux vis-à-vis de l'huile de palme (objectif 2). Pour attendre ces objectifs, nous avons procédé à une description de chaque zone d'étude afin de fournir les données géologiques du terrain. Par la suite des méthodes classiques de caractérisation des minéraux argileux ont été utilisées pour identifier les différentes phases minérales constitutives de ces matériaux. Enfin, nous avons déterminé leurs propriétés physico-chimiques et texturales. Les résultats qui découlent de cette étude sont présentés sous forme de deux articles correspondant respectivement aux deux zones d'étude. Le premier (§II.2) accepté à *Clay Minerals (MS-EF-12-10-R4)*, porte sur la détermination des propriétés physico-chimiques et minéralogiques des smectites de Sabga. Le second (§II.3), qui s'inscrit dans la continuité du premier, est soumis à *Applied Clay Science (CLAY5197)* et porte sur la minéralogie, les propriétés physico-chimiques des smectites de Bana et leur aptitude à décolorer l'huile de palme. Un résumé élargi des deux articles précède l'ensemble des résultats présentés dans les sous-sections (§II.2) et (§II.3).

II.1. Résumé des articles

Dans cette étude, douze échantillons de matériaux ont été collectés respectivement à Sabga (06) et Bana (06). Le but de cette étude était de déterminer la minéralogie et les propriétés physico-chimiques des matériaux récoltés, afin d'évaluer leur potentielle utilisation en tant que adsorbant dans la décoloration de l'huile de palme. Les résultats de différentes techniques analytiques révèlent que ces échantillons de matériaux sont principalement constitués de smectites dioctaèdriques et de kaolinite comme minéraux argileux. En plus de ces minéraux argileux, on note la présence du talc dans les échantillons de Bana. Le test de Greene-Kelly réalisé par saturation au lithium précise la nature montmorillonique de smectite dioctaèdrique. Des teneurs variées de cristobalite, quartz, feldspaths, ilmenite, anatase, hématite et heulandite sont présentes dans la majorité des échantillons, et représentent le

cortège des minéraux dits accessoires (impuretés). La composition chimique des argiles de Sabga montre une prédominance des oxydes majeurs SiO_2 (66-70%), Al_2O_3 (13-16%) et Fe_2O_3 (2-7%), la même observation a été faite sur les matériaux de Bana. La détermination des propriétés physico-chimiques des argiles de Sabga donne les résultats suivants: capacité d'échange cationique (CEC): 38 à 46 meq/100g ; surface spécifique comprise entre 33 et 90 m^2/g . Les échantillons d'argiles de Bana présentent une capacité d'échange cationique (CEC) entre 50 et 60 meq/100g et une surface spécifique de l'ordre de 50 à 68 m^2/g . L'étude du comportement électrophorétique des échantillons montre que la mobilité diminue avec l'augmentation du pH entre 3,0 et 4,5. Au-dessus de la valeur de pH de l'ordre de 4,5, la mobilité électrophorétique reste constante avec une valeur moyenne de $3,2 \mu\text{m.s}^{-1}.\text{v}^{-1}.\text{cm}^{-1}$. Ce phénomène est dû à la présence de la kaolinite et de minéraux non argileux. Le pouvoir décolorant d'un échantillon d'argile de Bana est de 55% pour une durée de traitement de 75 minutes à $97 \pm 1^\circ \text{C}$.

II.2. Smectite clay from Sabga deposit (Cameroon): Mineralogical and Physicochemical Properties (MS-EF-12-10-R4)

J.R. MACHE^{1, 2, 3,*}, P. SIGNING², A. NJOYA³, F. KUNYU⁴,

J.A. MBEY^{2, 5}, D. NJOPWOUO² AND N. FAGEL¹

¹ UR AGEs Argiles, Géochimie et Environnements sédimentaires, Département de Géologie, Université de Liège, B18, Allée du 6 Août, B-4000 Liège, Belgique

² Laboratoire de Physico-chimie des Matériaux Minéraux, Département de Chimie Inorganique, Université de Yaoundé 1, B.P. 812 Yaoundé, Cameroun

³ Mission de Promotion des Matériaux Locaux, B.P 2396 Yaoundé, Cameroun

⁴ Université de Yaoundé I, Département de Science de la Terre, B.P. 812 Yaoundé, Cameroun

⁵ Laboratoire Environnement et Minéralurgie, UMR 7569 CNRS-Université de Lorraine, 15 Avenue du Charmois, B.P. 40. F-54501, Vandœuvre-lès-Nancy Cedex, France

* Corresponding author: e-mail: jamache@yahoo.fr ; Tel: +3243662229;
Fax: +3243662029

ABSTRACT:

The physicochemical and mineralogical characterization of the < 250 µm particle-size fraction from six clay-rich samples from the Sabga deposit (North-west, Cameroon) were carried out in order to evaluate their potential applications. Analyses revealed that the major clay mineral was dioctahedral smectite along with small amounts of kaolinite in three clay samples. Cristobalite, feldspars, ilmenite and heulandites were also found as accessory minerals. A Li-saturation test (Greene-Kelly test) revealed the montmorillonitic nature of the smectite component. The chemical composition of the bulk clays consists of (66-70%) SiO₂, (13-16%) Al₂O₃ and (2-7%) Fe₂O₃. These clays present mineralogical (high montmorillonite content) and physico-chemical (cation exchange capacity (CEC): 38 to 46 meq/100g and specific surface areas ranging from 33 to 90 m²/g). These physical and chemical properties are fully compatible with potential uses in environmental applications. After some pretreatment (purification, chemical modification), these materials could also be used in refining edible oil as adsorbent, waste water treatment and wine technology.

KEYWORDS: smectite, mineralogy, physicochemical properties, Cameroon

INTRODUCTION

Nowadays, clay minerals are important natural materials with a great variety of industrial applications, e.g. ceramics, nanocomposites, oil drilling, waste isolation, and paper industries. Chemical applications of clay minerals include their use as adsorbents, decolorizing agents, ion exchangers, and molecular-sieve catalysts (Fowden et al., 1984; Murray, 1995). Among clays, smectites, which belong to the 2:1 group of phyllosilicates are known for their high cation exchange capacity and high adsorption capacity, chemical and mechanical stability, high specific surfaces area and swellability (Kloprogge et al., 1999; Hussian et al., 2011). The crystal structure of smectite is constituted by two tetrahedral sheets and an octahedral sheet. Tetrahedral sheets are formed by the association of SiO_4^{4-} tetrahedrons, each sharing three corners with the adjacent tetrahedra. Octahedral sheet is usually formed by a gibbsite-like sheet with Al as the central atoms (Mg in brucite). The oxygen of the free corners of each tetrahedral connects the tetrahedral sheet and the octahedral sheet to form a common plane octahedral sheet. The 2:1 layer is characterized by 8 tetrahedral sites and 6 octahedral sites. When two-thirds of the octahedral sites are occupied (4/6 sites are occupied) the layer is said to be dioctahedral and, when all the six octahedral sites are occupied, the layer is said to be trioctahedral. Negative charge defect occurs when the central cation is substituted by a lower charge cation (e.g., Al^{3+} replaces Si^{4+} in tetrahedral sheet or Fe^{2+} replaces Al^{3+} in octahedral sheet). The negative charge of the layers related to these substitutions is balanced by hydrated exchangeable cations in the interlayers (mostly Ca^{2+} , Mg^{2+} and Na^+). Smectites are characterized by a layer charge between 0.4 and 1.2 e^- per unit cell (Madejova' et al., 1998; Brigatti et al., 2006).

Clay minerals are abundant in Cameroon due to its location and the variability of geological basement (Njoya et al., 2001, 2006). However, it is difficult to locate the deposits of smectite clays in tropical zones such as Cameroon where the lateritic red soil is ubiquitous and kaolinite is the dominant clay mineral due to high hydrolysis conditions (Njoya et al., 2001). At present, the uses of smectite clays in Cameroon in many industrial applications (pharmaceutical, cosmetic and agro-alimentary), are developed, requiring the importations of these clay materials.

The main objective of the present study is to identify and characterize the smectite clay deposit of Sabga (North-west, Cameroon), with a view for potential industrial applications.

GEOLOGICAL SETTING AND SAMPLE LOCATION

The area under study is part of the Bamenda Mountains, situated on the Cameroon Volcanic Line (CVL). The study area is located between the Bamboutos Mountains to the south west and the Oku massive to the north east. This volcanic province is made up of both mafic and felsic rocks lying on a panafrican or older basement (Fig. 1) ([Kamgang et al., 2008](#)). On the one hand, the felsic lavas are mainly represented by trachytes, with subordinated benmoreites and alkaline to peralkaline rhyolites ([Kamgang et al., 2007](#)). Two main volcanic episodes were defined New K-Ar geochronological data (18 and 22 Ma and the second is from 12.5 to 13.5 Ma). These felsic rocks mainly originated through fractional crystallization process from mafic magmas, with crustal contamination ([Kamgang et al., 2007](#)). On the other hand, the mafic rocks are basalts to mugearites ([Kamgang et al., 2008](#)). Most of them were contaminated by the continental crust during their transit to the surface. One group of samples contains high Eu, Sr and Ba, reflecting a mantelic origin rather than any crustal contamination. It is argued that these characteristics were acquired by a mixture of melts formed by partial melting of mantle pyroxenites with melt formed in mantle peridotites. Such pyroxenites were observed as mantle xenoliths in the Adamaua province ([Kamgang et al., 2008](#)).

The area under study lies between longitudes 10°18' E to 10°21' E and latitudes 06°00' N to 06°02'N and covers part of the Mezam Division in the North-west Region of Cameroon, with Bamenda as regional headquarters.

The clay-rich materials were sampled from different sites (S) and sampling points (P) along different profiles or outcrop (Figs.2 and 3). Sample S115 was taken at S1, P1; samples S421, S422 and S423 were taken at S3, P9; samples S601 and S602 were taken on S3 at two different outcrops of sampling point P8. In the laboratory, the samples were dried at ambient temperature, grounded and sieved at 250 µm. the samples were homogenized and quartered to ensure the representativity of the initial material. All the following analyses were performed on this 250 µm size fraction.

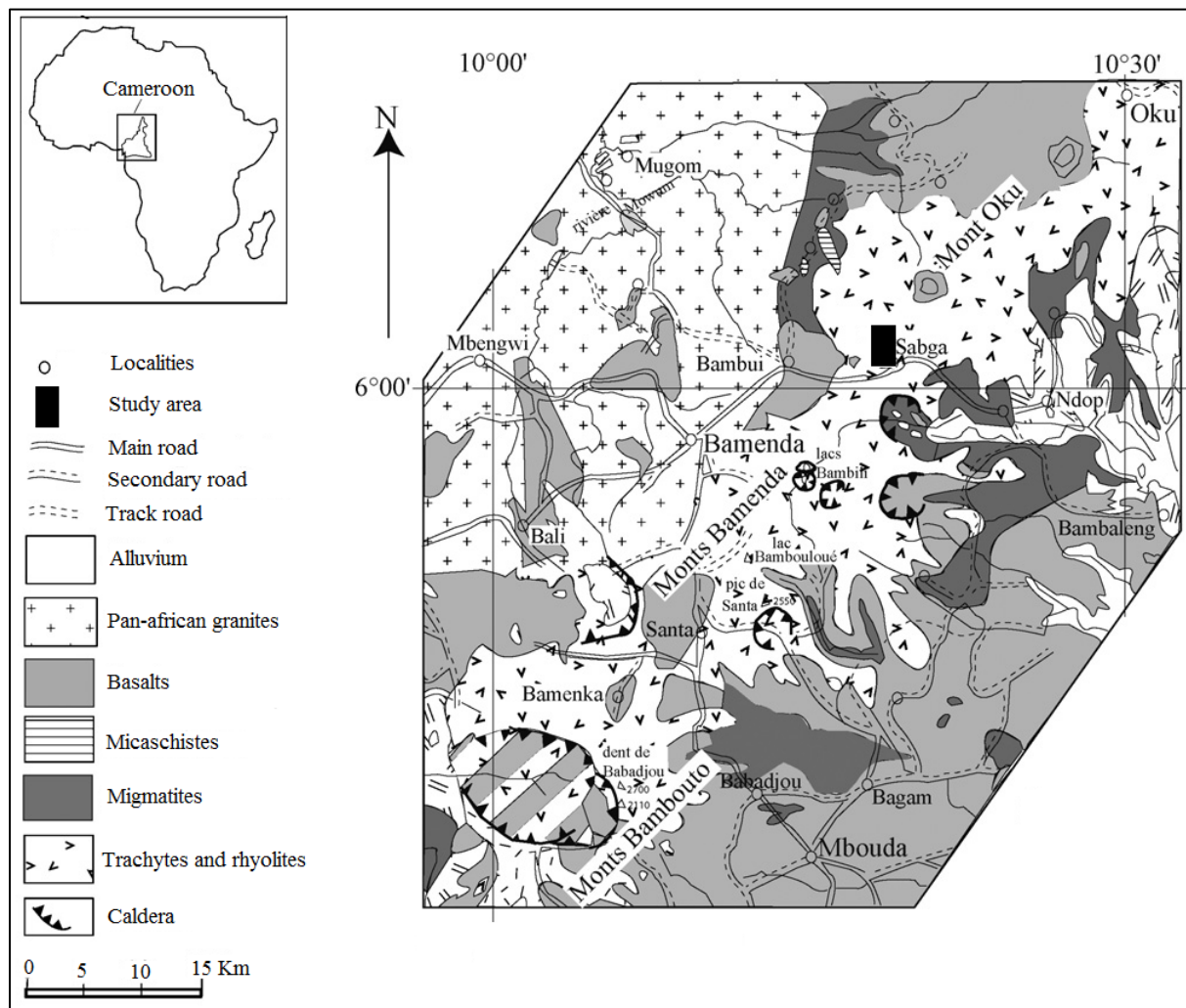


FIG. 1. Geological map of the Bamenda Mountains showing the location of study area (modified from Kamgang et al., 2008)

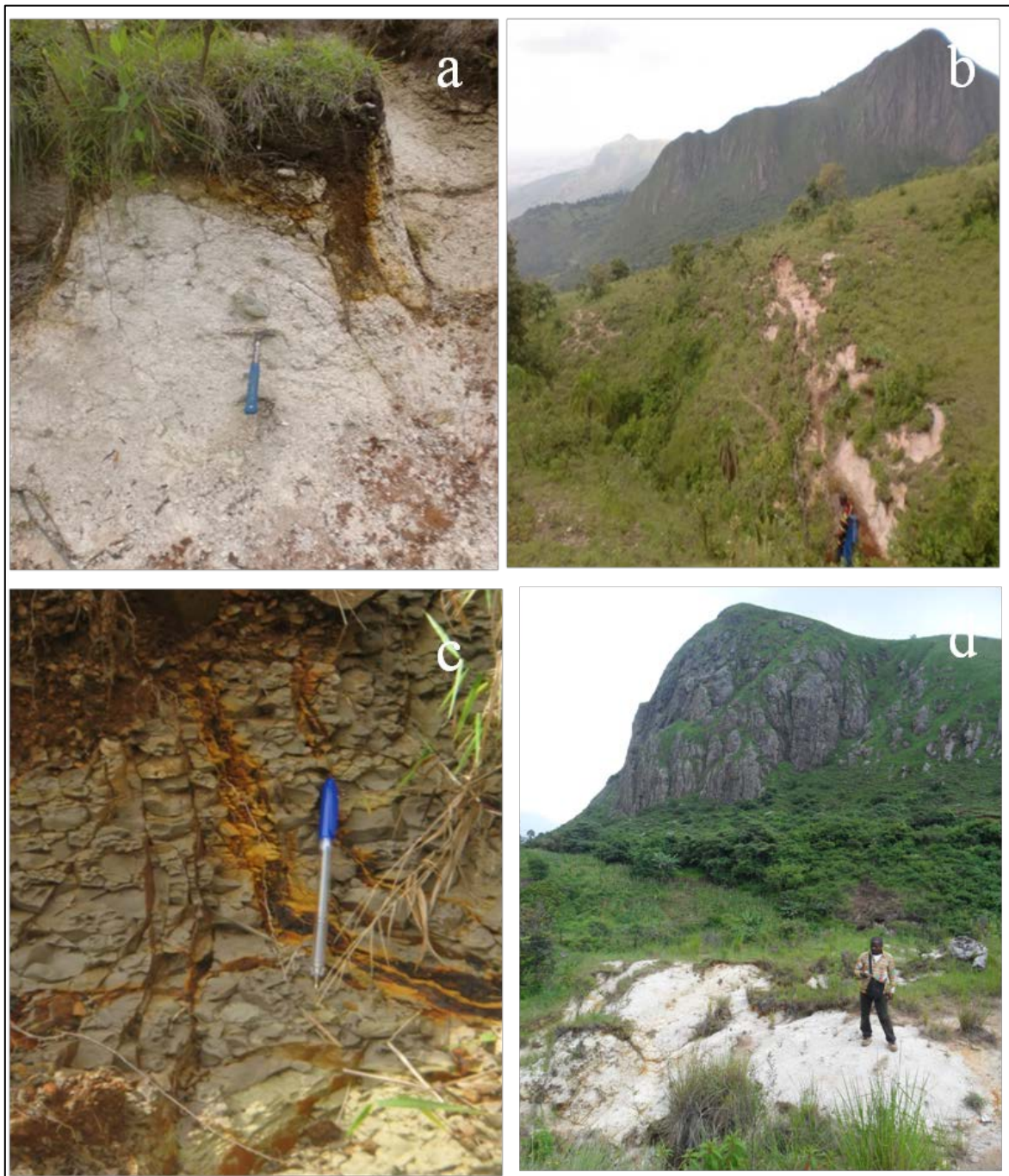


FIG. 2. General views of the Sabga clay deposit. (a) Geological outcrop showing the texture of sample S601; (b) Partial view of the site 3; (c) Geological outcrop (profile 1) showing sample S115; (d) Partial view of the site 1.

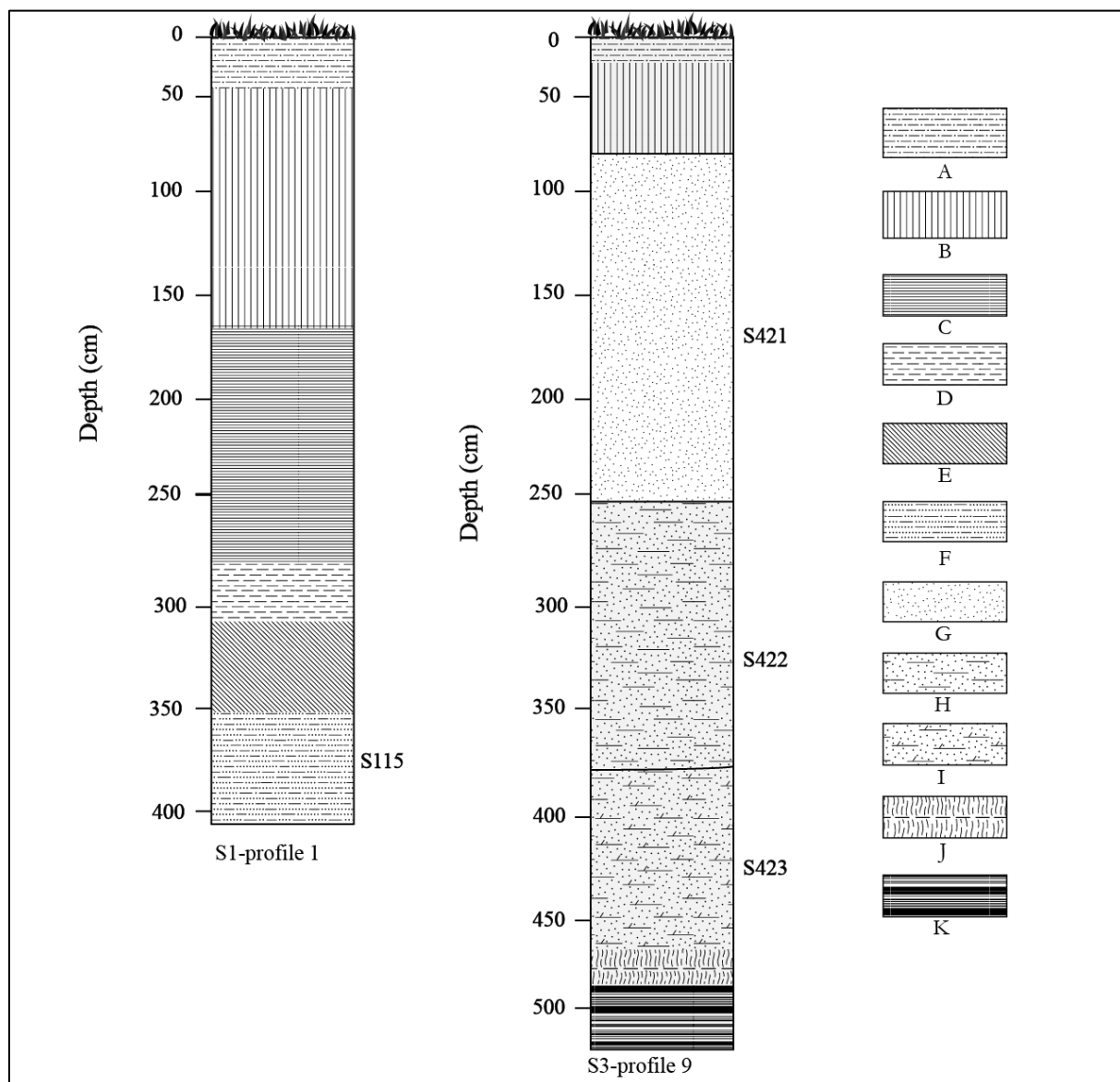


FIG. 3. Morphology of profiles of the clayey materials: A – dark clayey sand layer; B– reddish brown clayey layer spotted with yellow nodules; C – yellow clayey layer mixed with white patches and spotted nodules; D–reddish brown clayey layer mixed with white patches; E – white clayey layer mixed with brown patches; F – whitish grey clayey layer; G – cream white clayey layer; H – cream white clayey layer spotted with rusty patches; I – cream white humid clayey layer spotted with rusty patches; J – greenish grey humid clayey sand layer spotted with rusty patches; K – grey clayey sand humid layer spotted with rusty patches.

METHODS

Mineralogical analyses

The X-ray diffraction (XRD) analysis was first performed on non oriented powder of the dried $< 250 \mu\text{m}$ fraction. This was done using a Bruker AXS model D8 Advance diffractometer, with Cu-K α radiation, under 40 kV and 30 mA operating conditions. The XRD patterns were recorded over the 2° - $45^\circ 2\theta$ angular range using a step scan $0.02^\circ 2\theta$ and a step time of 2 seconds.

Additional measurements were performed on oriented aggregates ([Moore & Reynolds, 1989](#)) prepared from the $< 2 \mu\text{m}$ fraction obtained by suspension in distilled water of 1–2 g of the bulk clay samples. The suspension was first sieved at $63 \mu\text{m}$ to limit particle settling during decantation. The sieving also reduced the amount of impurities within the clay aggregates. The $< 2 \mu\text{m}$ fraction is taken from the suspension after a settling time calculated according to Stoke's law, placed on a glass slide and the XRD patterns were thus recorded between 2° and $30^\circ 2\theta$ using the same step size and time per step parameters. These oriented aggregates were subjected to three successive treatments: air drying, glycolation and heating to 500°C for 4 hours, in order to confirm the nature of clay phases. The Greene-Kelly test, modified by ([Lim & Jackson, 1986](#)) was also performed. To do so, the clay suspension was washed with 2N LiCl solution overnight. Samples were then rinsed with demineralized water, and prepared as oriented aggregates. XRD analyses on oriented clay mounts were conducted according to the following sequence: air-dried slide (N), heated at 300°C (H300, 2H), and finally overnight glycerol solvated (Gl). The Greene-Kelly test was carried out so as to characterize the swelling clay; in particular to differentiate smectites with tetrahedral substitution from those with octahedral substitution. After K-saturated of this $< 2 \mu\text{m}$ size fraction with 2N KCl solution, samples were then washed several times with demineralized water to remove chloride excess. XRD analyses on oriented clay mounts were performed successively in air-dried conditions (K-N), after heating to 110°C for 2 h (K-110), and after exchange with ethylene glycol (K-EG). K-saturation was done to identify the genetic conditions of the smectites ([Thorez, 2000](#)).

Fourier transform infra-red (FTIR) were recorded on the $< 250 \mu\text{m}$ fraction with a Fourier Transform Spectrometer Bruker IFS 55 (Nancy, France). The spectra were acquired on a mixture containing 15 % of the clay powder with oven-dried KBr. The spectra, recorded from 4000 cm^{-1} to 600 cm^{-1} with a resolution of 4 cm^{-1} , were obtained by accumulating 200 scans.

Differential scanning calorimetry (DSC) and thermo-gravimetry (TG) analyses were carried out on ~ 45 mg of the < 250 µm fraction of clay samples using a TG-DSC instrument by SETARAM with a heating rate of 5°C/min from ambient temperature to 700 °C (Liege, Belgium).

Scanning electron microscopy (SEM) images were performed on a Philips microscope model XL30 (Liege, Belgium). Phase identification of the clay was also access by energy dispersive X-ray spectroscopy (EDX). The images were obtained while operating in secondary electron detector at a voltage of 10 kV. The < 250 µm fraction was dispersed over a sample holder and gold-sputtered for (EDX) analysis.

Chemical analyses were carried out using emission spectrometry (Nancy, France). Approximately 1 g of clay < 250 µm powder was molded in fused lithium borate (LiBO_2) and dissolved in nitric acid. Inductive Coupled Plasma by Atomic Emission Spectrometry (ICP-AES) was used for the determination of major elements and Inductive Coupled Plasma by Mass Spectrometry (ICP-MS) was used for trace elements. Relative analytical uncertainties were estimated at 1-5% for major elements except for P_2O_5 (10%). They were up to 5% for most of the trace element concentrations except for Cu (10%). However, uncertainty was high (>10%) for any trace element displaying a low concentration (< 0.1 ppm).

Physical and textural analyses

Cation exchange capacities (CEC) were measured by saturating 300 mg of the < 250 µm fraction using ammonium acetate (1 N, pH = 7). The amount of ammonium fixed by the solid phase was determined by Kjeldahl distillation (Dohrmann, 2006).

The pH of the natural samples was measured with an analytical radiometer TIM 845 after stirring the 1:5 sample/milli Q water suspensions for 10 min and standing for 30 min.

The specific surface areas and total pore volume of the samples were determined from nitrogen adsorption and desorption isotherms at 77 K, obtained from a Carlo Erba Sorptomatic 1990 volumetric device, after outgassing the samples overnight at room temperature at a pressure lower than 10^{-4} Pa (Gregg & Sing, 1982). The specific surface area (SSA) was calculated from adsorption data by applying the Brunauer-Emmet-Teller (B.E.T) method.

RESULTS AND DISCUSSION

Mineralogical composition

The XRD patterns of the six samples show a broad basal reflection $d(001)$, ranging from 13.40-15.19 Å, characteristic of smectite clays (Fig. 4). The peak at 4.47 Å is related to the (02 ℓ) or (11 ℓ) reflection series. This value close to 4.47 Å indicates that the smectite clay is dioctahedral. The associated mineral detected in three clay samples (S421, S422 and S423) is kaolinite which is characterized by the (001) basal reflection at 7.10 Å on bulk powders. Accessory minerals such as cristobalite, feldspars and ilmenite were detected in all the samples. Their typical reflections are observed at 4.06-4.10 Å, 3.19-3.31 Å, and 3.71-3.75 Å, respectively. In addition, heulandite is present in sample S601 by reflections located at 8.85 and 7.83 Å.

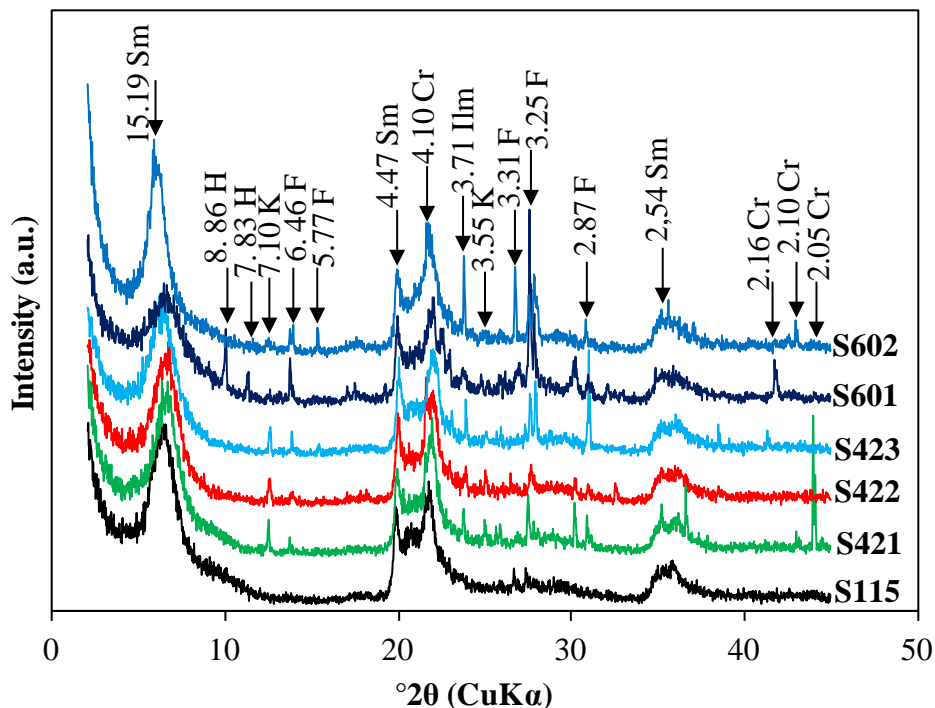


FIG. 4. X-ray powder diffraction patterns of the < 250 µm fractions.
 Sm: smectite; K: kaolinite; F: feldspars; H: heulandites; Cr: cristobalite;
 Ilm: ilmenite

For sample S115, the XRD patterns obtained for oriented preparation after different treatments are presented in Fig. 5. The Ethylene glycol treatment of the natural clay material lead to an increase of the basal interlayer spacing from 13.40 Å to 16.66 Å which is again typical of smectitic clay minerals (Fig. 5a).

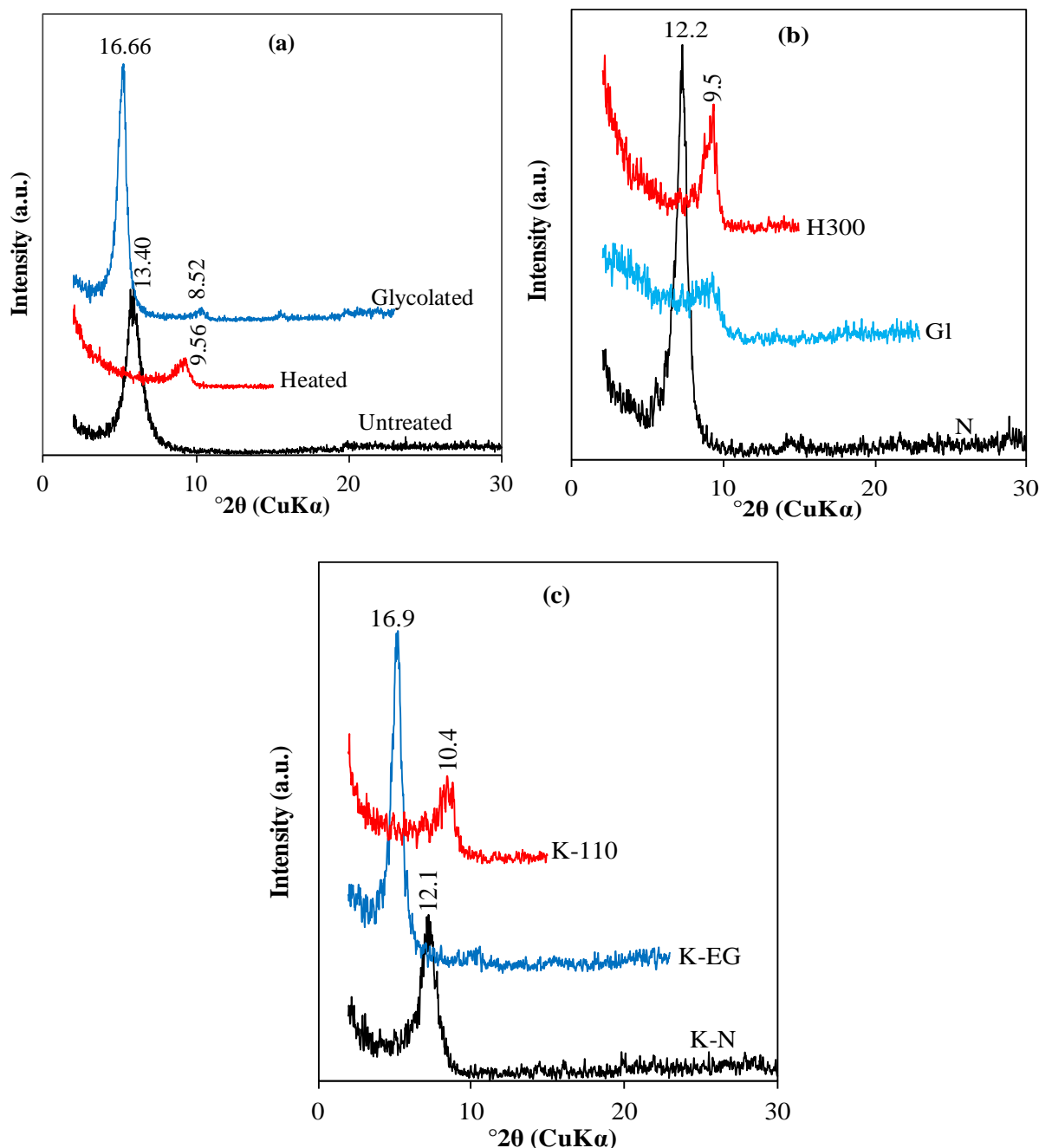
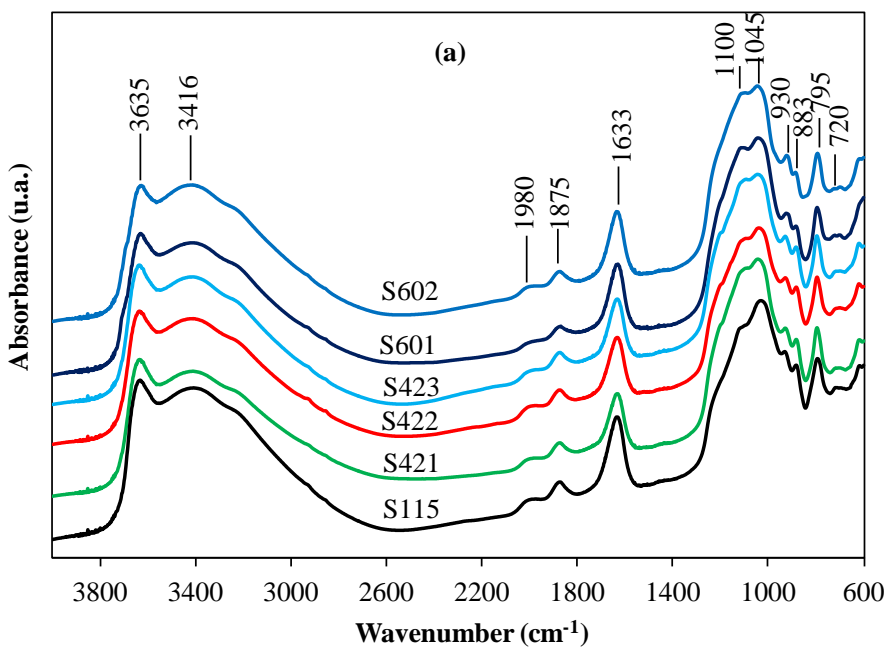


FIG. 5. XRD patterns of the oriented $< 2\mu\text{m}$ fraction of sample S115. (a) XRD patterns for untreated, heated at 500°C and glycolated specimen. (b) XRD patterns obtained after Li-saturation (Greene-Kelly test) for natural (N), treated with glycerol (Gl) and heated at 300°C (H300). (c) XRD patterns obtained after K-saturation for natural (K-N), treated with ethylene glycol (K-EG) and heated at 110°C (K-110).

On the heated sample, the collapse at 9.6 Å of the basal spacing further confirms the smectite nature of the samples (Fig. 5a; Holtpzapffel, 1985). The inability of all samples to re-expand beyond 9.5-9.8 Å with glycerol after Li-saturation and heat treatment, (Greene-Kelly test, Fig. 5b) indicates that these smectite are montmorillonite with an origin for layer charge located in the octahedral sheet (Fig. 5b). According to the Greene- Kelly test, this charge is neutralized by the migration of Li^+ ions into empty sites of the dioctahedral sheet (Malla & Douglas, 1987; Hradil et al., 2004). For K^+ saturated specimens, all oriented clay samples have basal spacings of ~12 Å, which expands to ~ 17 Å after glycolation (Fig. 5c). Such expansion after K-saturation and glycolation is typical of low-charge smectites (Komarneni & Breval, 1985).

The infrared absorption spectra show a sharp band around 3635 cm^{-1} due to OH stretching (Fig. 6a). This band, clearly visible on Fig. 6b, corresponds to AlAlOH stretching of smectite (Madejová et al., 1994) and a broad band of water around 3416 cm^{-1} due to the overlapping asymmetric ν_3 and symmetric ν_1 (H-O-H) stretching of H-bonded water (Madejová, 2003; Hajjaji et al., 2001). The bands at $1637\text{-}1630 \text{ cm}^{-1}$ are due to adsorbed water (Hajjaji et al., 2001). The Si-O stretching band (Fig. 6c) is observed in the IR spectra of both di-and tri-octahedral smectites, montmorillonite at $1031\text{-}1046 \text{ cm}^{-1}$. The band observed at 882 cm^{-1} , is assigned to the deformation δOH of AlFe-OH. The infrared spectra of the natural clays also revealed the presence of SiO_2 impurities. The bands at 698 , 794 , 1875 and 1984 cm^{-1} could all be ascribed to cristobalite (Moenke, 1974; Graetsch, 1988). The bands near 1985 cm^{-1} are combination and overtone bands of these impurities.



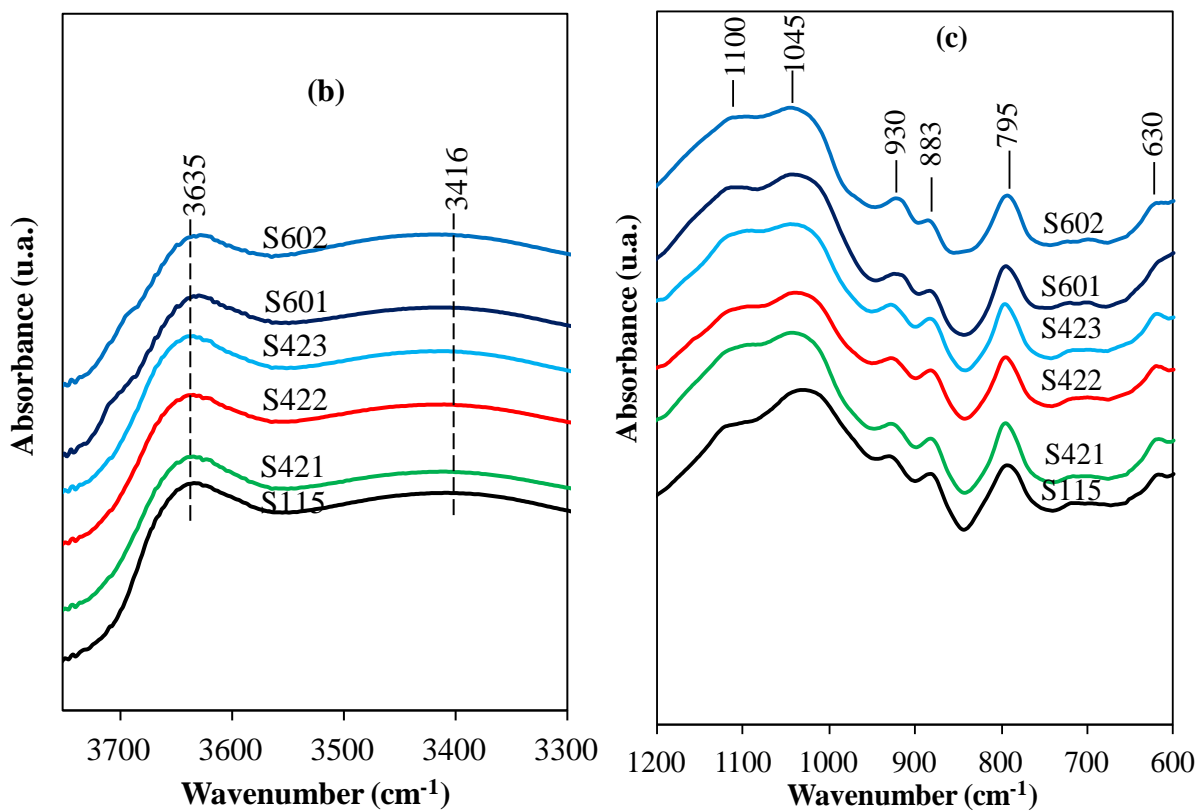


FIG. 6. FTIR spectra of the $< 250 \mu\text{m}$ fractions: (a) complete spectrum, (b) OH stretching domain (c) Si-O stretching domain

Thermal analyses of all the samples revealed five endothermic peaks in all clay samples (Fig. 7). The first large endothermic peak near 107°C corresponds to the removal of adsorbed water (Mackenzie, 1970). The second and third endothermic peaks (weak) at 147°C and 215°C are attributed to the loss of adsorbed and smectite interlayer water respectively. The fourth peak near 488°C corresponds to the elimination of water caused by dehydroxylation of coordinated and structural water molecule. The last endothermic peak near 650°C corresponds to the removal of OH groups of smectite.

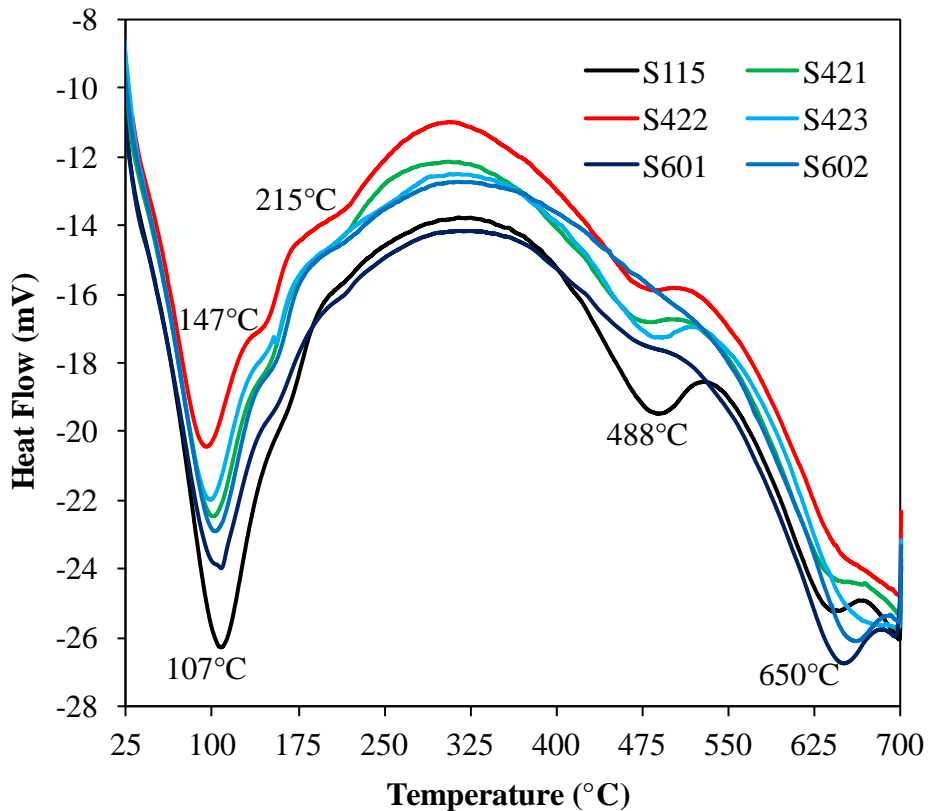
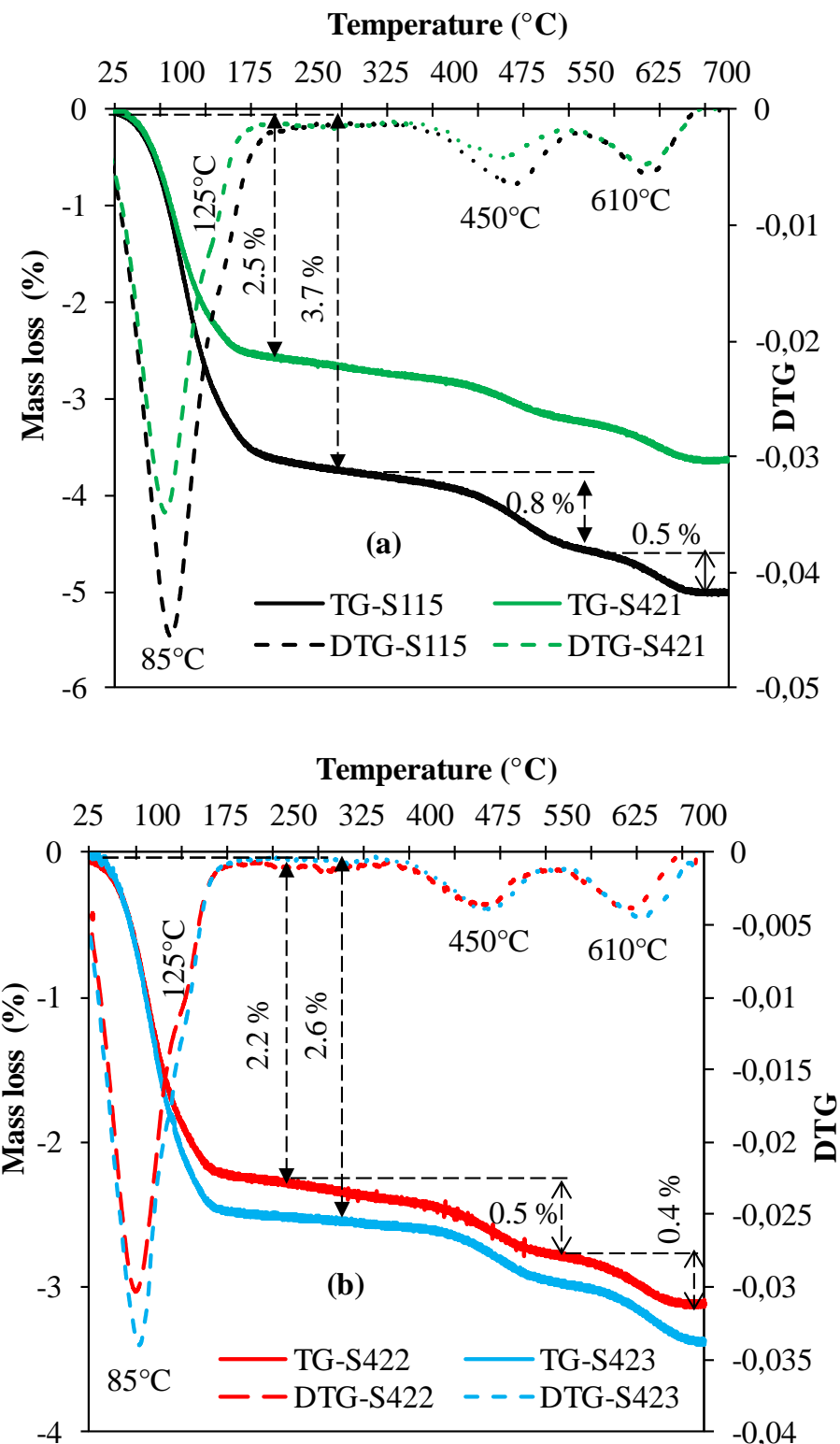


FIG. 7. DSC curves for the < 250 µm fractions.

The TG curves of the natural clays show two well-defined weight loss regions due to the loss of adsorbed water below 200°C and dehydroxylation of structural water near 500°C (Fig.8). The minor weight loss region above 605-630°C (0.6-1%) is due to the dehydroxylation of the clay sheets of smectite. The mass loss, due to adsorbed water molecules (70-175°C), ranges between 2.2 and 3.7 %. The coordinated water released (450-500 °C) leads to mass loss between 0.4 and 0.8 %. The mass loss, observed at 605-630°C ranges between 0.6 and 1.0%. Total weight losses range between 3.1 and 5.0 %. The wide range of dehydroxylation temperature (450-630°C) observed here, is consistent with dioctahedral smectites.

The TG derivative curves (DTG) of all samples show three sharp endothermic peaks (Fig. 8). Given that all samples are mainly composed of swelling clay minerals, the first peak (70- 85°C) is likely due to the loss of adsorbed water of montmorillonite. The two endothermic peaks at 450 and 605-630°C are attributed to the loss of water caused by dehydroxylation of structural water molecule of phyllosilicates contents in the clay samples (Fig. 8).



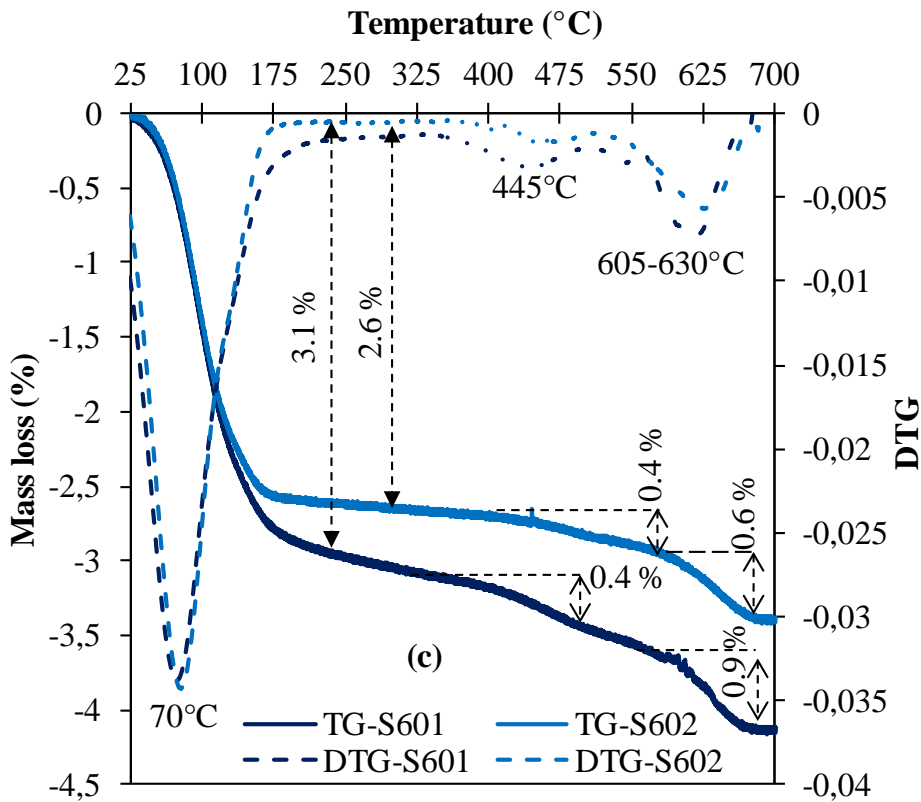


FIG. 8. TG (solid lines) and DTG (dotted lines) for the < 250 µm samples. (a) samples S115 and S421; (b) samples S422 and S423; (c) samples S601 and S602.

Chemical composition

Table 1 shows the chemical composition of major elements of the six clay samples from the Sabga area. The most abundant oxides are SiO₂, Al₂O₃ and Fe₂O₃ whereas K₂O, CaO, Na₂O, MgO, TiO₂ and MnO are present only in small quantities. SiO₂ values range between 66 and 70 %. Al₂O₃ contents vary between 13 and 16%. The SiO₂/Al₂O₃ ratio is greater than 4 for all the samples owing to the sandy content of the sample. Fe₂O₃ values for four samples (S115, S421, S422 and S423) are > 5%, samples S601 and S602 contains 3.4 and 2.6 % respectively. The Na₂O (0.2-1.1 %) and K₂O (0.4-2.8%) contents can be related to the presence of minor amounts of Na/K-feldspars. Remarkable is the large variation in the content of Ba, Ce, La, Nb, Nd, Zn, Sr and Zr with that of Zr ranging from 520 to 600 ppm, Ce from 101 to 199 ppm and of Ba from 142 to 348 ppm. The Zn content is high and varies between 108 and 223 ppm. The XRD measurements cannot confirm whether these elements are incorporated in the clay structure or are present as impurities of secondary minerals. Trace

elements such as As, Cu, Cr and Ni are absent in all samples, but Pb is present in minor amounts ranging between 10 and 57 ppm.

Major elements (Oxides in wt. %)	Samples					
	S115	S421	S422	S423	S601	S602
SiO ₂	68.23	67.52	66.29	66.26	66.12	69.97
Al ₂ O ₃	13.57	15.08	15.37	15.10	15.96	14.06
Fe ₂ O ₃	6.60	5.49	5.75	6.26	3.38	2.62
MnO	0.01	0.01	0.01	0.06	0.09	0.17
MgO	0.44	0.28	0.31	0.30	0.49	0.74
CaO	0.68	0.83	0.96	1.02	0.94	0.98
Na ₂ O	0.21	0.75	0.74	0.90	1.08	1.08
K ₂ O	0.44	1.25	1.27	1.49	2.76	1.71
TiO ₂	0.21	0.26	0.26	0.25	0.27	0.25
P ₂ O ₅	< L.D.	< L.D.	< L.D.	0.03	0.03	< L.D.
L.O.I.	10.51	9.06	9.38	8.50	8.51	9.06
Total	100.91	100.52	100.34	100.18	99.63	100.64
SiO ₂ /Al ₂ O ₃	5.03	4.48	4.31	4.39	4.14	4.98

L.O.I = Loss on ignition; <L.D. = < to detection limits.

TABLE 1. Major elemental compositions of the clay < 250 µm samples.

The scanning electron micrographs and an energy dispersive spectrometry analysis of three natural clays are presented in (Fig. 9). The EDX spectrum shows that the selected grains contain Al, Si and O which are dominant associated with various quantities of Fe, Na, K, Mg and Ca. Through EDX, a larger amount of Si in the regions was identified, which confirms the presence of fine cristobalite, in agreement with the XRD results. The SEM micrographs of natural clays reveal the presence of particle and sheets. We observed that porosity is uniformly distributed throughout the samples. The results of chemical analyses of major elements showed that the six clay samples display similar compositions.

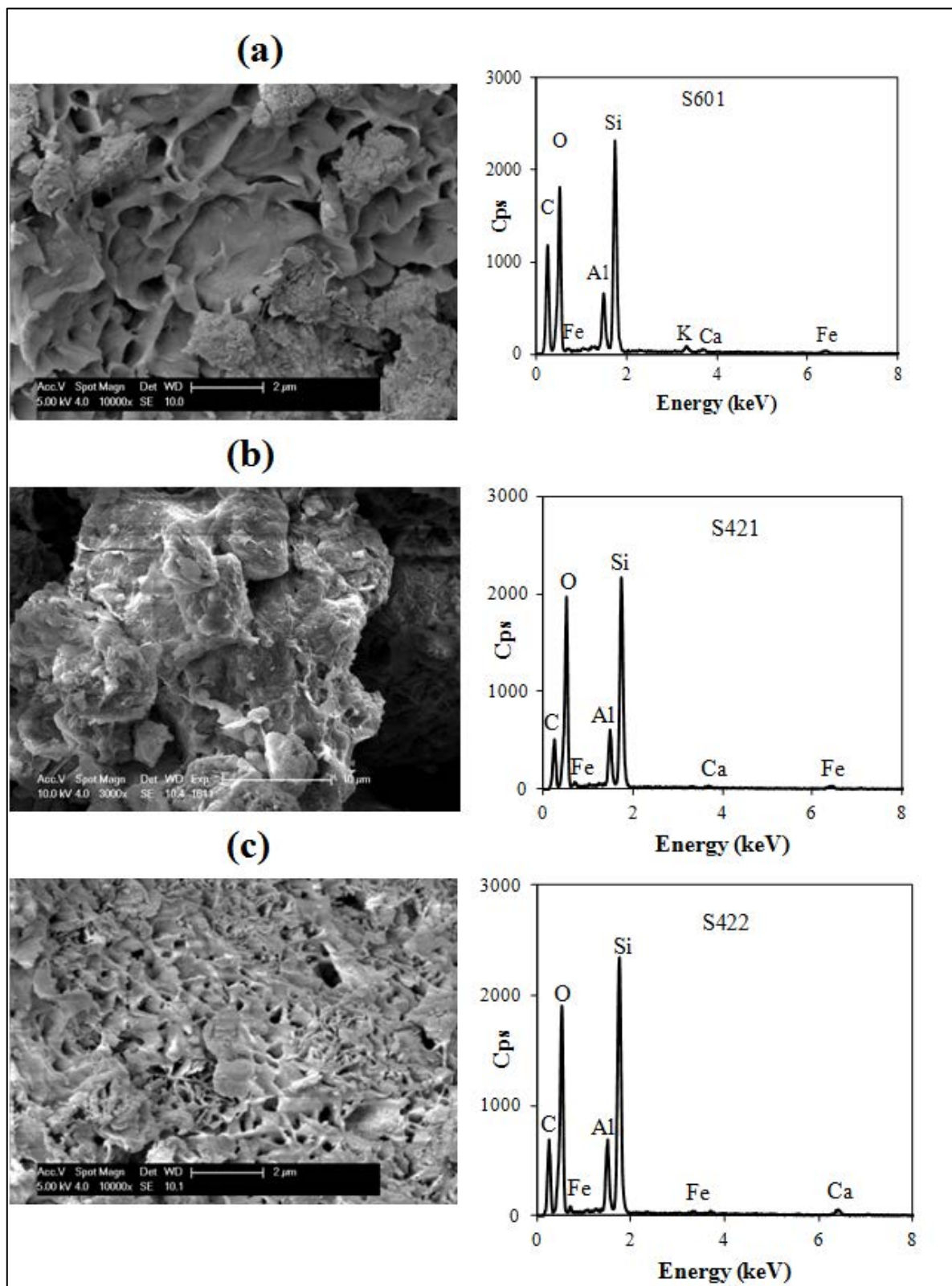


FIG. 9. Left: SEM micrographs for three $< 250 \mu\text{m}$ clay samples (S601, S421 and S422 from top to bottom) and right: their respective EDX spectra. (a) smectite with honeycomb texture, (b) wavy subhedral montmorillonite particle and (c) smectite with honeycomb texture.

Except for montmorillonite and kaolinite, the estimation of minerals contents was calculated using the equation defined by [Yvon et al. \(1982\)](#)

$$T(x) = \sum_1^n M_i \times P_i(x) \quad (1)$$

where:

- $T(x)$ is the percentage of oxide of chemical element “ x ”;
- M_i the percentage of mineral “ i ” in sample containing chemical element “ x ” and $P_i(x)$ the proportion of element “ x ” in mineral “ i ” (calculated from the ideal mineral formula).

This calculation is based on the results of qualitative mineralogical identification (XRD, FTIR, DSC-TG analyses) and the chemical composition of the samples reported in Table 1. The quantification of montmorillonite and kaolinite contents was performed on the basis of XRD and according to the method of [Cook et al. \(1975\)](#). First, the relative content of clay minerals (montmorillonite + kaolinite) was estimated from the relative intensity of the peak at 4.47 Å on the XRD patterns obtained for the < 250 µm fractions. In a second step an estimate of the relative proportion of montmorillonite and kaolinite was obtained from the relative (001) reflection intensities for these two clay minerals on the XRD patterns obtained for the < 2 µm fractions (glycolated specimens). The related error for this calculation is estimated at 10 %.

The mineralogical reconstitution scheme was done as follow:

- K_2O , Na_2O and CaO were used for feldspars (detected by XRD);
- TiO_2 , was used for ilmenite (detected by XRD);
- Al_2O_3 , was used for heulandite (detected by XRD) after subtracting the contribution for kaolinite, montmorillonite and feldspars ;
- SiO_2 was converted into cristobalite (detected by XRD) after subtracting the contribution from montmorillonite, feldspars, kaolinite and heulandite. The result of mineralogical composition for all samples is given in Table 2. Montmorillonite is the mineral present in the highest abundance (minimum 44 %), followed by cristobalite and feldspar. Note that these materials are heterogeneous and a size fractionation may be requested for specific mono-mineral applications (e.g. enrichment in montmorillonite for pharmaceutical or cosmetic applications).

Samples	% Minerals					
	Montmorillonite	Kaolinite	Cristobalite	Feldspars	Ilmenite	Heulandite
S115	59	-	38	8	1	-
S421	54	2	32	18	1	-
S422	56	1	30	18	1	-
S423	51	2	30	21	1	-
S601	48	-	19	25	1	14
S602	44	-	36	24	1	-

TABLE 2. Mineralogical composition of the clay < 250 µm samples.

Physical properties

The specific surface areas (SSA), the pore volume (V_p) and micropore volume (V_{mic}) of the different clay materials investigated are reported in Table 3. The specific surface area of the samples ranges between 33 and 90 m^2/g . For all the samples, except for S601 and S602, the SSA increases with the amount of montmorillonite (Tables 2 and 3). For samples S601 and S602, the difference may be due to variable proportion of external and internal SSA as suggested by (Dogan et al., 2007). It should also be noted that the presence of impurities or the weathering alteration may also affect the specific surface area of the samples.

Samples	SSA (m^2/g)	V_p (cm^3/g)	V_{mic} (cm^3/g)	C.E.C (meq/100g)	pH
S115	90	0.129	0.040	42	5.5
S421	68	0.128	0.031	46	4.9
S422	74	0.141	0.033	42	5.1
S423	33	0.132	0.031	38	5.4
S601	55	0.084	0.023	41	5.4
S602	72	0.141	0.032	46	5.4

TABLE 3. (SSA) specific surface area, (V_p) pore volume and (V_{mic}) micropore volume resulting from the analysis of nitrogen adsorption-desorption isotherms, CEC and pH of clay < 250 µm samples.

The nitrogen adsorption-desorption isotherms at 77 K are similar for all samples (3 samples reported in Fig. 10). The sharp N_2 -adsorption isotherm corresponds to the type II according to the IUPAC recommendation (Sing et al., 1985). The total pore volume (V_p) was

estimated from the volume of nitrogen held at the relative pressure $P/P_0=1$. A micropore volume value (V_{mic}) was evaluated from the volume absorbed between the relative pressure of 0.10 and 1.0. The values of pore volumes range between 0.084 to 0.141 cm^3/g and the micropore volume values range from 0.023 to 0.04 cm^3/g .

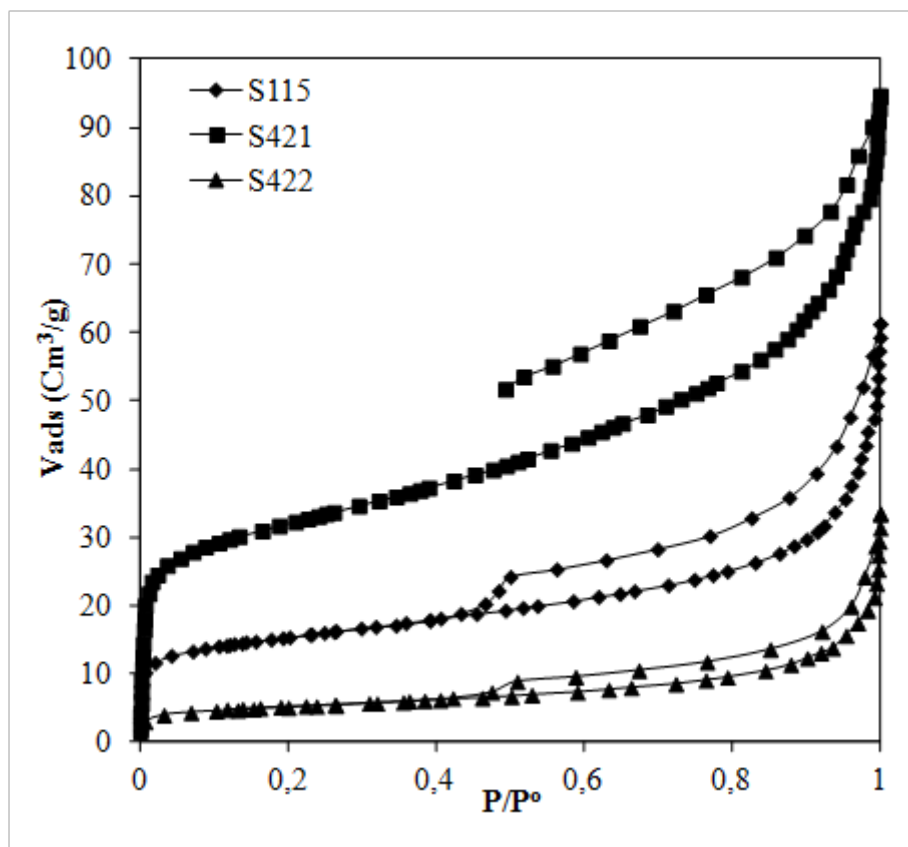


FIG. 10. Selected N_2 adsorption-desorption isotherms for three $< 250 \mu\text{m}$ clay samples.

The ammonium acetate method revealed CEC values ranging between 38 and 46 meq/100g (Table 3). These values are lower than the typical CEC for pure montmorillonite (60-120 meq/100g). However these CEC values are consistent with the relative proportion of montmorillonite ranging between 44 and 59% (Table 2). Finally, the pH values (Table 3) range between 4.9 and 5.5, indicating an acid character of the clays and the absence of carbonates.

Genesis of the clay materials

The clayey materials studied in Sabga are located in both the lower and higher parts of landscape with altitude varying between 1500 and 1700 m, along hilly slopes and road cutting. The mineral paragenesis (montmorillonite + cristobalite + feldspar \pm kaolinite \pm ilmenite \pm heulandite) indicates that the smectitic clays are closer to surrounding trachyte as parent rocks. This paragenesis also indicates that the clay formation is still going on, with alteration of feldspars. Moreover, no hydrothermal indicator mineral as pyrite, hydroxyl apatite or any ore associated minerals was fund ([Njoya et al., 2006](#)). It can be concluded that the smectitic clay deposits of Sabga are from residual origin. The exploitable thickness varies from 2 to more than 4 m, with a maximum of 1 m lateritic cover, indicating advanced argilic alteration and a well drained hilly environment.

These results are close to those obtained at the surrounding areas. Indeed considering the parent rocks, they are similar to the residual clay materials of the bentonite group of the North West Region at Santa, Bambili and Mbengwi ([Thiobault & Le Berre, 1985](#)), and at Baba ([Njopwouo, 1993](#)), formed from the weathering of trachytic and trachy- phonolitic rocks on a well drained hilly environment. These results can also be compared to the composition of the white bentonite in San Juan Province, Argentina made of montmorillonite and cristobalite as major minerals ([Allo & Murray, 2004](#)). However Sabga clays differ from the quartz-rich smectitic clays (i.e., vertisol) of the northern part of Cameroon formed in a confined environment under a Sahelian climate ([Eno Belinga et al., 1977, Kamga et al., 2001](#)).

CONCLUSION

The results of this study show that clay deposits from Sabga in North-west Cameroon mainly consist of montmorillonite with variable amounts of accessory minerals such as cristobalite, feldspars, ilmenite and heulandites. Trace of kaolinite was also present in three clay samples (S421, S422 and S423) in addition to the montmorillonite. The chemical compositions of these natural clay-rich samples are of SiO_2 (66-69%), Al_2O_3 (13-16%) and Fe_2O_3 (2-7 %), with minor amounts of K_2O , CaO , Na_2O , MgO and TiO_2 .

From the mineralogical and physicochemical characteristics of these clay-rich materials, they can be found uses in many classical applications of clay materials such as the retention of heavy metal, oil refining, foundry bonding, civil engineering, waste disposal, cosmetics, adhesives, catalysts, paints, inks and in agriculture. Although natural montmorillonite can be used in many applications, it is also of interest to improve its capability. Hence acidic activation may be of great interest in the use of the material as refining agent of oils or color removal from other liquids. Preparation of sodium-montmorillonite from Sabga deposit is also of interest due to the technical applications of the Na-montmorillonite ([Hartwell, 1965](#)). Organoclay preparation is another aspect of modification that is of interest in polymer-clay composites preparation.

In the framework of valorization of Cameroonian local resources, the actual uses that are to be considered in short and medium term are oil refining, waste water treatment and civil engineering.

Acknowledgements

The authors are grateful to Erasmus Mundus ACP for a PhD fellowship for the stay of Jacques Richard Mache at the University of Liege (Belgium). They gratefully appreciate the help of Fabien Thomas (Laboratoire Environnement et Minéralurgie, Nancy, France).

REFERENCES

- Allo W.A. & Murray H.H. (2004) Mineralogy, chemistry and potential applications of a white bentonite in San Juan province, Argentina. *Applied Clay Science*, **25**, 237-243.
- Brigatti M.F., Galan E. & Theng B.K.G. (2006) Structure and mineralogy of clay minerals. Pp. 309-377 in: *Handbook of Clay Science* (F. Bergaya, B. K.G. Theng & G. Lagaly, editors), Elsevier, 1, Oxford.
- Brunauer S., Deming L.S. & Teller E. (1940) On a theory of Van der Waals adsorption of gases. *Journal of the American Chemical Society*, **62**, 1723-1732.
- Cook H.E., Johnson P.D., Matti J.C. & Zemmels I. (1975) Methods of sample preparation and X-ray diffraction data analysis in X-ray mineralogy laboratory. Pp. 997–1007 in: *Initial Reports of the DSDP* (A.G. Kaneps, editor). Printing Office, Washington, DC.
- Dogan M., Dogan A.U., Yesilyurt F.I., Dogan A., Buckner I. & Wurster D.E. (2007) Baseline studies of the Clay Minerals Society special clays: specific surface area by the Brunauer, Emmett, Teller (BET) method. *Clays and Clay Minerals*, **55**, 534-541.
- Dohrmann R. (2006) Cation exchange capacity methodology II: A modified silver-thiourea method: *Applied Clay Science*, **34**, 38-46.
- Eno Belinga S.M., Ekodeck G.E., Njeng E. & Ossah N.H. (1977) L'altération argileuse des roches basiques de la région de Maroua Nord-Cameroun. *Annales de la Faculté des sciences, Université de Yaoundé*, **23**(24), 65-77.
- Fowden L., Barrer R.M. & Tinker R.B. (1984) Clay Minerals: Their Structure, Behaviour and Use. *Philosophical Transactions of the Royal Society of London, Series A, Mathematical and Physical Sciences*, **311**, 219-432.
- Graetsch H. (1988) Structural characteristics of opaline and microcrystalline silica minerals. pp. 209-232 in: *Silica. Physical Behavior, Geochemistry and Materials Applications. Reviews in Mineralogy* (P.J. Heaney, C.T. Prewitt & G.V. Gibbs, editors). Mineralogical Society of America, 29, Washington, DC.
- Gregg S.J. & Sing K.S.W. (1982) Adsorption, Surface Area and Porosity, Academic Press, London.
- Hajjaji M., Kacim S. & Boulmane M. (2001) Mineralogy and firing characteristics of clay from the valley of Ourika (Morocco). *Applied Clay Science*, **21**, 203-212.
- Hartwell J.M. (1965) The diverse uses of montmorillonite. *Clay Minerals*, **6**, 111-118.

- Holtzapffel T. (1985) Les Minéraux Argileux : Préparation, Analyse diffractométrique et Détermination, pp. 77-109. Société Géologique du Nord, France.
- Hradil D., Grygar T. S., Kova M. H., Ka P.B., Lang K., Schneeweiss O.I. & Chva' Tal M. (2004) Green earth pigment from the Kadan region, Czech Republic: use of rare Fe-rich smectite. *Clays and Clay Minerals*, **52**, 767–778.
- Hussin F., Aroua M.K. & Daud W.M.A. (2011) Textural characteristics, surface chemistry and activation of bleaching earth. *Chemical Engineering Journal*, **170**, 90-106.
- Kamga R., Nguetnkam J.P. & Villieras F. (2001) Caractérisation des argiles du nord Cameroun en vue de leur utilisation dans la décoloration des huiles végétales. Pp 247-257 in : *Actes de la première conférence sur la valorisation des matériaux Argileux au Cameroun* (C. Nkoumbou & D. Njopwouo, editors). Yaoundé, Cameroun.
- Kamgang P., Njonfang E., Chazot G. & Tchoua F. (2007) Géochimie et géochronologie des laves des monts Bamenda (ligne volcanique du Cameroun). *Comptes Rendus Geosciences*, **339**, 659-666.
- Kamgang P., Njonfang E., Chazot G. & Tchoua F. (2008) Geochemistry and geochronology of mafic rocks from Bamenda Mountains (Cameroon): Source composition and crustal contamination along the Cameroon Volcanic Line. *Comptes Rendus Geoscience*, **340**, 850-857.
- Kloprogge J.T., Komarneni S. & Amonette J.E. (1999) Synthesis of smectite clay minerals: A Critical Review. *Clays and Clay Minerals*, **47**, 529-554.
- Komarneni S. & Breval E. (1985) Characterization of smectites synthesised from zeolites and mechanism of smectite synthesis. *Clay Minerals*, **20**, 181-188.
- Lim C.H. & Jackson M.L. (1986) Expandable phyllosilicate reactions with lithium on heating. *Clays and Clay Minerals*, **34**, 346–352.
- Mackenzie R.C. (1970) Simple phyllosilicate based on gibbsite and brucite-like sheets. Pp. 498-537 in: *Differential Thermal Analysis of Clays* (R.C. Mackenzie, editor). Academic Press, New York.
- Madejová J., Komadel P. & Cicel B. (1994) Infrared study of octahedral site populations in smectites. *Clay Minerals*, **29**, 319-326.
- Madejová J., Bujda'k J., Janek M. & Komadel P. (1998) Comparative FT-IR study of structural modifications during acid treatment of dioctahedral smectites and hectorite. *Spectrochimica Acta Part A*, **54**, 1397-1406.

- Madejová J.(2003) FTIR techniques in clay mineral studies. *Vibration Spectroscopy*, 31,1-10
- Malla & Douglas. (1987) Problems in identification of montmorillonite and beidellite. *Clays and Clay Minerals*, **35**, 232-236.
- Moore D.M. & Reynolds R.C. (1989) X-ray Diffraction and the Identification and Analysis of Clay Minerals, pp.179-201. Oxford University Press, Oxford.
- Moenke H.H.W. (1974) Silica, the three-dimensional silicates, borosilicates and beryllium silicates. Pp. 365-382 in: *The infrared spectra of minerals* (V.C. Farmer, editor). Mineralogical Society, London.
- Murray H.H. (1995) Clays in industry and the environment. Pp. 49-55 in: *Clays Controlling the Environment, Proceedings of the 10th International Clay Conference, Adelaide, Australia, 1993* (G.J. Churchman, R.V. Fitzpatrick & R.A. Eggleton, editors). CSIRO Publishing, Melbourne, Australia.
- Njopwouo D. (1993) Chimie, Minéralogie, Texture et comportement rhéologique des argiles comestibles au Cameroun. Pp.1-90 in: *Etudes Préliminaires* (D. Njopwouo, editor). Rapport Séjour Scientifique, France.
- Njoya A., Ekodeck G.E., Nkoumbou C., Njopwouo D. & Tchoua M. F. (2001) Matériaux argileux au Cameroun: gisements et exploitation. Pp. 13-30 in : *Actes de la première conférence sur la valorisation des matériaux Argileux au Cameroun* (C. Nkoumbou & D. Njopwouo, editors). Yaoundé, Cameroun.
- Njoya A., Nkoumbou C., Grosbois C., Njopwouo D., Njoya D., Courtin N.A., Yvon J. & Martin F. (2006) Genesis of Mayouom kaolin deposit (West Cameroon). *Applied Clay Science*, **32**, 125-140.
- Panda A.K., Mishra B.G., Mishra D.K. & Singh R.K. (2010) Effect of sulphuric acid treatment on the physico-chemical characteristics of kaolin clay. *Colloids and Surfaces A: Physicochemical and Engineering Aspects*, **363**, 98-104.
- Sing K.S.W., Everett D.H., Haul R.A.W., Moscou L., Pierotti R.A., Rouquérol J. & Siemieniewska T. (1985) Reporting physisorption data for gas/solid systems with special reference to the determination of surface area and porosity. Pure and applied Chemistry, **57**(4) 603-619.
- Thiobault P.M. & Le Berre P. (1985) *Les argiles pour brique B.R.G.M.* CRMO, 65, MINMEE, Cameroun.

- Thorez J. (2000) Cation-saturated swelling physils: an XRD revisit. Pp. 71-85 in: *Proceedings of the First Latin-American Clay Conference* (C.F. Gomes, editor). Associacao Portuguesa de Argilas, Madeira.
- Yvon J., Lietard O. & Cases J.M. (1982) Minéralogie des argiles kaoliniques des Charentes. *Bulletin de Minéralogie*, **105**, 431-437.

II.3. Mineralogical, Physicochemical Properties of smectite clays from Bana (Western Cameroon) and Preliminary test as Potential oil bleaching earth

J.R. Mache^{a, b, c,*}, P. Signing^b, J.A. Mbey^d, F. Thomas^d, D. Njopwou^b, N. Fagel^a

^a UR AGES Argiles, Géochimie et Environnements sédimentaires, Département de Géologie, Université de Liège, B18, Allée du 6 Août, B-4000 Liège, Belgique

^b Laboratoire de Physico-chimie des Matériaux Minéraux, Département de Chimie Inorganique, Université de Yaoundé 1, B.P. 812 Yaoundé, Cameroun

^c Mission de Promotion des Matériaux Locaux, B.P 2396 Yaoundé, Cameroun

^d Laboratoire Environnement et Minéralurgie, UMR 7569 CNRS-Université de Lorraine, 15 Avenue du Charmois, B.P. 40. F-54501, Vandœuvre-lès-Nancy Cedex, France

* Corresponding author: e-mail: jamache@yahoo.fr ; Tel: +3243662229;
Fax: +3243662029

ABSTRACT

In this study, six clay samples collected from Bana (West Region of Cameroon) were investigated for their physical, chemical, mineralogical and thermal behavior. The purpose was to evaluate their potential use as raw materials in bleaching palm oil. Chemical analysis, X-ray diffraction and infrared spectroscopy results indicated that these materials are composed mainly of montmorillonite (70-77%), mica (5-9%), kaolinite (2-9%). Accessory minerals such as: quartz, anatase and feldspars are also present. These materials exhibited Cation Exchange Capacity (CEC) from 50 to 60 meq/100g and have specific surface area of 50 to 68 m²/g. For electrophoretic behavior of the samples, the mobility decreases with increasing pH between 3.0 and 4.5. Above a pH value of 4.5, the mobility remains constant with an average value of 3.2 μm.s⁻¹.v⁻¹.cm⁻¹. This phenomenon is due to the presence of non-clay minerals and kaolinite. The bleaching capacity of this natural clay is 55% for 75 minute bleaching time at 97 ±1°C. This bleaching power of smectite-rich clays from Bana can be enhanced by chemical treatment with mineral acids.

Keywords: Smectite, mineralogy, thermal analysis, electro-kinetics, bleaching, palm oil

1. INTRODUCTION

Smectites are widely spread in nature as the main components of bentonite. Montmorillonite is the most common mineral of the smectite group classified into sodium or calcium types depending on dominant exchangeable ion (Zhansheng et al. 2006). It may contain kaolinite, micas, feldspars, cristobalite and quartz such as additional clay minerals and accessory minerals. Smectites, belonging to the 2:1 group of clay minerals have many industrial applications in a broad range of industry and other activities (Slávka et al., 2008; Harvey and Lagaly, 2006). They are widely used in civil engineering, as slurry cut-off walls (Garwin and Hayles, 1999), landfill sites and radioactive waste storage (Hanchar et al., 2004; Montes et al., 2005; Seki and Yurdakoç, 2007), palletizing iron ores, foundry bond clay, drilling mud, sealant, animal feed bond, agricultural carrier, cat box adsorbent, catalyst and catalyst support, adsorbent in the oil industry and for environmental protection (Bergaya et al., 1996), bleaching agents for mineral and vegetable oils (Taylor et al., 1989; Srasra et al., 1989; Christidis et al., 1997). These wide applications of smectites are strongly related to their ability to form thixotropic gels with water and also their capability to adsorb large amounts of water, a high specific surface area and cation exchange capacity (Lumdsen et al., 1995; Wu et al., 1999).

Due to its geographical location, Cameroon has large deposits of clay materials. Since three decades, numerous studies have been conducted on Cameroonian clay materials and their potential uses. These studies were carried out on talc (Nkoumbou et al., 2006, 2008), halloysite (Njopwouo and Wandji, 1982) and kaolin clays which so far represent the largest clay deposit available in Cameroon (Njopwouo and Wandji 1985; Elimbi et al., 2003; Njoya et al., 2006; Pialy et al., 2008; Ekosse, 2010). The potential uses of these clay materials have been carried out to develop ceramic products such as bricks, tiles, refractories and fine porcelain (Djangang et al., 2007, 2008; Elimbi et al., 2002; Kamseu et al., 2007; Pialy et al. 2009), geopolymmer cements (Lemougna et al., 2011; Tchakounté et al., 2012), mineral filler in rubber reinforcement and as catalyst in the polymerization of styrene (Njopwouo et al., 1988) and, most recently, in the development of nano-composite films from cassava starch and kaolin (Mbey et al., 2012).

In the framework of the valorization of Cameroonian local resources, the use of smectite clays from Cameroon as bleaching adsorbent of vegetable oils are of special interest. Some clay materials such as vertisols soil from the northern Cameroon have already been studied for this purpose (Djoufac et al., 2007; Nguenkam et al., 2008). None of the above studies

deals with smectite clays from the Western region of Cameroon. For these reasons, the search of smectite clay deposits, their characterization and potential valorization as bleaching earth of vegetable oils is very necessary.

The main objectives of this work were to characterize the clay materials from Bana (Western-Cameroon) in terms of mineralogical composition, to determine their physico-chemical properties, such as cation exchange capacity and N₂-adsorption-desorption behavior and also to evaluate their potential use in oil bleaching, which are limited to the traditional uses in therapy and consumption by women. It should be noted that only few data devoted to the geological setting of the Bana Mountains are reported in the literature. Several techniques such as X-ray diffraction (XRD), Fourier Transform Infra Red Spectroscopy (FTIR), Scanning Electron Microscopy (SEM), Thermal analyses (DTA and TGA), chemical analyses by Inductive Coupled Plasma by Atomic Emission Spectrometry (ICP-AES) and Inductive Coupled Plasma by Mass Spectrometry (ICP-MS) were used to obtain accurate informations about these clay materials. This study is a part of the wide research program whose objective is to valorize local clay materials for potential industrial applications generally with special attention in Cameroon.

2. GEOLOGICAL SETTING AND CONTEXT

The Tertiary Bana volcano-plutonic complex (5°84'E - 5°1'N) is located at the southeast of the West Cameroon Highlands, in the central part of the Cameroon Volcanic Line (CVL). It occupies an area of 4 × 7 km (ca. 55 km²) ([Keupouo et al., 2006](#)). The Bana complex forms a prominent mountainous scarp culminating at 2097 m above sea level, rising 600 m above the general level of the countryside to the south and 350 m to the northwest. This complex is bounded to the south by an elevated (up to 1500 m) crystalline basement encompassing Neoproterozoic granite and gneisses cross cut by mafic and felsic dykes. The complex consists of plutonic rocks of syenodiorite, alkalic granite and calc-alkalic granite, and volcanic rocks of alkalic rhyolite, quartz trachyte, FeO-Al₂O₃ -TiO₂ -rich rocks, transitional plagioclase – phryic basalts, benmoreite to rhyolitic welded tuffs and basanite, alkalic olivine basalt and hawaiite ([Kuepouo, 2004](#)). The average rain fall in this district is about 1300-2500 mm per year.

The clay samples were collected from two different sites. The first site is a granite saprolite road cutting profile outcropping at altitude of 1600 m. It consists of reddish lateritic soil of about 2 m thick in the top and white to yellowish granite saprolite of 18 m thick in the

lower part. The second site is an homogeneous yellowish dyke of about 0.5 m in width and about 13 m in height within the granitic rock outcropping about 1 km southern of the first site. The two clays are actually exploited by local population for therapy and consumption (geophagia). However, no scientific data (mineralogical and physico-chemical properties) has been available to ascertain if these materials are suitable for this purpose and according to their characteristics, or if other applications could be possible.

3. MATERIALS AND METHODS

The clay samples used in the present study were collected at Bana ($5^{\circ}09'00''N$, $10^{\circ}17'00''E$) in the West region of Cameroon (Fig.1). Six clay materials (named: BN25, BN35, BN45, BN61, BN81 and BN115) sampled in the field were taken by anger coring at different depth varying from 2.5 m to 11.5 m and 10 Kg of each sample was collected (Table 1). In the laboratory, all the samples were wet sieved through a size of 63 μm . Each sample was air-dried after decantation; the retained samples were quartered to ensure a representative sample. All the analyses were performed on the $< 63 \mu\text{m}$ fraction. The clay fraction ($< 2 \mu\text{m}$) of the Bana clay sample was obtained by sedimentation according to the Stocke's law. This fraction was used for electrokinetic and oriented preparation in X-ray diffraction. The crude palm oil (CPO) used for this present study was provided by SOCAPALM Co (Cameroon).

Sample	Depth (m)	Color	Moisture (%)	Particle size distribution (%)	
				Clay ($< 2 \mu\text{m}$)	Silt ($2- 63 \mu\text{m}$)
BN25	2.5	Yellow	10.2	9.0	91.0
BN35	3.5	Pale -Yellow	10.2	7.8	92.1
BN45	4.5	Pale -Yellow	10.5	9.9	90.0
BN61	6.1	Pale -Yellow	10.5	9.5	90.5
BN81	8.1	Olive - Pale	11.5	8.6	91.4
BN115	11.5	Olive - Pale	11.5	7.5	92.5

Table 1. Characteristics of the clay materials.

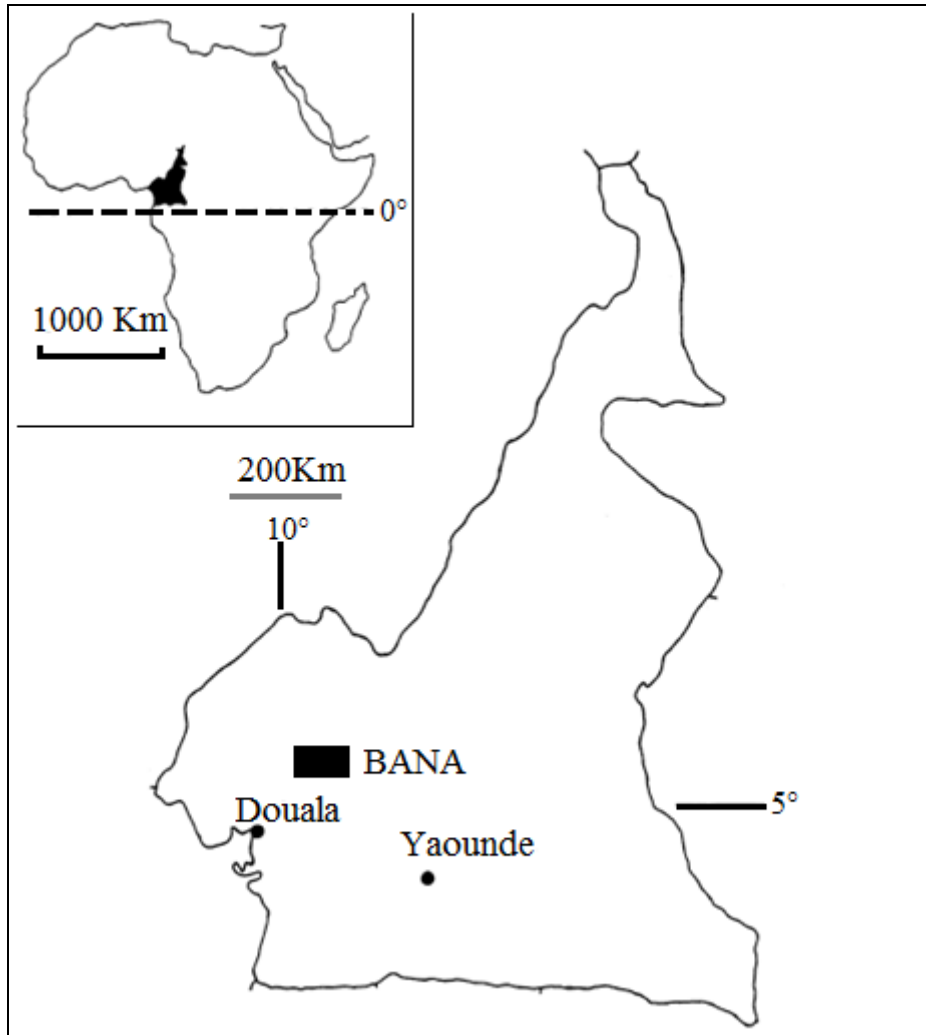


Figure 1: Location of Bana, Western part of Cameroon

The XRD analysis was done on a Bruker AXS model D8 Advance diffractometer, with Cu-K α radiation, under 40 kV and 30 mA operating conditions, to identify the mineralogical phases of the bulk clayey samples. The XRD patterns on the < 63 μm fraction were recorded between 2° and 70° using a step scan 0.02° and a step time of 3 seconds. Additional XRD measurements were made on oriented aggregates (Moore and Reynolds, 1989) and the data were recorded between 2° and 30° (2 θ) using a step scan 0.02° and a step time of 0.6 s. These oriented aggregates were subjected to three successive treatments: air drying, glycolation and heating to 500°C for 4 hours, in order to confirm the type of clay mineral phases. The Greene-Kelley test modified from Lim and Jackson (1986) was used to distinguish between octahedral and tetrahedral negative layer-charge deficiencies in the smectites. The test

consists of saturating the < 2µm clay fractions with 2 M LiCl solution overnight. The Li-exchanged fractions were then rinsed with demineralized water, and oriented aggregates have been prepared on glass slides. The XRD analyses on oriented clay fractions were conducted in sequence on the air-dried slide (N), heated at 300°C (H300, 2H), and finally overnight glycerol solvated (Gl). A d spacing (001) reflection at 9.6 to 10 Å, is indicative of montmorillonite (octahedral negative layer charge), while a spacing at 16.7 to 17.7 Å indicates beidellite (tetrahedral negative layer charge).

Chemical analyses were carried out at the *Service d'Analyse des Roches et des Minéraux* (SARM Nancy-France) using emission spectrometry. The samples were molded in fused lithium borate (LiBO_2) and dissolved in nitric acid. The major elements were determined by Inductive Coupled Plasma by Atomic Emission Spectrometry (ICP-AES), while trace and rare earth elements Inductive Coupled Plasma by Mass Spectrometry (ICP-MS). Relative analytical uncertainties were estimated at 1-5% for major elements except for P_2O_5 (10%). They were up to 5% for most of the trace element concentrations except for Cu (10%). However, uncertainty was high (>10%) for any trace element displaying a low concentration (<0.1ppm).

Infra red spectra were recorded from 4000 cm^{-1} to 600 cm^{-1} range with a resolution of 4 cm⁻¹, using accumulation of 200 scans, in diffuse reflection mode on KBr pellets made of 15 % clay in oven dried using a Bruker Fourier Transform Interferometer IFS 55.

Thermal analyses (DTA and TGA) were carried out at the Groupe d'Etude des Matériaux Hétérogènes of the Ecole Nationale Supérieure de Céramique Industrielle (Limoges, France). The temperatures investigated ranged from 20 to 1200 °C in an air atmosphere, with continuous recording. The heating rate was $5^\circ\text{C}.\text{min}^{-1}$.

Scanning electron microscopy (SEM) images were performed on a Philips microscope model XL30 to determine morphological and mineralogical features of the samples. The images were obtained while operating in secondary electron detector at a voltage of 10 kV. The samples were dispersed over a sample holder and gold-sputtered for analysis.

The mobility was measured by micro-electrophoresis using a Zetaphoremeter V by CAD Instrumentation (LEM, Nancy), in 10^{-3} M NaNO_3 background in a pH range from 3 to 10.

The specific surface areas and total pore volume of the samples were determined from nitrogen adsorption and desorption isotherms at 77 K, obtained from a Carlo Erba Sorptomatic 1990 volumetric device, after outgassing the samples overnight at room

temperature at a pressure lower than 10^{-4} Pa ([Gregg and Sing, 1982](#)). The specific surface area (SSA) was calculated from adsorption data by applying the Brunauer-Emmet-Teller (B.E.T) method.

Cation exchange capacities (CEC) were measured using cobaltihexamine $[\text{Co}(\text{NH}_3)_6\text{Cl}_3]$ as exchangeable ions. The amount of cobaltihexamine fixed by the solid phase was determined using UV-visible spectroscopy. The displaced cations were determined by atomic absorption spectrometry (Perkin-Elmer 1100B). The equilibrium pH of clay suspensions were measured using an analytical radiometer TIM 845.

For the bleaching experiment, 10 g of oil was placed in 300 mL jacketed glass reactor equipped with water circulation thermostated at the predetermined temperature, that is 80°C, 90°C and 97°C. When the content of reactor had reached the required temperature, usually in less than 20 minutes, a known amount of clay (% by mass of the palm oil) was added to the reactor and the mixture was stirred continuously during the desired time ranging from 5 to 120 minutes. The treated oils were filtered using Whatman no.1 filter paper and the absorbance of the crude and bleached oils were determined spectrophotometrically at 449 nm (SHIMAZU UV PC 2100 absorption spectrophotometer) by diluting 0.05g of bleached oil in 5 ml of acetone (analytical grade, Merck). The bleaching capacity of Bana clay was expressed as follow:

$$\text{Bleaching capacity} = 100 \times ((A_0 - A) / A_0)$$

Where A_0 and A are the absorbance of the crude and bleached oil, respectively.

4. RESULTS AND DISCUSSION

4.1. Mineralogical composition

The XRD patterns of six clay samples show a broad basal reflection d_{001} , ranging from 13.50 to 14.10 Å indicating the presence of smectite ([Fig.2](#)). The reflection (020 or 110) at 4.47 Å is notably broad, indicating a large crystallite size and/or a mixture of different water-layer thicknesses where the two water-layer structures appear to dominate. The (060) reflection at 1.49-1.50 Å for all samples indicates that the smectite was characterized as a dioctahedral smectite ([Moore and Reynolds, 1987; Emmerich et al., 2009](#)). Mica (9.48 Å) and kaolinite (7.22 Å) are the mineral phases associated to the smectite. In all samples, quartz (3.34 Å), anatase (3.51 Å) and K-feldspars (3.21-3.24 Å) are coexisted as accessory minerals.

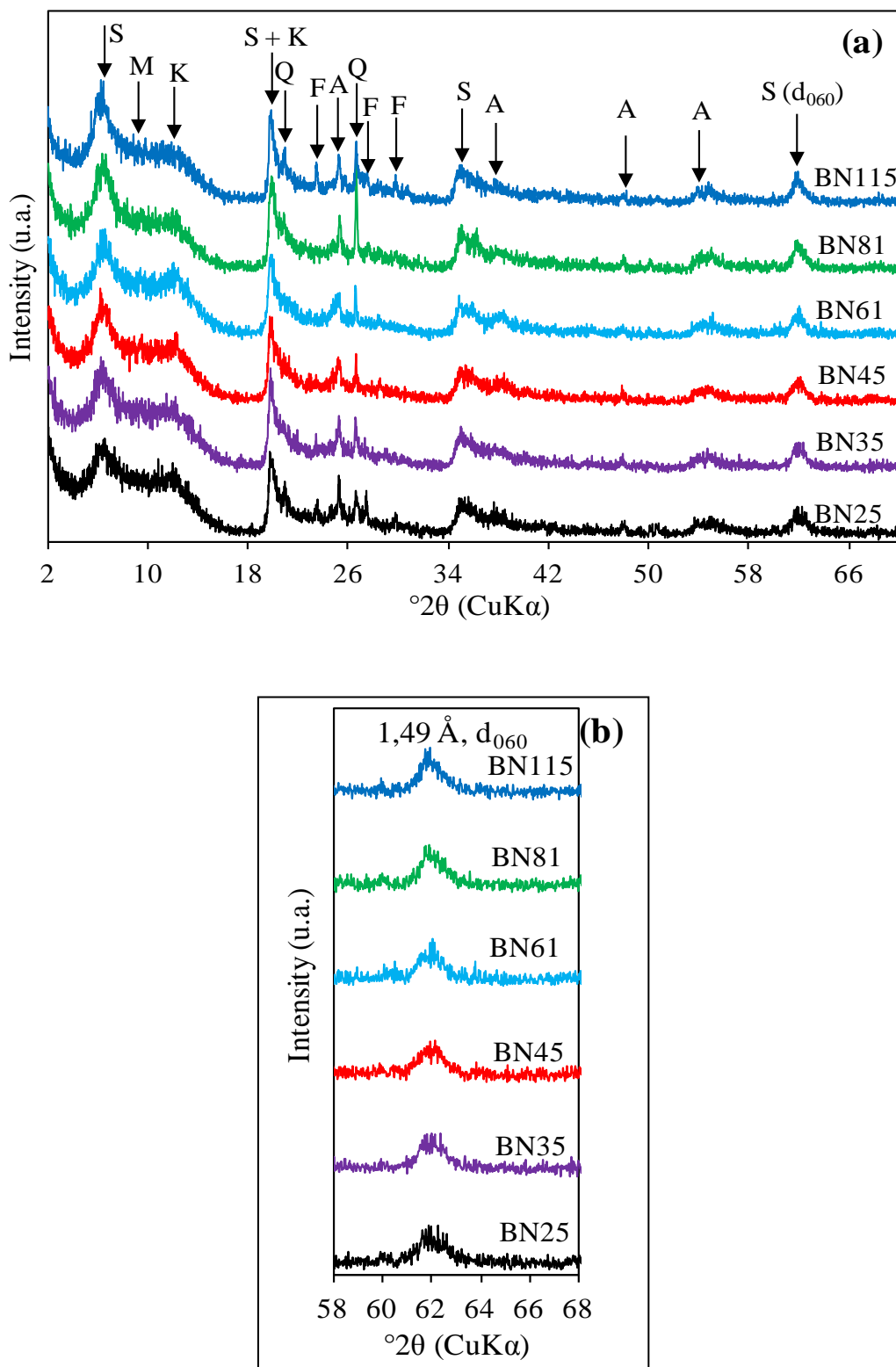


Figure 2: XRD patterns of randomly oriented samples of clays from Bana.

Sm: smectite; M: mica; Kln: kaolinite; Qtz: quartz; Fps: feldspars

The corresponding X-ray diffractograms of oriented aggregate of the clay fraction (e.g. sample BN81) on glass slide, corresponding to the specimen that has been air-dried, saturated with ethylene glycol and heated at 500°C is presented in Fig.3. The basal spacing of smectite expanded from ~15.0 Å to ~16.7 Å after saturation with ethylene glycol, and collapsed to ~9.8 Å after heating at 500°C, confirming the presence of a swelling clay mineral (Holtpzapffel, 1985; Wolters et al., 2009; Moraes et al., 2010). The inability of all samples to re-expand beyond 9.8 Å with glycerol after Li-saturation and heated treatment at 300°C, indicates that these smectite are montmorillonite with a layer charge origin located in the octahedral sheet. According to the Greene- Kelly test, this charge is neutralized by the migration of Li⁺ ions into empty sites of the dioctahedral sheet due to divalent cation substitution (Jaynes and Bigham, 1987; Malla and Douglas, 1987; Hradil et al., 2004).

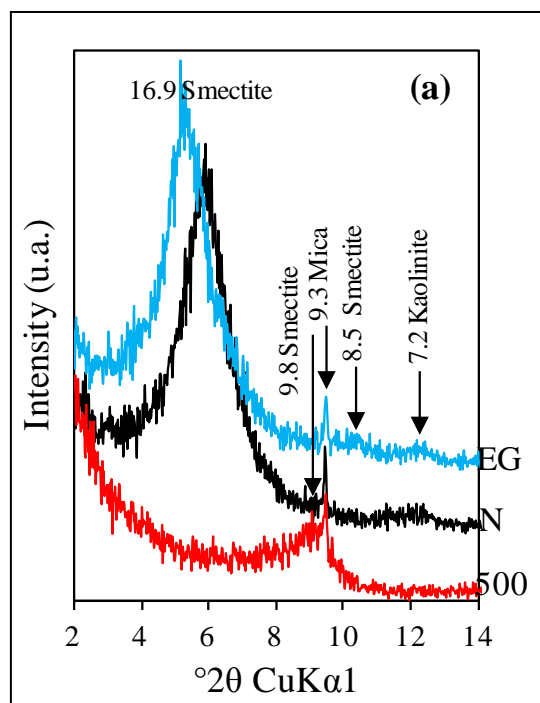
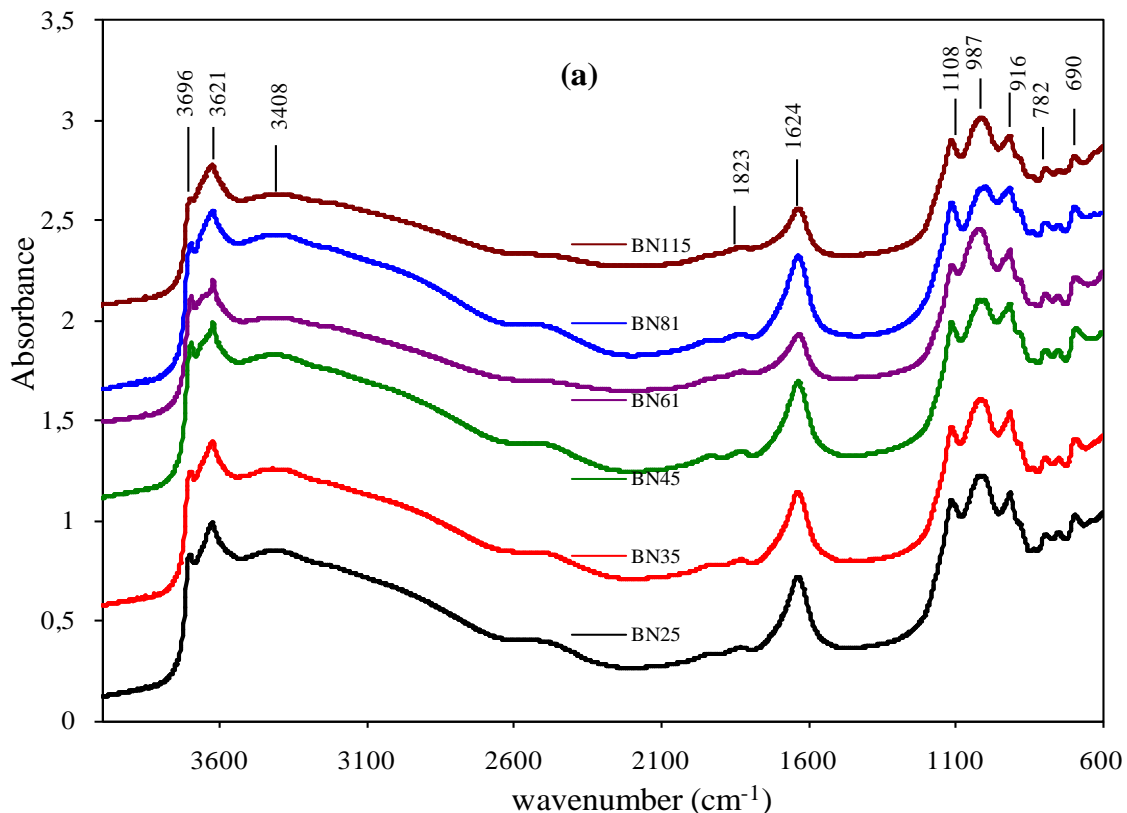


Figure 3: XRD patterns of the oriented $< 2 \mu\text{m}$ fraction the clay sample: (a) air-dried (N), ethylene glycol (EG), and heated (500); (b)

The mineralogical composition of the $< 63 \mu\text{m}$ fraction samples, which was found from X-ray diffractograms, was determined by using its characteristic reflections (001). It consists of predominantly montmorillonite (70-77%) and substantial amounts of mica (5-9%), kaolinite (2-9%), quartz (1-4%), anatase (2%) and K-feldspars (1-6%) (Table 2).

The FTIR spectra of the < 63 μm fraction samples are showed in Fig 3. The spectra for all samples show a band at 3621 cm^{-1} , corresponding to stretching vibrations of AlAlOH or AlMgOH in smectite. The broad bands around 3408 and 1624 cm^{-1} are due to the stretching and bending vibration of adsorbed water, respectively (Farmer, 1974). However, lattice OH-stretching vibrations of samples (BN25, BN35, BN81 and BN115) are broader than that of samples BN45 and BN61. The bands at 916 cm^{-1} are attributed to an Al-OH-Al bending vibration (Madejovà et al., 1992). The absorbency at 3621 and 916 cm^{-1} confirms the dominant presence of dioctahedral smectite with (Al-Al-OH and Mg-OH-Al) stretching and bending bands. The weak band at 3696 cm^{-1} corresponds to Al-OH stretching vibration of kaolinite (Famer and Palmeri, 1975), this result confirms the presence of kaolinite detected by X-ray diffraction. In the spectra of all samples, the band at 1108 cm^{-1} and the broad shoulders at 987 cm^{-1} were observed, these two bands correspond to Si-O stretching vibrations in smectite and those around 690 cm^{-1} are due to the bending mode of the same vibrations. The weak bands observed around 782 cm^{-1} for the six samples may be related to quartz (Madejovà and Komadel, 2001), which is in good agreement with the XRD results.



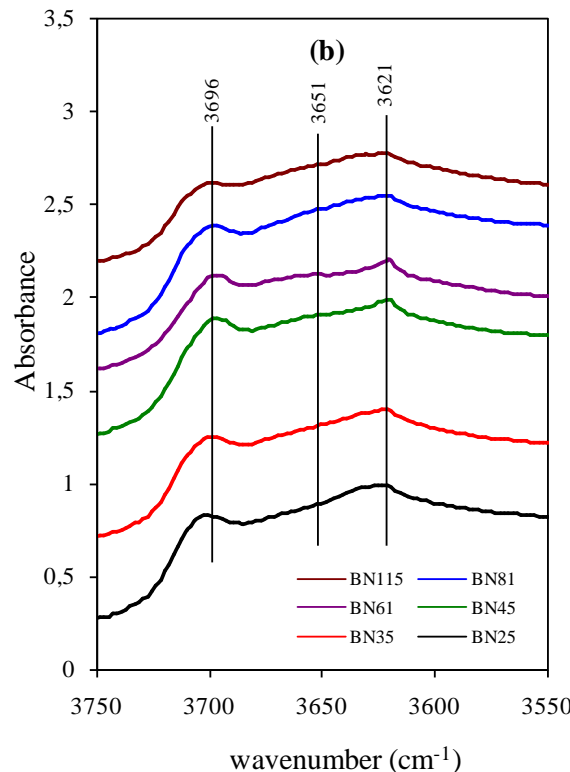
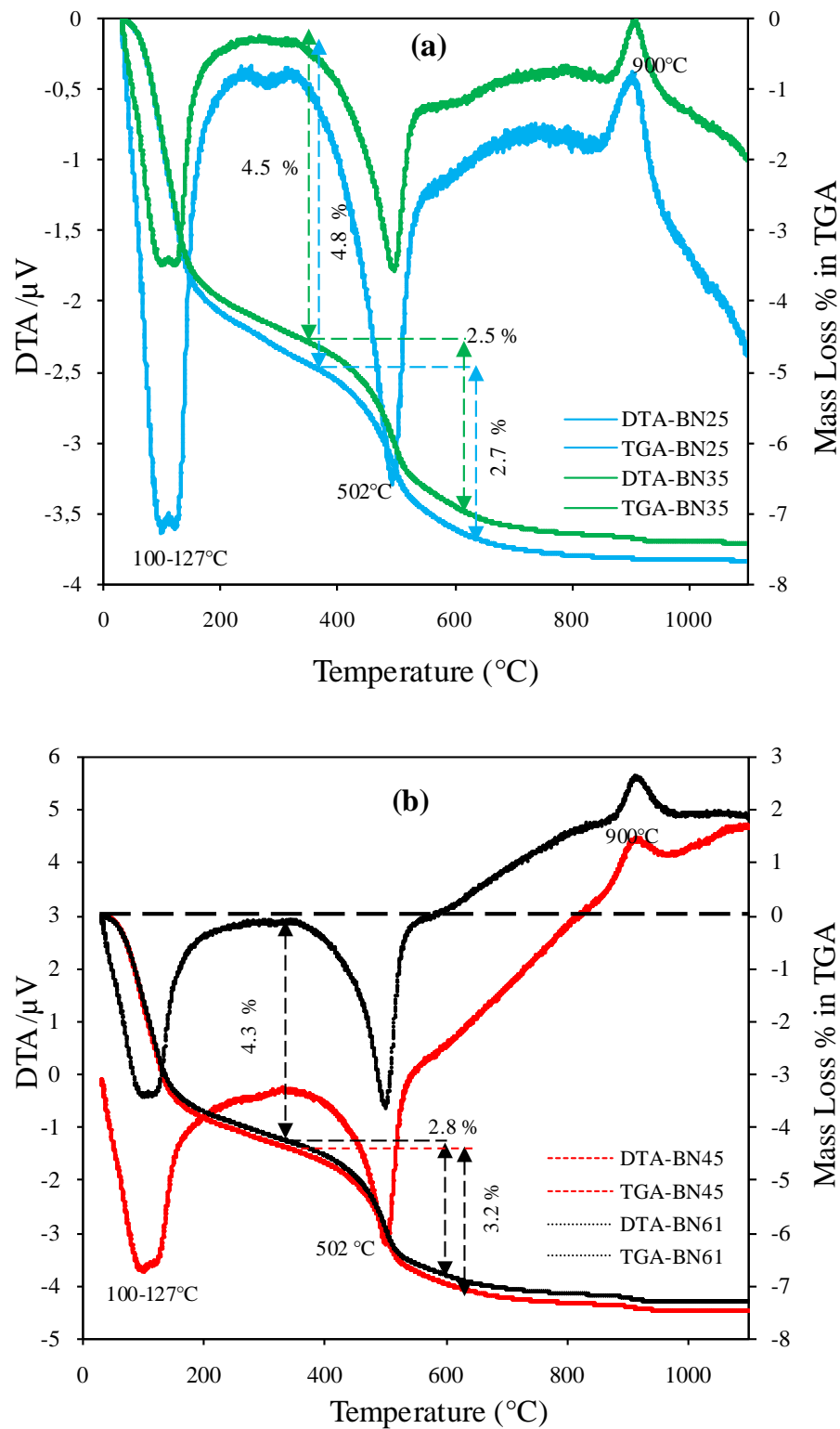


Figure 4: Infrared spectra of the clay samples: (a) complete spectrum; (b) OH stretching domain.

The IR spectra of all samples shown in Fig.4 prove some similarity in terms of chemical composition and provided further information on mineralogical composition of the samples. The dominant clay mineral is dioctahedral smectite in all samples. The weak intensity band of kaolinite reveals the low content of this clay mineral associated with smectite. The results of IR spectroscopy are in accord with the XRD analysis. No substantial differences in mineralogical phases among the six samples collected from Bana.

The TGA curves (Fig.5) show two well-defined weight loss regions. The first region observed between 25 and 350 °C corresponds to the mass loss approximately 5 %, which may be due to water physisorbed, adsorbed onto the external surface or hydration water, coordinated to exchangeable interlayer cations and adsorbed between the clay mineral layers (Moraes et al., 2010). The presence of water is corroborated by the bands assigned to the O-H stretching and angular deformation vibrations of H-O-H in residual hydrated water within the interlayer space seen at 1624 and 3408 cm⁻¹ in the IR spectra of the six samples.

The mass losses due to dehydroxylation, according to the reaction $2(\text{OH}) \rightarrow \text{H}_2\text{O} + \text{O}$ observed in the second region (400-750 °C) did not vary dramatically; these mass losses range between 2.4-3.2 %.



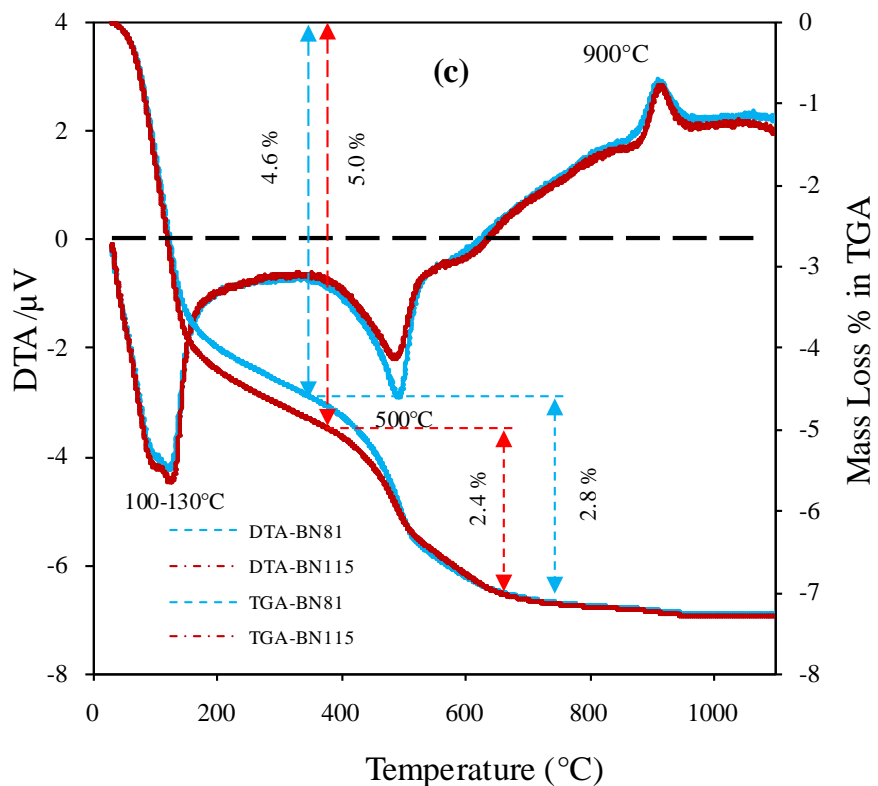


Figure 5: DTA and TGA curves of the clay samples.

The DTA curves of the six samples studied show two sharp endothermic peaks. The first endothermic peak, characteristic of water desorption-dehydration is ranging from 100 to 130 °C; a second endothermic peak, ranging from 450 to 600 °C is caused by dehydroxylation (Fig.5). The lower dehydroxylation temperature observed at (500-502 °C), may be related probably to the Fe_2O_3 content and the larger Fe content in the octahedral site in the smectite structure (Aranha Da Paz et al., 2012). Brigatti (1983) observed the same lower dehydroxylation temperature, which is typical of smectite with high iron content, iron reduces the thermal stability of 2:1 clay minerals according to the reduced bond energy ($\text{Mg-OH} > \text{Al-OH} > \text{Fe-OH}$); this reduction in stability is corroborated by the presence of 3620 cm^{-1} band in the IR spectra that is assigned to the OH stretching of these groups (Wolters and Emmerich, 2007; Moraes et al., 2010). A final double peak (endo-exothermic) corresponds: the first around 800°C is related to the structure destruction while the second at 900°C is attributed to a new phase formation (recrystallization) (Carty et al., 1998; Pialy et al., 2008; Aranha Da Paz et al., 2012).

The thermal behavior of the materials studied revealed closer similarities, confirming the results obtained by X-ray diffraction and IR spectroscopy on the mineralogical composition.

Scanning electron microscopy (SEM) was used to provide further features on morphology of the samples studied. Fig.6 shows that the dioctahedral smectite (montmorillonite), which is the dominant clay mineral, has the form of flakes, honeycomb texture or wavy subhedral form. [Christidis et al \(1995\)](#) show that the honeycomb texture forms of montmorillonite are due to dehydration of the specimens under vacuum. Crystals or grains of iron and titanium (Fig.6), respectively, were found in the materials, probably contained in the mineral phases, which corroborate the results of X-ray patterns, confirming the presence of smectite and anatase, two minerals that have iron and titanium respectively.

Based on the results given by X-ray diffraction, Infra-red spectroscopy, thermal analysis and scanning electron microscopy, the clays studied show clearly that the dioctahedral smectite (montmorillonite) is recognized as the dominant mineral associated with kaolinite, mica and some impurities such as quartz, feldspars and anatase. Also, these six clay samples present a similar behavior in terms on mineralogical composition and morphological characteristics.

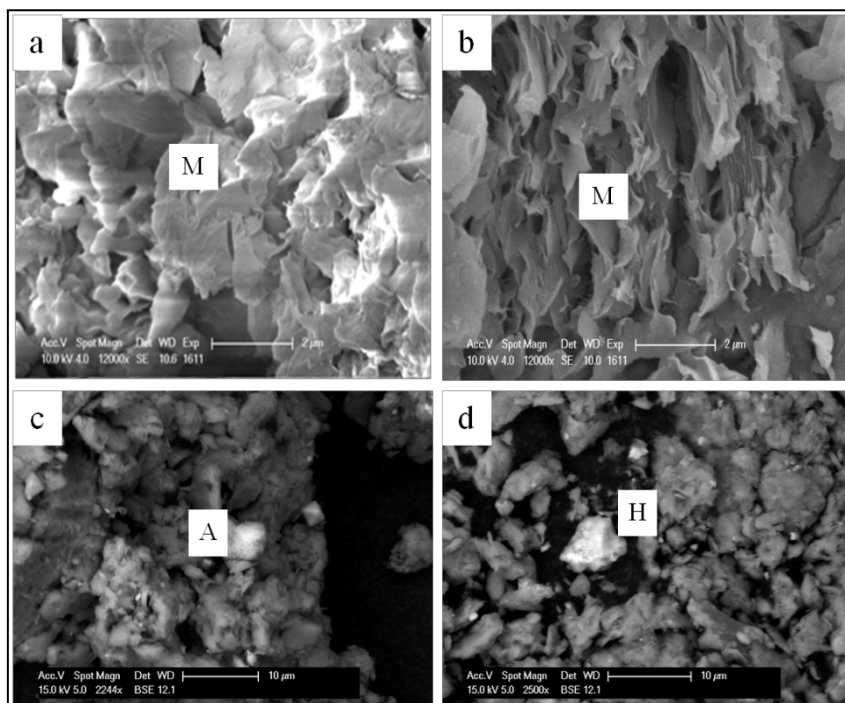


Figure 6: SEM images and EDX of the clay samples: (Montmorillonite (M) with honeycomb texture and a wavy subhedral form, (A) grain of anatase and (B) grain of hematite)

4.2. Chemical composition

The chemical compositions of the < 63 µm fractions were analyzed for the major elements and the results are presented in Table 3. The most abundant oxides in all of the samples were SiO₂, Al₂O₃ and Fe₂O₃ because their mineralogy is dominated by smectite. The six samples exhibited a similar TiO₂ content, ranging between 2.10 to 2.31 %, the presence of this oxide is coherent with the presence of anatase revealed by X-ray diffraction. However, MgO, K₂O and CaO contents were almost the same in all of the samples. These six clay samples also had relatively small Na₂O and MnO contents. All samples were characterized by high amounts of SiO₂ (values ranged between 49.14 to 52.67 %) and relative amounts of Al₂O₃ (values ranged from 22.45 to 23.82 %). The Al₂O₃ content within the clays depends on the intensity of kaolinization. A higher Al₂O₃ content indicates more kaolinization of a clay sample ([Yanik, 2011](#)). The small amounts of Al₂O₃ content in these samples suggest a low content in kaolinite.

	Samples					
	BN25	BN35	BN45	BN61	BN81	BN115
SiO ₂	49.14	51.41	50.04	50.11	51.43	52.67
Al ₂ O ₃	23.10	23.37	23.82	23.41	22.84	22.45
Fe ₂ O ₃	9.06	6.43	7.31	7.25	6.02	5.51
MnO	0.01	0.01	0.01	0.01	0.01	0.01
MgO	1.58	2.40	2.79	2.88	2.04	2.30
CaO	0.08	0.08	0.07	0.08	0.05	0.05
Na ₂ O	0.01	0.01	0.01	0.01	0.01	0.02
K ₂ O	0.84	0.47	0.38	0.13	0.53	1.01
TiO ₂	2.21	2.24	2.17	2.10	2.15	2.31
P ₂ O ₅	0.12	0.15	0.13	0.19	0.24	0.21
L.O.I.	14.08	13.34	13.89	13.46	14.00	13.46
Total	100.22	99.91	100.60	99.62	99.32	100.00
SiO ₂ /Al ₂ O ₃	2.12	2.19	2.10	2.14	2.25	2.34
Smectite	72.8	75.3	77.0	70.5	77.2	74.1
Mica	4.9	7.5	8.7	9.0	6.4	7.2
Kaolinite	9.1	4.9	2.5	7.2	1.8	4.1
Quartz	1.4	1.7	0.5	1.5	3.9	2.6
Anatase	2.2	2.2	2.2	2.1	2.2	2.3
K-feldspars	4.9	2.8	2.2	0.8	3.1	5.9
Oxyde de fer	9.1	6.4	7.3	7.3	6.0	5.5

L.O.I : Loss on ignition

Table 2: Major elements and mineralogical compositions (wt. %) of clay samples.

In addition the $\text{SiO}_2/\text{Al}_2\text{O}_3$ ratio (2.12-2.34) is indicative of smectite clay with a ratio ~2.36. Bana clays are made essentially of clays such as smectite or mica. The Fe_2O_3 contents for all samples vary between 5.51 to 9.06 %, indicate that the iron cation are present in the interlayer of smectite or associated with another minerals like hematite. The loss on ignition for all samples ranged from 13.34 to 14.08 %.

The most abundant trace elements in these samples are Ba (96-241 ppm), Cr (541-554), La (251- 406 ppm), Nd (205-322 ppm), V (248-273 ppm), Y (256-365 ppm), Zn (108-137 ppm) and Zr (197-214 ppm). The results of chemical analyses showed that there is very little difference in the chemical composition of all the clay samples.

4.3. Physico-chemical and textural properties

- CEC and pH

The cobaltihexamine method revealed CEC values ranging between 50 and 59 meq/100g (Table 3). These values mainly result from the smectite phase, and coherent with the mineralogical composition of the samples. The presence of accessory minerals (anatase, quartz and feldspars) and also clay minerals (kaolinite, mica) accounting for these CEC values.

The clay samples have acidic pH values (Table 3). These values are ranging between 4.8 to 5.1, this result confirms the absent of calcite, as already revealed by XRD.

Samples	S_{SA} (m ² /g)	Pore volume (cm ³ /g)	Microporous volume (cm ³ /g)	CEC (UV) (meq/100g)	CEC (chem) (meq/100g)	pH
BN25	50	0.099	0.021	55	56	4.9
BN35	58	0.093	0.025	54	54	4.8
BN45	68	0.102	0.031	50	50	5.1
BN61	49	0.101	0.020	50	49	5.1
BN81	62	0.108	0.027	56	61	5.1
BN115	55	0.109	0.026	59	62	4.9

Note: UV: *derived from the measurement of cobaltihexamine concentrations by U.V-visible spectroscopy*; Chem: *derived from analysis of displaced cations*

Table 3: CEC, equilibrium pH, Specific Surface Area (SSA) and pore volumes of clay samples

- ***Electrokinetic***

In the whole range of investigated pH (2 to 10), the mobility is negative as observed by the electrophoretic mobilities (EM) (Fig. 7). This negative mobility indicates that the clay surface is negatively charged. A relative constant mobility between pH = 4.5 and pH = 10 is observed for an EM average value of $3.3 \mu\text{m/s/V/cm}$. A shift of the EM towards $-0.5 \mu\text{m.s}^{-1}.\text{v}^{-1}.\text{cm}^{-1}$ is recorded for pH below 4.0. No isoelectric point is observed within 4.3-10 pH range. The constant behavior between pH 4.5 and 10 is concordant with the montmorillonite behavior due to the permanent charge of this clay. The absence of an isoelectric point is usual in clays with permanent crystalline charge like smectites (Thomas et al., 1999; Avena et al., 2003; Tombacz & Szekeres, 2006; Duc et al., 2006). The shift of the EM at lower pH is usual for minerals having pH-dependant charge (variable charge) such as quartz, microcline, anatase or goethite (Thomas et al., 2002). The EM dependence to pH is also observed for kaolinite (Alkan et al., 2005). The observed EM shift is then attributed to the kaolinite content with a contribution of non-clay minerals such as anatase and microcline.

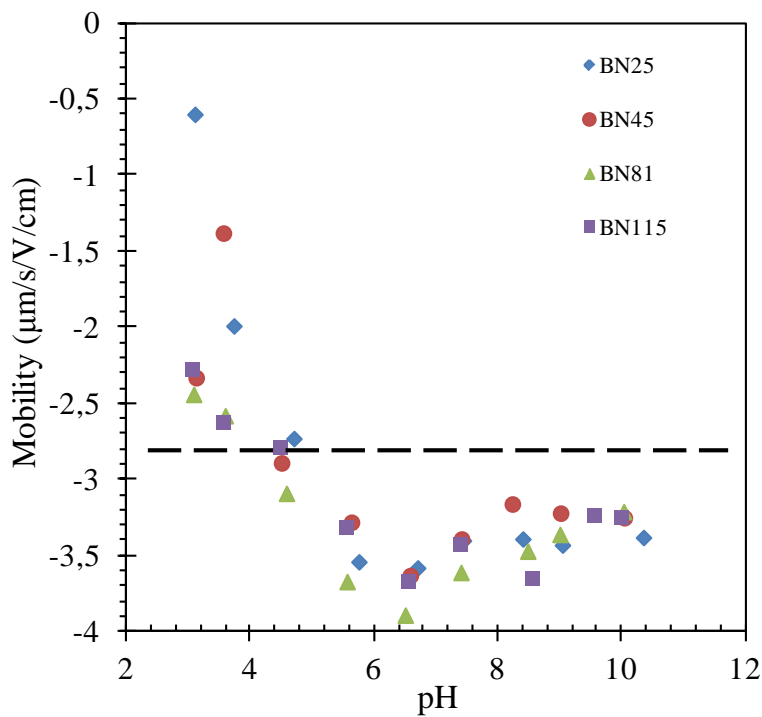


Figure 7: Electrophoretic mobility of the clay fraction in 10^{-3} M NaNO_3 as function of pH

- ***Adsorption-desorption isotherm and BET surface area***

The N_2 adsorption-desorption isotherms of the natural clays (Fig. 8) display very similar shapes. An hysteresis indicates the presence of a relatively open mesoporosity. The isotherms of all clays are classified as type III on the basis of IUPAC recommendations. This isotherm type characterizes notable mesoporous structures. The hysteresis loop of these samples is similar to type H3. This type of isotherm is characteristic of materials for which the affinity between adsorbate and adsorbent is lower than that between the adsorbate molecules.

The specific surface areas (SSA), the pore volume and micropore volume of the different clay materials investigated are reported in Table 2. The specific surface area of the samples ranges between 49 and 68 m^2/g . For all the samples, except for BN81, the SSA increases with the amount of smectite (Table 2 and 3). For sample BN81, the difference may be due to variable proportion of external and internal SSA as suggested by [Dogan et al. \(2007\)](#). The average pore volume, determined by [Dubinin-Radushkevitch](#) equation, is $\sim 0.1 \text{ cm}^3/\text{g}$. The high SSA confirms the high smectite mineral content in this clay. The high SSA area is important factor when the clay minerals are used as absorbent. These values of specific surface area are coherent with the mineralogical composition of the samples.

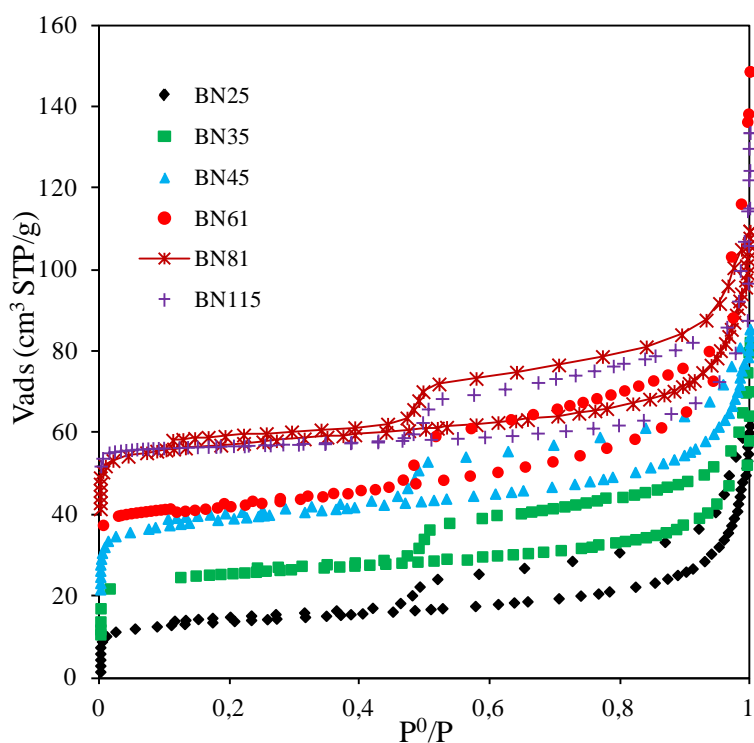


Figure 8: N_2 adsorption/desorption isotherms of the clay samples.

Based on the results provided by mineralogical composition and physico-chemical properties, which are almost similar for all clay samples studied, the sample named BN81 taken at 8.1 m of depth along the profile was chosen to evaluate the potential uses as bleaching earth.

4.4. Bleaching test

In order to examine the potential use of the natural clay collected from Bana area in the decolouration of palm oil, a decolouration test was carried out by varying the bleaching time from 5 to 90 minutes at 97°C. The beta-carotene is the pigment responsible for the color of crude palm oil. The bleaching capacities of the natural clay to remove this pigment at different contact time are presented in Fig. 9. One observes that the bleaching performance of the natural clay increases with the increase in bleaching time, reaching a maximum value of 55 % after 75 minutes. Also, it can be seen from Fig. 9 that the bleaching capacity of the clay studied increases rapidly during the first 45 minutes and progresses slightly thereafter. The result is in agreement with those reported by [Berbesi \(2006\)](#) which stated that the contact time for effective bleaching typically ranges from 15 to 45 minutes, with 20 to 30 minutes being most common. The first fast step of decolouration represents the chemical interaction between the Brönsted sites and /or to direct binding at Lewis sites on clay surfaces and beta-carotene, while the second slow step may probably indicate physical adsorption of beta-carotene on those molecules adsorbed during the first step ([Christidis et al., 2003](#)). The positive effect of increasing contact time may be improvement of the bleached color and pigment removal ([Berbesi, 2006](#)).

Two industrial clays named Enge and Flor B80 produced by Engelhard (Netherland) and South African Industrial Clay (South Africa), respectively, studied by [Nguetnkam et al. \(2008\)](#) in bleaching palm oil at optimum conditions (3 %, 95 °C and 2.5h) show the bleaching powers around 80 %. The results provided by smectite-rich clay from Bana show a weak bleaching power than industrial clays, which have bleaching capacities twice greater than natural clay from Bana.

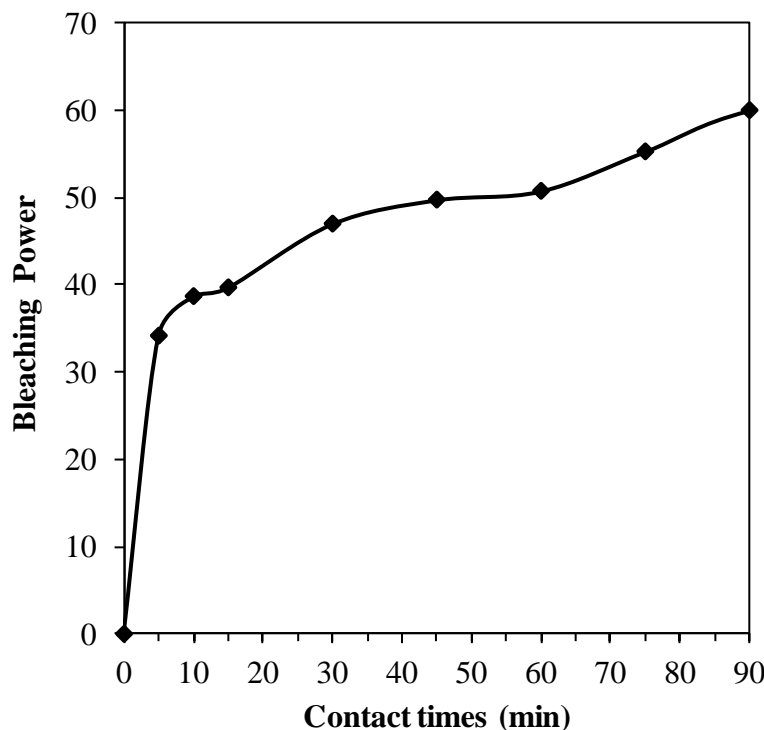


Figure 9. Kinetic of palm oil bleaching at $(97 \pm 1^\circ\text{C})$ by BN81 clay sample.

The highest bleaching efficiency of both industrial clays is related to their mineralogical structure and adsorptive properties including surface area, particle size distribution, porosity, and surface acidity which play an important role in the bleaching performance of clays. This bleaching power of industrial clays is due to their chemical treatment by acid.

The yield of the natural sample is of interest given that; the bleaching capacity of commonly used clay-based bleaches is achieved through acid, alkaline or organic activation of montmorillonite based clay ([Srasra et al., 1989](#); [Christidis et al., 1997](#); [Hussin et al., 2011](#)). The bleaching capacity of the Bana clay could then be optimized through activation.

CONCLUSION

Characterization of the natural clays from Bana area (Western Cameroon) by X-ray diffraction, infra-red spectroscopy, scanning electron microscopy, chemical and thermal analyses showed that the main clay mineral is montmorillonite ($\geq 70\%$) associated to kaolinite and mica. Accessory minerals such as anatase, feldspars and quartz are also present. The Specific Surface Area (SSA), cation exchange capacity (CEC) and electrophoretic mobility values are consistent with the high montmorillonite content of these clay materials. This montmorillonite content is of interest for application in oil bleaching. Decolouration tests yield an interesting bleaching power of 55 %. To enhance this bleaching potential, acid activation of the Bana's clay is actually under investigation and further bleaching experiments will be carried out to optimize the bleaching potential of the Bana clays.

Acknowledgements

The authors are grateful to European Commission for the Erasmus Mundus ACP for a PhD fellowship for J.R Mache at the University of Liege (Belgium).

REFERENCES

- Alkan, M., Demirbaş, Doğan, M., 2005. Electrokinetic properties of kaolinite in mono- and multivalent electrolyte solutions. *Microporous and Mesoporous Material* 83, 51-59.
- Aranha Da Paz, S.P., Angelica, R.S., De Freitas, R., 2012. Mg-bentonite in the Parnaiba Paleozoic basin, northern Brazil. *Clays and Clay Minerals* 3, 265-277.
- Avena, M.J., Mariscal M. M., Carlos, P., De, P., 2003. Proton binding at clay surfaces in water. *Applied Clay Science* 24, 3-9.
- Bergaya, F., Dion, P., Alcover, J.F., Clinard, C., Tchoubar, D., 1996. TEM study of kaolinite thermal decomposition by controlled-rate thermal analysis. *Journal of Materials Science* 31, 5069-5075.
- Berbesi, R., 2006. Achieving optimal bleaching performance. *Oil Mill Gazetteer* 112, 1-5.
- Brigatti, M.F., 1983. Relationship between composition and structure in Fe-rich smectites. *Clay Minerals* 49 (5), 444 - 445.
- Carty, W.M., Senapati, U., 1998. Porcelain-raw materials, processing, phase evolution, and mechanical behavior. *Journal of American Ceramic Society* 1998, 8, 3-20.
- Christidis, G.E., Scott, P.W., Marcopoulos, T., 1995. Origin of the bentonite deposits of Eastern Milos and Kimalos, Greece: geology, geological, mineralogical and geochemical evidence. *Clays and Clay Minerals* 43, 63-77.
- Christidis, G.E., Scott, P.W., Dunham, A.C., 1997. Acid activation and bleaching capacity of bentonites from the Island of Milos and Chios, Aegean, Greece. *Applied Clay Science* 12, 329-347.
- Christidis, G.E., Kosiari, S., 2003. Decolorization of vegetable oils: a study of the mechanism of adsorption of b-carotene by an acid-activated bentonite from Cyprus. *Clays and Clay Minerals* 51(3), 327–333.
- Djangang, C.N., Elimbi, A., Melo, U.C., Nkoumbou, C., Lecomte, G., Yvon, J., Bonnet, J.P., Njopwouo, D., 2007. Characteristics and Ceramic Properties of Clays from Mayouom deposit (west Cameroon). *Industrial Ceramics* 27(2), 79-88.
- Djangang, C.N., Elimbi, A., Lecomte, G.L., Soro, J., Nkoumbou, C, Yvon, J., Blanchart, P. Njopwouo, D., 2008. Refractory ceramics from clays of Mayouom and Mvan in Cameroon. *Applied Clay Science* 39(1-2), 10 -18.

- Djoufac, W.E., Elimbi, A., Panczer, G., Nyada Nyada R., Njopwouo, D., 2006. Caractérisations physico-chimiques et minéralogiques des vertisols de Garoua (Nord Cameroun). *Annales de Chimie des Sciences de Matériaux* 31, 75-90.
- Djoufac, W.E., Kamga, R., Figueras, F., Njopwouo, D., 2007. Acid activation and bleaching capacity of some Cameroonian smectite soil clays. *Applied Clay Science* 37, 149-156.
- Dogan, M., Dogan, A.U., Yesilyurt, F.I., Dogan, A., Buckner, I., Wurster, D.E. 2007. Baseline studies of the Clay Minerals Society special clays: specific surface area by the Brunauer, Emmett, Teller (BET) method. *Clays and Clay Minerals* 55, 534-541.
- Duc, M., Gaboriaud, F., Thomas, F., 2006. Coupled chemical processes at the clay-electrolyte interface. A batch titration study of MX80 and Swy2 montmorillonites. *Journal of Colloid and Interface Science* 300, 616-625.
- Ekosse, G.E., 2010. Kaolin deposits and occurrences in Africa: Geology, mineralogy and utilization. *Applied Clay Science* 50(2), 212-236.
- Elimbi, A., Njopwouo, D., 2002. Firing characteristics of ceramics from the Bomkoul kaolinitic clay deposit (Cameroun). *Tile and brick International* 18(6), 364-369.
- Elimbi, A., Yeugouo, E., Nenwa, J., Liboum., Njopwouo, D., 2003. Caractérisations chimiques et minéralogiques de deux matériaux du gisement argileux de Bakong (Cameroun). *African Journal of Material and Minerals* 06(1), 13-19.
- Emmerich, K., Wolters, F., Kahr, G., Gerhard, L., 2009. Clay profiling: the classification of montmorillonites. *Clays and Clay Minerals* 57 (1), 104-111.
- Farmer, V.C., 1974. The infrared Spectra of Minerals. Mineralogical Society. London
- Farmer, V.C., Palmieri F., 1975. The characterization of soil minerals by infrared spectroscopy. In: Giesecking, E.J. *Soil Components*. 2, Springer-Verlag, NewYork, pp. 573-670.
- Garwin, S.L., Hayles, C.S., 1999. The chemical compatibility of cement-bentonite cut-off wall material. *Construction and Building Materials* 13, 329-341.
- Gregg, S.J., Sing, K.S.W., 1982. *Adsorption, Surface Area and Porosity*, Academic Press.
- Harvey, C.C., Lagaly, G., 2006. Conventional applications. In: Bergaya, F., Theng, B.K.G., Lagaly, G. (Eds.), *Handbook of Clay Science*. Elsevier, pp. 501-541.
- Hanchar, J.M., Stroes-Gascione, S., Browning, I., 2004. Scientific basic for nuclear waste management. XXVIII. *Materials Research Society Sympocium Proceedings*. Materials research Society, Warrendale, Pennsylvania.

- Hradil, D., Grygar, T. S., Kova, M. H., Ka, P .B., Lang, K., Schneeweiss, O. I., Chva' Tal, M., 2004. Green earth pigment from the kadan' region, czech republic: use of rare Fe-rich smectite. *Clays and Clay Minerals* 52, 767–778.
- Holtzapffel, T., 1985. Les minéraux argileux, Préparation, Analyse diffractométrique et Détermination. Société Géologique de France, pub 12, 136 p.
- Hussin, F., Aroua, M.K., Daud, W.M.A., 2011. Textural characteristics, surface chemistry and activation of bleaching earth. *Chemical Engineering Journal* 170, 90-106.
- Jaynes, W.F., Bigham, J.M., 1987. Charge reduction, octahedral charge, and lithium retention in heated, Li-saturated smectites. *Clays and Clay Minerals* 35, 440-448.
- Kamseu, E., Leonelli, C., Boccaccini, D.N., Veronesi, P., Miselli, P., Pellacani, G., Melo, U.C., 2007. Characterization of Porcelain Compositions using two china Clays from Cameroon. *Ceramics International* 33(5), 851-857.
- Kuepouo, G., 2004. Geology, Petrology and Geochemistry of the Tertiary Bana Volcano-Plutonic Complex, Cameroon Line, Central Africa. Ph.D. Thesis, Kobe University, Japan, 301p.
- Kuepouo, G., Tchouankoue, J.P., Nagao, T., Sato, H., 2006. Transitional tholeiitic basalts in the Tertiary Bana volcano-plutonic complex, Cameroon Line. *Journal of African Earth Sciences* 45, 318–332.
- Lemougna, P.N., MacKenzie, J.D.K., Melo, U.C., 2011. Synthesis and Thermal Properties of Inorganic Polymers (geopolymers) for Structural and Refractory Applications from Volcanic Ash. *Ceramics International* 37, 3011-3018.
- Lim, C.H., Jackson, M.L., 1986. Expandable phyllosilicate reactions with lithium on heating. *Clays and Clay Minerals* 34, 346–352.
- Lumdson, D.G., Evans, L.J., Bolton, K.A., 1995. The influence of pH and chloride on the retention of cadmium, lead, mercury and zinc by soils. *Journal of Soil Contamination* 4, 137-150.
- Madejová, J., Komadel, P., Cicel B., 1992. Infrared spectra of some Czech and Slovak smectites and their correlation with structural formulas. *Geologica Carpathica, Series Clays.* 1, Bratislava, Juene 1992. pp. 9-12.
- Madejovà, J., Komadel, P., 2001. Baseline studies of the clay minerals society source clays: infrared methods. *Clays and Clay Minerals* 49, 410-432.
- Malla, P.B., Douglas, L.A., 1987. Problems in identification of montmorillonite and beidellite. *Clays and Clay Minerals* 35, 232-236.

- Mbey, J.A., Hoppe S., Thomas, F., 2012. Cassava starch-kaolinite composite film. Effect of clay content and clay modification on film properties. *Carbohydrate Polymers* 88(1), 213-222.
- Moraes, D.S., Angélica, R.S., Costa, C.E.F., Rocha Filho, G.N., Zamian, J.R., 2010. Mineralogy and chemistry of a new bentonite occurrence in the eastern Amazon region, northern Brazil. *Applied Clay Science* 48, 475- 480.
- Montes, G., Geraud, H.Y., Duplay, J., Reuschle, T., 2005. ESEM observations of compacted bentonite submitted to hydration/dehydration conditions. *Colloids and Surfaces A: Physicochemical Engineering Aspects* 262, 14-22.
- Moore, D.M., Reynolds, Jr., R.C., 1997. X-Ray Diffraction and the Identification and Analysis of Clay Minerals. Oxford University Press, Oxford.
- Moore, D.M., Reynolds, R.C., 1989. X-ray Diffraction and the Identification and Analysis of Clay Minerals. Oxford University Press, Oxford. pp.332
- Nguetnkam, J.P., Kamga, R., Villiéras, F., Ekodeck, G.E., Yvon, J., 2008. Assessing the bleaching of some Cameroonian clays on vegetable oils. *Applied Clay Science* 39, 113-121.
- Njopwouo, D., Wandji, R., 1982. Un gisement d'halloysite à Balengou (Ouest-Cameroun). *Revue Scientifique et Technique, Série Science de la Terre* 2, 41-54.
- Njopwouo, D., Wandji, R., 1985. Minéralogie de l'argile kaolinitique Bomkoul (Cameroun). *Revue Scientifique et Technique, Série Science de la Terre* 1(3-4), 71-81.
- Njopwouo, D., Roques, G., Wandji, R., 1988. A contribution to the study of the catalytic action of clays on the polymerisation of styrene: Reaction mechanism. *Clay Minerals* 23(1), 35-43.
- Njoya, A., Nkoumbou, C., Grosbois, C., Njopwouo, D., Njoya, D., Courtin, A.N., Yvon, J., Martin F., 2006. Genesis of Mayouom kaolin deposit (Western Cameroon). *Applied Clay Science* 32(1-2), 125-140.
- Nkoumbou, C., Njopwouo, D., Villiéras, F., Njoya, A., Yonta, G.C., Ngo Njock, L., Yvon, J., Tchoua, F.M., 2006. Geological study and physico-chemical Characteristics of Talc of Boumnyebel (Centre-Cameroun). *Journal of African Earth Sciences* 54, 61-73.
- Nkoumbou, C., Villiéras, F., Barres, O., Bihannic, I., Pelletier, M., Razafitianamaharavo, A., Metang, V., Yonta Ngoune, C., Njopwouo, D., Yvon, J., 2008. Physicochemical properties of talc ore from Pout-kelle and Memel deposits (central Cameroon). *Clay Minerals* 43 (2), 317-337.

- Pialy, P., Nkoumbou, C., Villieras, F., Razafitianamaharavo, A., Barres, O., Pelletier, M., Ollivier, G., Bihannic, I., Njopwouo, D., Yvon, J., Bonnet, J.P., 2008. Characterization for industrial applications of clays from Lembo deposit, Mount Bana (Cameroun). Clay Minerals 43, 415- 435.
- Pialy, P., Tessier-Doyen, N., Njopwouo, D., Bonnet, J.P., 2009. Effects of densification and mullitization on the evolution of the elastic properties of a clay-based material during firing. Journal of the European Ceramic Society 29(9), 1579-1586.
- Srasra, E., Bergaya, F., Van Damme, H., Ariguib, N.K., 1989. Surface properties of activated bentonite: decolorization of rape seed oil. Applied Clay Science 4, 411- 421.
- Seki, Y., Yurdokoc, K., 2007. Identification and characterization of Fe-rich smectites in the Camlica Region of western Turkey. Clays and Clay Minerals 42, 153-160.
- Taylor, D.R., Jenkins, D.B., UngermaNN, C.B., 1989. Bleaching with alternative layered minerals: a comparison with acid activated Montmorillonite for bleaching Soybean oil. Journal of the American Oil Chemists' Society 66, 334-341.
- Tchakoute, H.K., Elimbi, A., Mbey, J.A., Ngally Sabouang, C.J., Njopwouo, D., 2012. The effect of adding alumina-oxide to metakaolin and volcanic ash on geopolymers products: A comparative study. Construction and Building Materials 35, 960-969.
- Thomas, F., Michot, L.J., Vantelon, D., Montargès, E., Prélot, B., Cruchaudet, M., Delon, J.F., 1999. Layer charge and electrophoretic mobility of smectites. Colloids and Surfaces 159, 351-358.
- Thomas, F., Prélot, B., Villiéras, F., J.M., 2002. Electrochemical properties of solids at the Aqueous-solid interface and heterogeneity of surface. Comptes Rendus Geoscience 334, 633-648.
- Tombácz, E., Szekeres, M., 2006. Surface charge heterogeneity of kaolinite in aqueous suspension in comparison with montmorillonite. Applied Clay Science 34, 105–124.
- Wolters, F., Lagaly, G., Kahr, G., Nueesch, R., Emmerich, R., 2009. A comprehensive characterization of dioctahedral smectites. Clays and Clay Minerals 57, 115-133.
- Wolters, F., Emmerich, K., 2007. Thermal reactions of smectites-relation of dehydroxylation temperature to octahedral structure. Thermochimica Acta 462, 80-88.
- Wu, J., Laird, D.A, Thompson, M.L., 1999. Sorption and desorption of copper on soil clay components. Journal of Environmental Quality 28, 334-338.
- Yanik, G., 2011. Mineralogical, crystallographic and technological characteristics of Yaylayolu kaolin (Kütahya, Turkey). Clay Minerals 46, 397-410.

Zhansheng, W., Chun, L., Xifang, S., Xiaolin, X., Bin, D., Jin'e, L., Hongsheng, Z., 2006.
Characterization, acid activation and bleaching performance of bentonite from
Xinjiang. Chinese Journal of Chemical Engineering 14(2), 253-258.

CHAPITRE III

INFLUENCE DU TRAITEMENT ACIDE SUR LES PROPRIETES PHYSICO-CHIMIQUES, MINERALOGIQUES ET TEXTURALES DES ARGILES DE BANA ET SABGA

Introduction

Afin d'améliorer les propriétés de surfaces des deux argiles camerounaises riches en smectite dioctaédrique (montmorillonite), il a été procédé à l'activation acide qui est un traitement chimique généralement employé pour optimiser la capacité d'adsorption de ce type de matériau en vue de leur utilisation comme terres décolorantes dans l'industrie de raffinage des huiles végétales.

La montmorillonite est un minéral argileux dit gonflant formé de deux couches de tétraèdres siliciques liées au centre d'une couche d'octaèdre aluminique. La neutralisation de la charge électrique négative des couches résultant de la substitution isomorphique des ions Al^{3+} par Fe^{2+} et Mg^{2+} dans les sites octaédriques et les ions Si^{4+} et Al^{3+} dans les sites tétraédriques, est assurée par des cations dits échangeables tels que Na^+ et Ca^{2+} situés entre les couches (espace inter-feuillet). Le caractère non-structural de ces cations échangeables offre des possibilités plus simples de leur remplacement par des ions positifs tels que les protons (H^+). L'activation à l'acide sulfurique a été utilisée pour remplacer les cations interfoliaires des matériaux argileux par des protons. Les modifications structurales, physico-chimiques et texturales dues à ce traitement ont été suivies par diffraction des rayons X (DRX), spectroscopie infrarouge (FTIR), microscopie électronique à balayage (MEB), analyse thermique (ATD/ATG), analyse chimiques (ICP-AES/MS), absorption atomique (AAS), analyse par électrophorèse capillaire (CIA) et aussi par la détermination de surface spécifique (BET), capacité d'échange cationique (CEC) et potentiel d'hydrogène des produits obtenus. Le présent chapitre présente l'évolution structurale, physico-chimique et texturale des matériaux après traitement acide.

Les résultats de cette étude sont présentés à la section (§III.2) ci-dessous sous la forme d'un article soumis à *Colloids and Surfaces A: Physicochemical and Engineering Aspects*.

III.1. Résumé de l'article

Dans cette étude, deux argiles collectées dans les localités de Bana et Sabga respectivement des régions de l'Ouest et Nord-ouest du Cameroun à base de smectite dioctaédrique, ont été activées par de l'acide sulfurique à diverses concentrations de 0,5 à 4,0N à 80°C pendant 2 heures. Les modifications structurales et texturales subies par ces matériaux ont été suivies par diffraction de rayon X, spectroscopie infrarouge à transformée de Fourier, microscopie électronique à balayage, adsorption d'azote à 77 K et granulométrie laser. Il ressort de ces investigations que l'activation à l'acide sulfurique provoque une dissolution partielle de la smectite, tandis que les minéraux qui lui sont associés (cristobalite, quartz, feldspars et kaolinite) ne subissent pas d'altération notable. Cette dissolution partielle, plus marquée dans l'échantillon de Bana (BN) que dans celui de Sabga (S), s'accompagne d'une augmentation de leur surface spécifique. Au cours de ce traitement la surface spécifique passe de 65 à 134 m²/g pour Bana à une concentration de 4N et pour Sabga de 74 à 84 m²/g dans les mêmes conditions. Les courbes de distribution des tailles de particules montrent que le volume de particule en fonction de la taille augmente avec le traitement acide pour les échantillons de Bana et reste inchangé pour ceux de Sabga. L'activation procède par un remplacement des cations interfoliaires par les protons, il s'ensuit une baisse des valeurs de capacité d'échange cationique et le pH des produits activés. L'augmentation linéaire de la surface spécifique des deux argiles avec la concentration de l'acide indique que ces matériaux peuvent subir des traitements à des concentrations en acide plus élevées. Les propriétés de surfaces ainsi identifiées montrent que ces matériaux activés peuvent être considérés comme des adsorbants prometteurs pour la décoloration des huiles végétales.

III.2. Acid activation of smectite clays from Cameroon: Effect on mineralogical and physico-chemical properties

Jacques Richard Mache^{a, b, c, *}, Pierre Signing^b, Jean Aimé Mbey^d,
Angelina Razafitianamaharavo^d, Daniel Njopwouo^b, Nathalie Fagel^a

^a UR AGES Argiles, Géochimie et Environnements sédimentaires, Département de Géologie,
Université de Liège, B18, Allée du 6 Août, B-4000 Liège, Belgique

^b Laboratoire de Physico-chimie des Matériaux Minéraux, Département de Chimie
Inorganique, Université de Yaoundé 1, B.P. 812 Yaoundé, Cameroun

^c Mission de Promotion des Matériaux Locaux, B.P 2396 Yaoundé, Cameroun

^d Laboratoire Environnement et Minéralurgie, UMR 7569 CNRS-Université de Lorraine, 15
Avenue du Charmois, B.P. 40. F-54501, Vandœuvre-lès-Nancy Cedex, France

* Corresponding author: e-mail: jamache@yahoo.fr; Tel: +3243662229;
Fax: +3243662029

ABSTRACT

Smectite clays from western Cameroon were treated with sulfuric acid solution of different concentrations 0.5, 0.7, 1.0 and 4.0 N at 80 °C for 2 hours. The physicochemical, mineralogical and morphological properties of the treated clays were assessed by several techniques. The sulfuric acid treatment causes structural modification of the dioctahedral smectite. The accessory minerals such as cristobalite, quartz, feldspars and anatase remain clearly unaltered by the acid attack. The analysis of the supernatant solutions after acid treatment reveals a leaching of octahedral and tetrahedral cations, the degree of which in amount increases with acid concentration. The smectite clays treated with sulfuric acid exhibited a lower cation exchange capacity (CEC). They also present a variation of their specific surface area (SSA) from 65 to 134 m²/g for the smectite from Bana and 74 to 84 m²/g for the smectite from Sabga. The different specific surface areas are linked with the abundance of smectite (SiO₂/Al₂O₃: 2.2; 6.5, respectively from Bana and Sabga) and the amount of impurities (cristobalite, quartz or silica residue) in the studied clay samples. Clays from Bana and Sabga can be considered as promising adsorbents in bleaching procedure of vegetable oils.

Keywords: smectite, acid activation, X-ray diffraction, thermal analyses, specific surface area

1. INTRODUCTION

Smectites, including bentonite, are 2:1 layered aluminosilicate clay minerals that are widely distributed in soils, sediments, and prehistoric clay deposits [1]. Due to isomorphic substitution in the tetrahedral Si and/or octahedral Al layers, smectites are characterized by structural negative charges that are compensated by exchangeable cations in the interlayer regions. These cations being non structural could easily be replaced by other positively charged atoms or molecules [2-5].

The industrial use of smectite is closely related to its reactivity and textural properties, which depend strongly on surface state modification. Several methods have been suggested in the literature to improve the physico-chemical properties of smectite clays such as pillaring or intercalation treatment which involves chemical and physical restricting of the clay mineral structure, microwave or heat treatment (physical treatment) which involves alteration of chemical composition and crystalline structure by the effect of temperature, and acid activation (chemical treatment) which involves alteration of structure and surface functional groups to increase capacity for adsorption or to create active site that encourage adsorption of specific ions or molecules [6].

Acid activation is a useful method to modify the catalytic behavior and enhance clay properties; mainly their sorptive properties [7, 9]. Thus, acid treatment is commonly required when clays are used in industry; for example, as catalysts or catalyst supports in alkylation and polymerisation reactions [10-17] and as a component in carbonless copying papers [18]. Probably, the most widely used acid-activated clays are the bleaching earths [19-22], which are capable of removing colour, odour and other impurities from cooking oils of vegetable and animal origin. These practical applications are a consequence of the existence of a high physico-chemical activity in the clay surface.

During the acid treatment, the first step of acid attack is to remove the exchangeable cations by protons. The second step is the leaching of Al, Mg and Fe from octahedral and tetrahedral sheets; but the SiO_4 groups of tetrahedral sheets stay largely intact [7]. Increasing of the specific surface area is an important physical change which is a function of the structure and removal of octahedral sheets.

In the present work, physicochemical and mineralogical characterizations of acid-activated smectite-rich clays from Cameroon treated at different sulfuric acid concentrations are investigated. The effect of acid concentration on some mineralogical and physicochemical properties such as particle size distribution, specific surface area and chemical evolution was

investigated. Previous works on the acid activation of clay minerals have been conducted by many researchers; these works have focused on the use of high acid concentrations during the treatment. Our choice is based on weaker range concentration.

2. MATERIALS AND METHODS

2.1. Materials

Two natural clays with a high content of dioctahedral smectite as main clay minerals associated with kaolinite, quartz, anatase, feldspars and cristobalite (Fig. 1) used in this experiment were sampled from Bana in the West Region of Cameroon (named BN clay sample) and Sabga in the North West Region of Cameroon (named S clay sample). The < 63 μm fractions were separated by wet sieving, decantation and subsequently dried at 110 °C. After drying, the clay samples were reduced by gentle grinding in an agate mortar. All the physico-chemical and mineralogical analyses were done on the < 63 μm fractions.

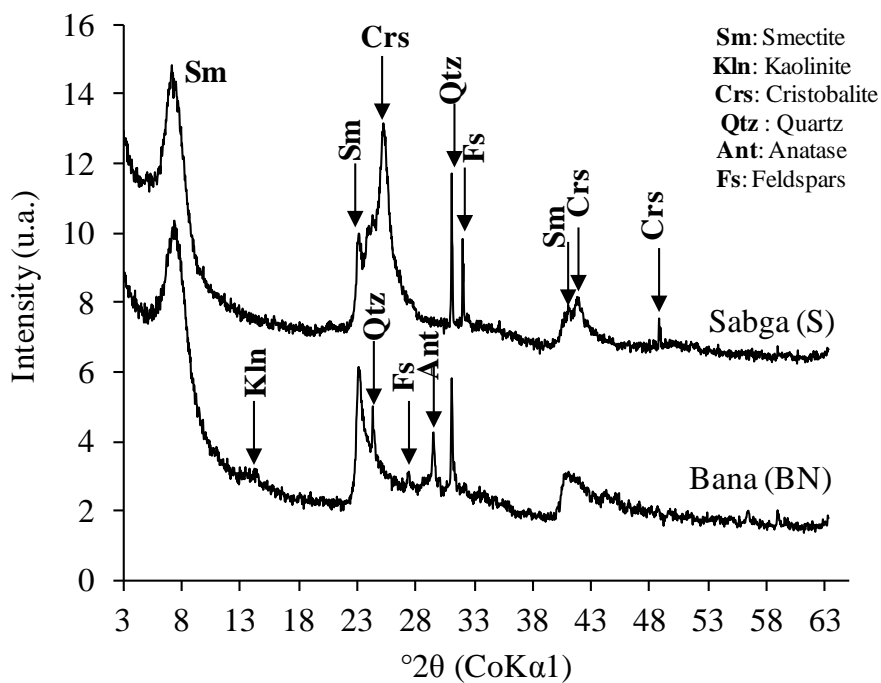


Fig 1. XRD patterns of the natural clay samples.

2.2. Methods

2.2.1. Acid activation

Acid activation was applied to both BN and S samples. For the acid activation, samples of 10 g were dispersed in 100 mL of 0.5, 0.7, 1.0 and 4.0 N H₂SO₄ (prepared from H₂SO₄ 96 % p.a, Fischer); the mixture clay-acid was stirred continuously in a jacketed glass reactor equipped with water circulation condenser and a thermometer at 80 °C for 2 hours. At the end of each run, and after cooling at room temperature, suspensions were filtered and the remaining solid phases were washed several times with pure water (MilliQ ultra filtration) to remove any unspent acid and until the filtrates were neutral (test of 5 % BaCl₂). After drying at 110 °C for 24 hours and gently ground in an agate mortar, the activated samples were designated as BN-0.5, BN-0.7, BN-1.0, BN-4.0 for the sample obtained from Bana and S-0.5, S-0.7, S-1.0, S-4.0 for those from Sabga with the suffix indicating the concentration of H₂SO₄ used during the activation. The activated samples were stored in the plastic bottles closed tightly for use.

2.2.2. Characterization of the materials

The acid activated clay samples were characterized by X-ray diffraction (XRD), Fourier transform infrared spectroscopy (FTIR), thermal analyses (DTA/TG), scanning electron microscopy (SEM), Inductive Coupled Plasma by Atomic Emission Spectrometry (ICP-AES), Capillary Ion Analyzer (CIA) and Atomic Absorption spectrometry (AAS), Specific Surface Area by using (N₂-adsorption at 77 K), Cation Exchange Capacity (CEC) and Particle Size Distribution (PSD).

The X-ray diffraction patterns were obtained with a D8 Bruker diffractometer with CoKα1 radiation ($\lambda=1.7902$). Experimental conditions were 35 kV, 45 mA, step scan 0.036° and step time 3.0 s. The XRD patterns were recorded in the range of 3-63°.

Major elements were determined at CRPG-CNRS (Nancy, France) by emission spectrometry using Inductive Coupled Plasma and Atomic Emission Spectrometry (ICP-AES) after fusion with lithium borate (LiBO₂) and dissolved in nitric acid (HNO₃). Relative analytical uncertainties were estimated at 1-2 % for major elements except for P₂O₅ (5 %).

The Fourier Transform Infra-Red and diffuse reflectance were used to investigate the short range of structural changes caused by the acid attack. The infrared spectra were recorded on a Bruker IFS 55 spectrometer equipped with a MCT detector. The analysis was done on

KBr pellets with 15 % of treated sample. For each sample, 200 scans with a resolution of 4 cm⁻¹ were recorded between 4000 cm⁻¹ to 600 cm⁻¹.

The TG–DTA measurements of the samples were done with a thermal analyzer (TA Instruments, Model STD 2960, simultaneous DTA-TGA) at a heating rate of 10 °C.min⁻¹ in an air atmosphere.

Changes in particle morphology were observed on a Philips microscope model XL30. The micrographs were obtained with a secondary electron detector, using an accelerating voltage of 15 kV. The samples were deposited on a sample holder with an adhesive carbon foil and covered with gold.

Nitrogen adsorption-desorption isotherms at 77 K were recorded on a step by step automatic home built set-up. Specific surface areas (SSA) were determined from adsorption data by applying the Brunauer-Emmet-Teller (BET) equation. Micropore and non-microporous surface areas were obtained using the t-plot method proposed by De Boer et al. (1996) [23]. Pore size distributions were calculated on the desorption branch using the Barrett-Joyner-Halenda method assuming parallel pore shape [24].

The particle size distribution (PSD) of the samples was determined on Malvern Instrument Mastersizer-2000 equipment. In order to avoid flocculation, the suspensions were sonicated for 5 min using an ultrasonic apparatus. They were then placed in the small-volume compartment, stirred at 2000 rpm and sonicated before measurement. The measuring ranges were 0.02-2000 µm. Each result obtained was the average of four measurements.

Cation Exchange Capacity (CEC) were measured using the chloride salt of cobaltihexamine [Co (NH₃)₆Cl₃] as exchangeable ions. The amount of cobalt hexamine fixed by the solid phase was determined using UV-visible spectroscopy. The displaced cations were determined by atomic absorption spectrometry (Perkin-Elmer 1100B). The pH values of the clays were measured with a 905 Titando pH-meter Instruments Ω Metrohm following stirring of a 1:5 sample/milli Q water suspension for 30 min and standing for 1 hour.

Capillary Ion Analyzer (CIA) and Atomic Absorption spectrometry (Analytik Jena, Model Nov AA 300) were used respectively to determine the amount of (Ca²⁺, Na⁺, K⁺, Mg²⁺) and (Si, Al, Cu, Co, Cr, Fe, Ni, Pb, Sr, Ti, V, Zn) in the obtained supernatant solutions after acid treatment.

3. RESULTS AND DISCUSSION

3.1. Structural modification under acid treatment

The XRD patterns of activated clays with 0.5, 0.7, 1.0 and 4.0 N H₂SO₄ solutions are presented in Fig. 2. Activation has affected mainly the 001-order (basal spacing) reflections of smectite: the intensity of the (001) reflection decreases significantly with increase in acid concentration.

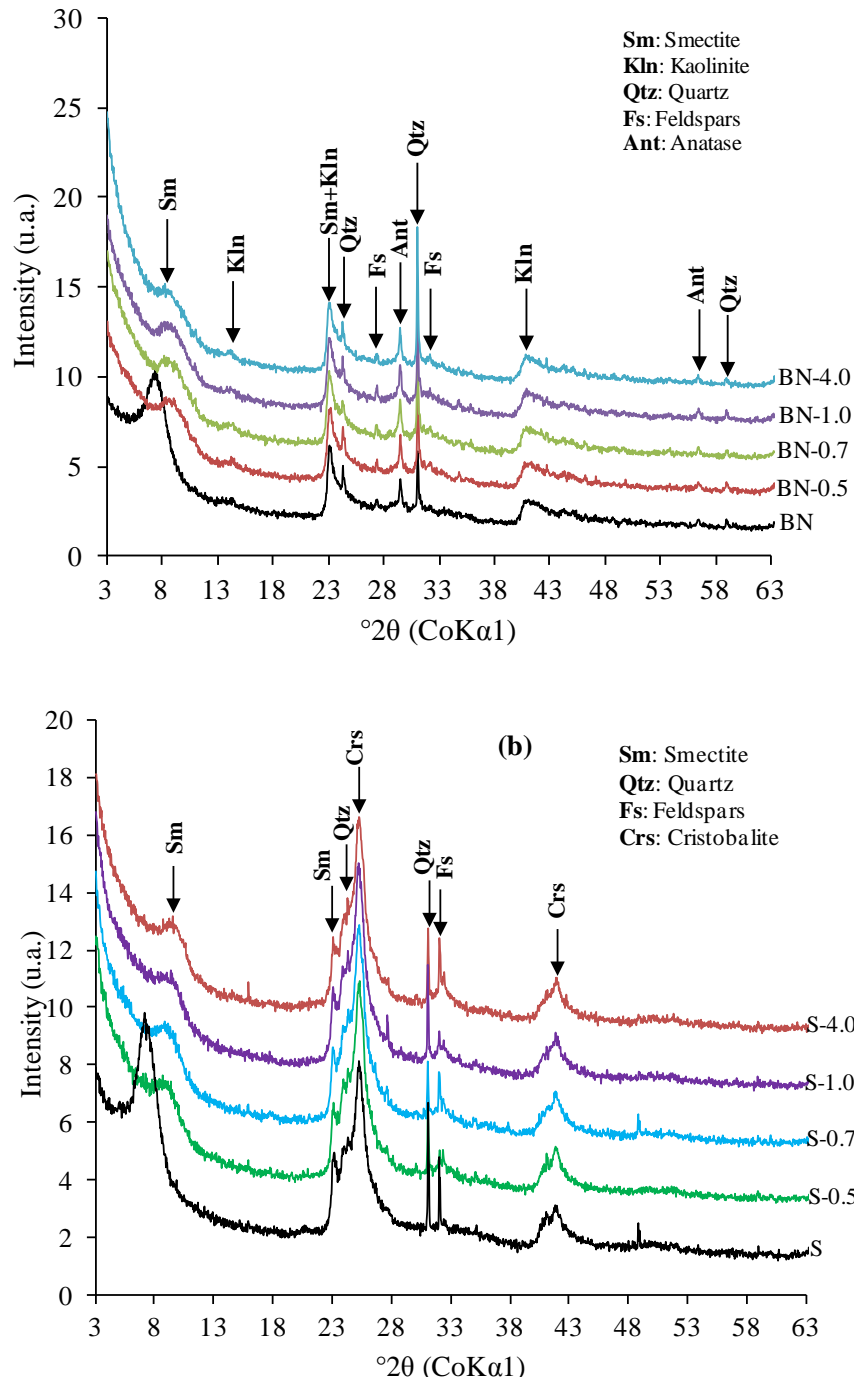


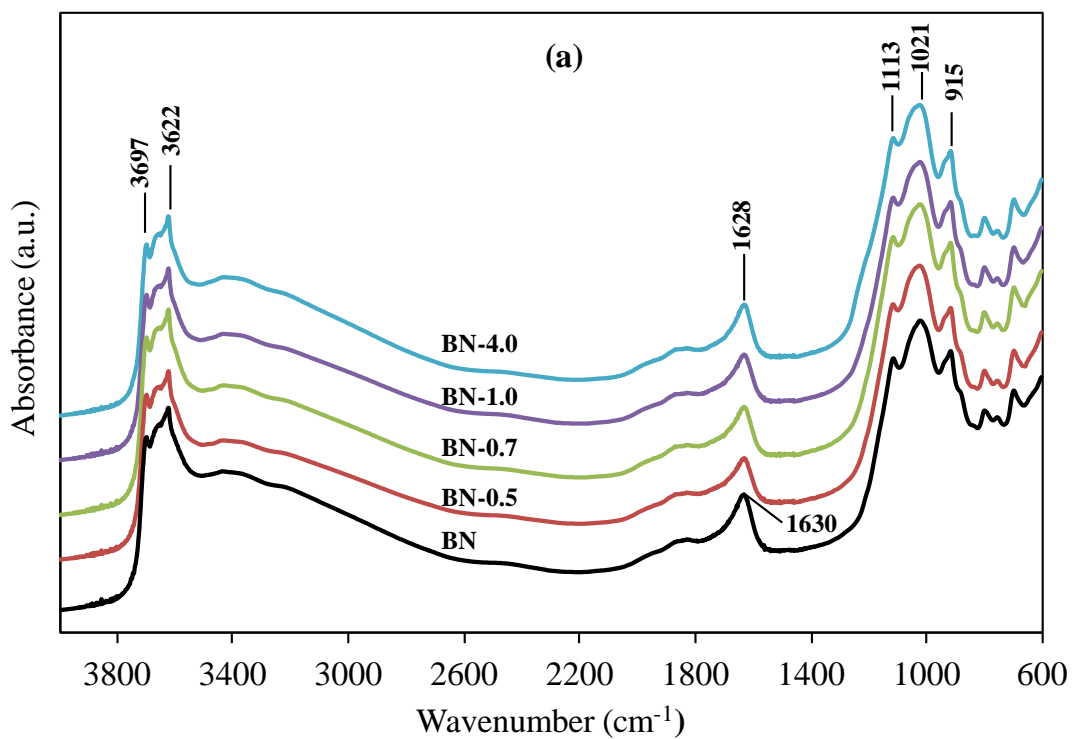
Fig 2. XRD patterns of acid activated clay samples: (a) Bana; (b) Sabga

The effect of acid concentration on the smectite structure is similar in both samples and it can be seen from Fig. 2 that the acid concentration at 4 N causes the most drastic changes. These observations are in agreement with those reported in the literature [8, 25]. Acid activated samples display a slight increase of the background in the range of $21^\circ 2\theta$ and $35^\circ 2\theta$ attributed to the deposition of amorphous products (SiO_2) from the acid attack on the octahedral layer and the exposure of the tetrahedral layer [8, 9]. In the XRD patterns of the acid treated clays from Bana (Fig. 2a), the d_{001} reflection of kaolinite remain unchanged; suggesting that acid activation up to 4 N does not affect its structure. The planes (11l) remain present for the whole range of concentrations used in this work, indicating that clay layers are not fully dissolved during acid treatment. The structural changes due to the treatment of the clays with H_2SO_4 are observed through the shift of d-spacing towards lower values with diminishing of the intensity and smoothing of the main smectite peaks in the diffractograms. This indication of the reduction in the peaks areas indicates the structural changes on the clay. The modification of clays enhances the visibility of the peaks corresponding to quartz, cristobalite and feldspars structures, so, acid activation affect only the smectite mineral. During the acid attack, the protons penetrate into the clay mineral layer of smectite and attack the structural OH groups. The resulting dehydroxylation is due to the successive release of the octahedrally coordinated atoms (Mg, Ca) occurring together with the elimination or substitution of the Al atoms from the tetrahedral sheets.

The X-ray of the two activated clays showed that acid treatment affects the intensity of the basal reflections d_{001} of the smectite; it also causes intense structural modifications and gradual dissolving of the octahedral sheets. However, the crystal structure of the smectite is still partly preserved even after treatment with 4.0 N H_2SO_4 . In the XRD pattern the reflection of associate minerals (quartz, cristobalite, and feldspars) were still detected, because their dissolution was much slower and no additional new phase was observed in the obtained products.

FT-IR spectra of untreated and treated clays are plotted in Fig. 3 and 4. In the O-H stretching domain, untreated and treated clays, depicted by one or two bands, respectively for S and BN samples. The intensity of hydroxyl stretching bands at 3697 cm^{-1} and 3622 cm^{-1} indicates the presence of kaolinite in the BN sample (Fig. 3a); these two bands were still well expressed, suggesting that kaolinite is less sensitive to acid leaching [8]. The band at 3636 cm^{-1} highlighted in Fig. 4a, corresponds to Al-Al-OH stretching of smectite [26]. The intensity of this band decrease with the increase of acid concentration. This progressive decreasing of the

band is related to the removal of octahedral cations, causing the loss of water hydroxyl groups and indicating the dissolution of dioctahedral structure smectite [27]. The bands at 1628-1632 cm⁻¹ (Fig. 3a and Fig. 4a) are attributed to water of hydration for both samples, these bands showed significant decrease in intensity with increasing acid concentration. The progressive widening of the 1021 cm⁻¹ and 1041 cm⁻¹ bands in the spectra of BN and S samples, respectively, were attributed to the Si-O stretching vibration (in-plane). However, the increase in intensity of the bands at 798 cm⁻¹ and 793 cm⁻¹, reveals the formation of amorphous silica (Fig. 3c, 4c) [9, 28].



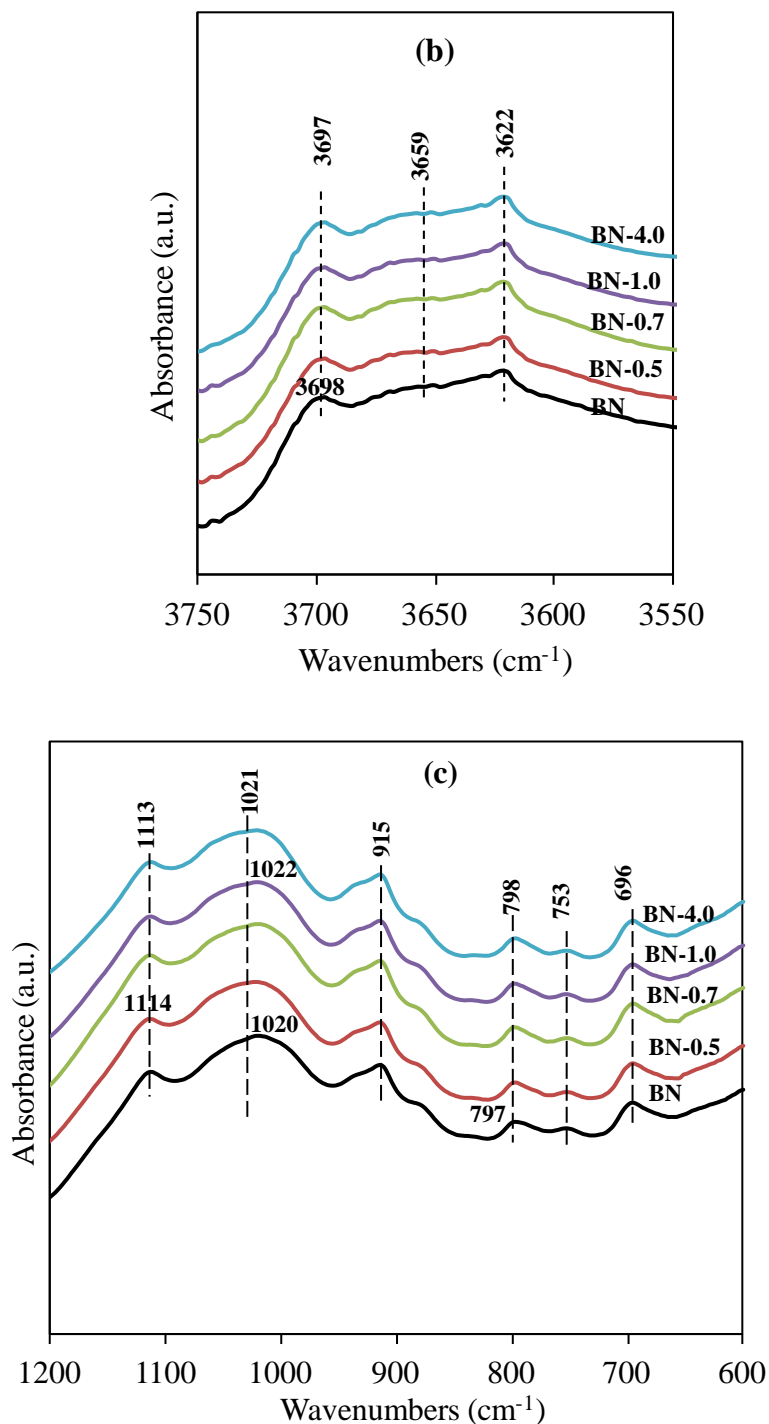
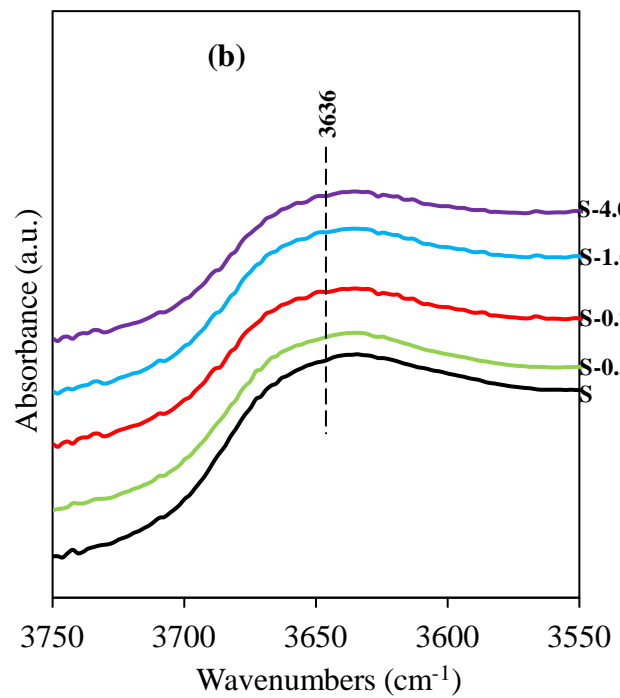
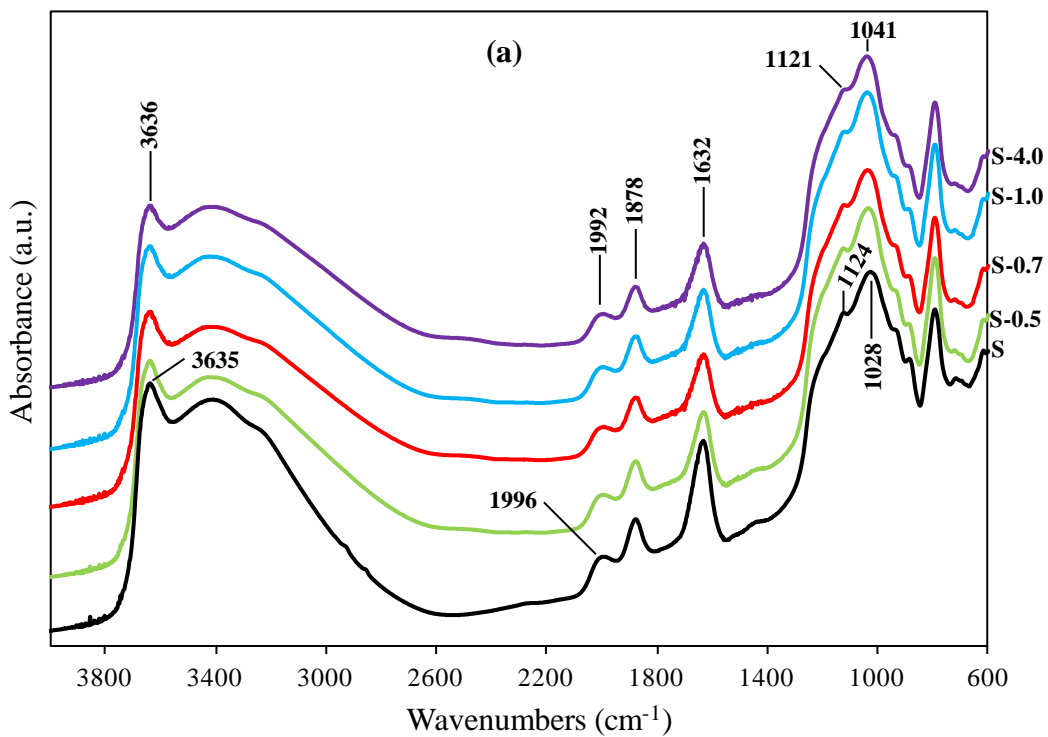


Fig 3. FTIR spectra of natural and activated clay Bana from Bana: (a) complete spectrum; (b) OH stretching domain; (c) Si-O stretching domain



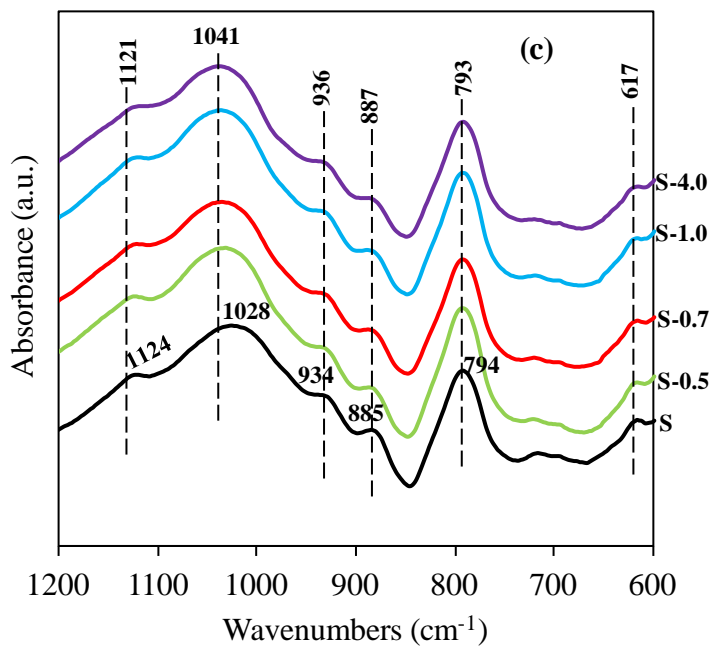
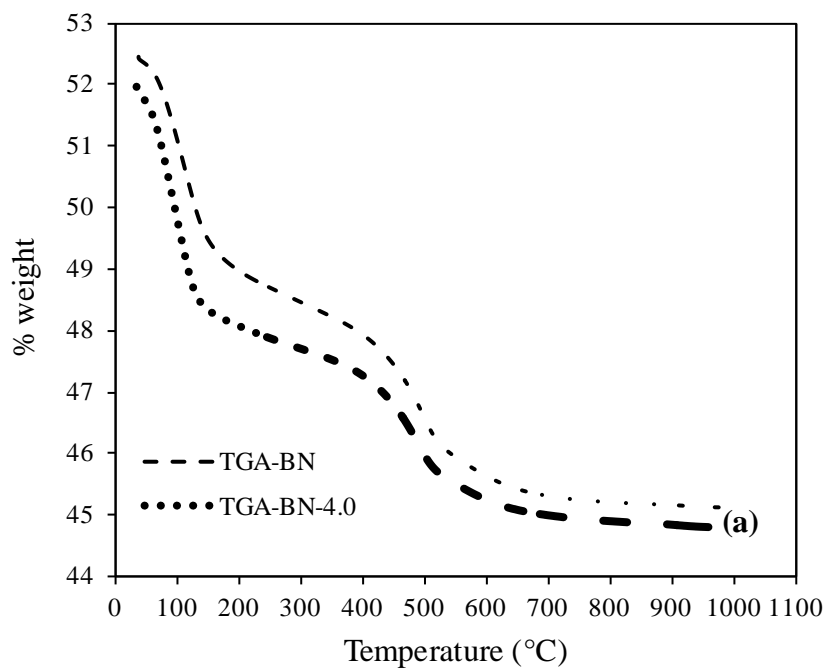


Fig 4. FTIR spectra of natural and activated clay from Sabga: (a) complete spectrum; (b) OH stretching domain; (c) Si-O stretching domain

The weak bands at 1113 cm^{-1} and 1121 cm^{-1} observed in BN and S spectra respectively, were assigned to the Si-O stretching vibration (out-of-plane). The intensity of Al-Al-OH bending bands at 915 cm^{-1} remains constant after treatment with various acid concentrations, suggesting that this band is associated not only with Al-Al-OH vibration of smectite but also with the vibrations of kaolinite [28]. This observation is in agreement with the results of the XRD analysis, which showed the presence of reflection d_{001} of kaolinite and residual of smectite after acid activation up to 4.0 N. The Al-Fe-OH band observed in the spectra of Sg samples (Fig. 4c) at 887 cm^{-1} , during activation, is considerably weaker; suggesting that the leaching of Fe cations in the octahedral sheets increased with acid concentration. The strong band at 793 cm^{-1} associated with cristobalite observed in Sabga clay survives not only the leaching process but increases also in intensity during the acid attack. The presence of cristobalite is clearly shown by XRD patterns. Furthermore, the bands at 696 cm^{-1} in BN samples showed the presence of quartz. The weak absorption band at 617 cm^{-1} observed in S samples can be identified as the perpendicular vibration of the octahedral cations (R-O-Si) where these are light (R=Al, Mg, Fe).

The effect of the acid activation process on the thermal behavior of the two smectite based clays (Fig. 5 and 6) are summarized as follows: (1) the losses of interlayer water is still

observed in the acid treated samples at the temperature near 100 °C; (2) the area of the dehydration (endothermic peaks at about 81 °C) remains essentially unchanged for Sabga sample (Sg) treated at 4N (Fig. 5b). However, the clay sample of Bana (BN) shows a change in the area of the endothermic peak associated with the dehydration of adsorbed water and interlayer water when the clay is treated with 4N acid (Fig. 5a); a total weight loss of 7.3 % and 5.6 %, respectively for untreated and treated clays is observed (Fig. 5a). The intensity of the main dehydroxylation peak at about 490 °C becomes weak when more concentrated acid is used (Fig. 6a). The exothermic peak observed at about 920 °C in the untreated sample due to the decrystallization becomes weaker after H_2SO_4 attack with 4N acid concentration; this result shows that the H_2SO_4 activation decrease the crystallinity of smectite phase in BN samples. For S samples, the two endothermic peaks observed at 490 and 635 °C due to the dehydroxylation of phyllosilicates (smectite) have been preserved in the Sabga treated samples (Fig. 6b), but occur at lower temperatures compared with the untreated sample (435 °C instead of 490 °C and 560 °C instead of 635 °C), the area of the dehydroxylation peaks becomes more diffuse in the treated sample (S), associated with a small weight loss (Fig. 5b).



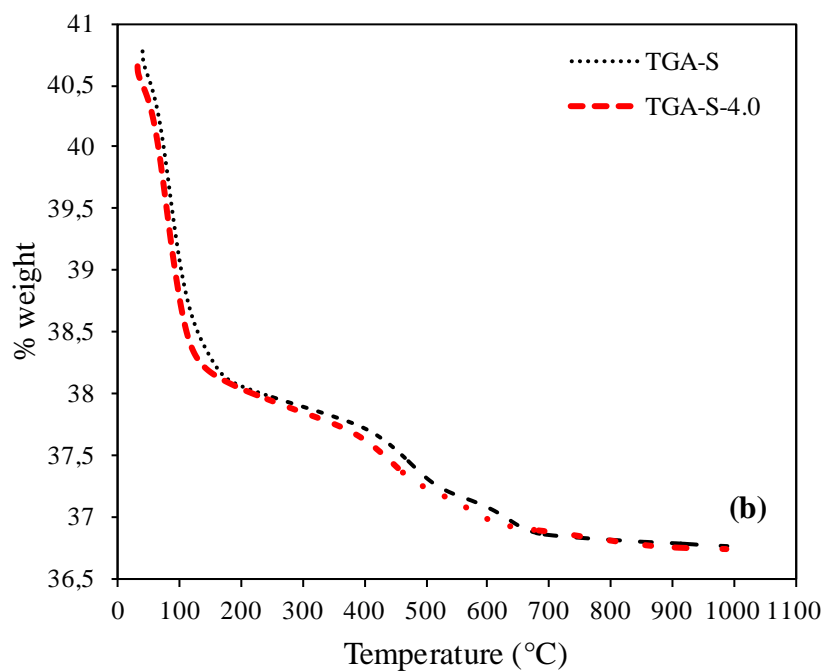
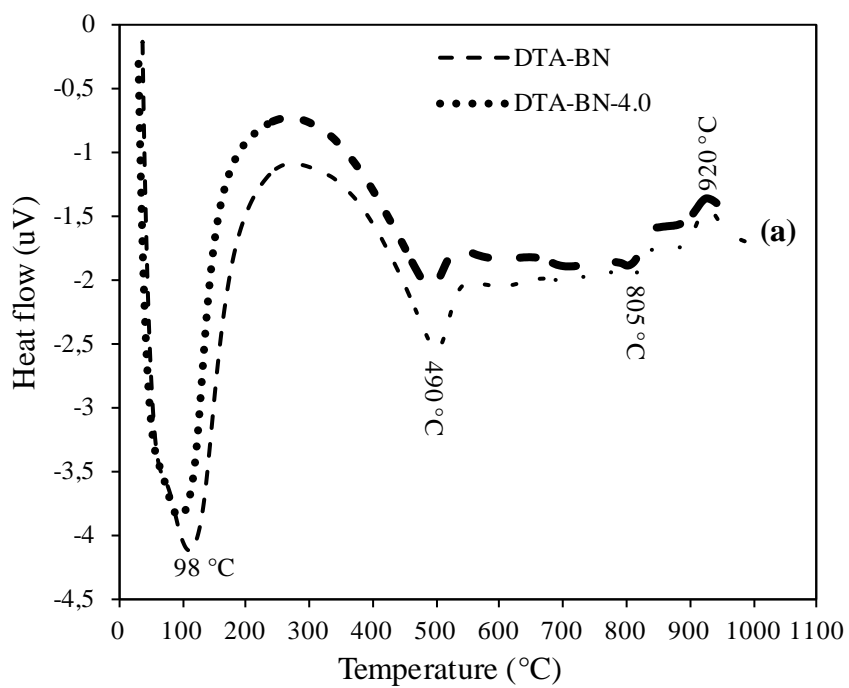


Fig 5. (a) TGA curves of untreated and treated sample “BN”; (b) TGA curves of untreated and treated sample “S”



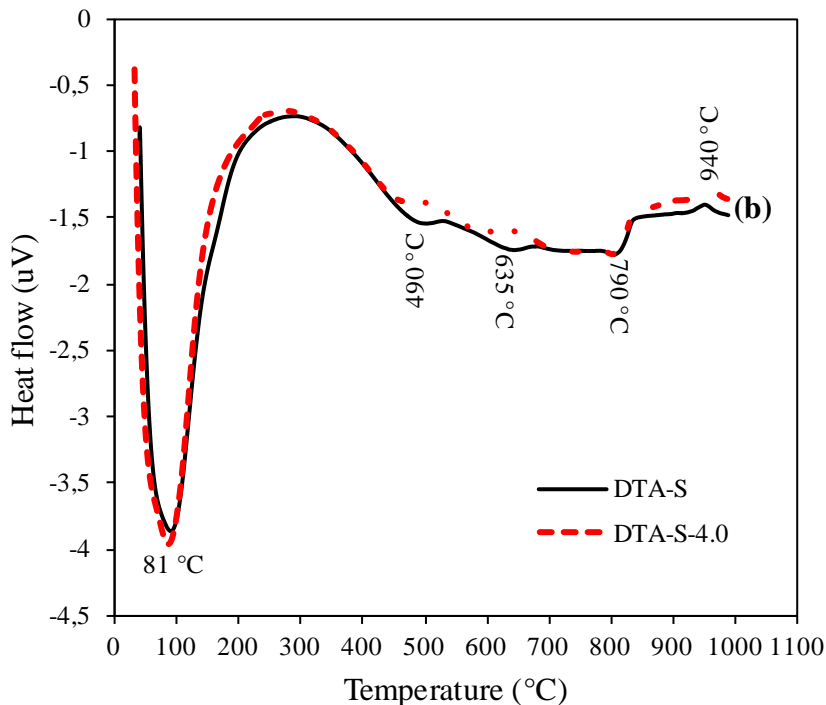


Fig 6. (a) DTA curves of untreated and treated sample “BN”, (b) DTA curves of untreated and treated sample “S”

The total weight loss observed between untreated and treated sample is respectively 4 % and 3.9 %; these weak changes observed during acid treatment in samples (S) confirms that the acid concentrations used in the present study does not destroy completely the structure of smectite phase (see XRD patterns of S sample in Fig 2b).

The crystallinity of the two clay samples decreases continuously with increase acid concentration; this increase affects some physico-chemical properties of clays.

3.2. Chemical evolution of smectites based clays with acid treatment

Major elements, performed by ICP-AES provided evidence of changes in the samples composition after acid treatment (Table 1). By increasing the sulfuric acid concentration from 0.5 to 4.0 N in both clay samples, it can be observed the reduction in the CaO content indicating that the Ca^{2+} cations were replaced by H^+ protons and/or polyvalent cations leached from octahedral sheet. In view of this net reduction during the treatment, Ca^{2+} cations are probably the exchangeable cation in both samples. As acid activation progressed, however, the percentages of Na_2O and K_2O remain almost unchanged while that of SiO_2 increases with increasing acid concentration. The same behavior was observed in the ratio of $\text{SiO}_2 / (\text{Al}_2\text{O}_3 + \text{Fe}_2\text{O}_3 + \text{MgO})$ which increased in both samples up to 4.0 N.

Major elements	BN	BN-4.0	S	S-4.0
SiO ₂	50.94	54.58	73.39	75.57
Al ₂ O ₃	22.39	20.52	11.43	11.00
Fe ₂ O ₃	5.52	4.93	4.83	4.37
MnO	0.01	0.00	0.01	0.00
MgO	1.85	1.76	0.35	0.09
CaO	0.05	< L.D.	0.55	0.11
Na ₂ O	0.02	0.02	0.26	0.25
K ₂ O	0.70	0.71	0.48	0.40
TiO ₂	2.31	2.45	0.17	0.18
P ₂ O ₅	0.26	0.14	0.03	< L.D.
P.F.	16.15	15.26	9.30	8.49
Total	100.20	100.38	100.79	100.46

< L.D.: below detection limit

Table 1. Chemical composition of major elements (% wt) of untreated and treated samples

The unchanged percentages of Na₂O and K₂O are most probably due to the presence of highly stable Na or K-feldspars, these observations were coherent with those revealed by XRD and FTIR analyses. The increase in the relative content of TiO₂ shows that the Ti⁴⁺ cations are located probably at the tetrahedral sites in the 2:1 layers of smectite similar to Si⁴⁺ cations. Samples activated with sulfuric acid caused the increase of the SiO₂ content which is due to remobilization of octahedral cations. The alterations of the original structure of the two clays were observed by the relative decrease in the octahedral sheets oxides such as MgO, Fe₂O₃ and Al₂O₃, but a significant proportion of the octahedral cations remained, following acid activation by 4.0 N H₂SO₄, and suggesting that the layered structure of the smectite clay in the two samples was partially destroyed. The difference in the amounts of the octahedral sheets oxides removed from the samples reflected the possible presence of the cations (Mg, Fe and Al) both in readily soluble or exchangeable forms (e.g. Mg) and in admixtures that are more resistant to acid attack (e.g. feldspars). The loss of ignition at 1100 °C of the activated samples decreases with increasing acid concentration, due to the dehydroxylation of octahedral cations (AlAlOH, AlFeOH and AlMgOH) from the structure smectite, which forms water molecules lost. Similar results were obtained by Gates et al. (2002) and Amari et al. (2010) [21, 29].

The effect of acid concentration on the dissolution of the cations from the two clay samples during acid treatment is shown in Table 2.

Ions	BN	BN-1.0	BN-4.0	S	S-1.0	S-4.0
Ca	0.21	< 120	< 300	2.62	328.85	< 300
Mg	0.05	107.95	208.49	1.09	89.47	< 200
K	0.75	< 200	< 500	1.80	< 200	< 500
Na	-	-	-	1.51	225.76	432.00
Al	0.94	1195	2176	22.43	504	647
Si	33.33	193	774	131	238	470
Fe	0.12	392	904	15.70	464	482
Ti	0.00	0.00	0.00	0.00	0.00	0.00
Cu	-	-	-	0.02	0.25	0.26
Co	0.00	0.34	0.60	0.01	0.27	0.46
Cr	-	-	-	0.00	0.03	0.01
Ni	-	-	-	0.00	0.24	0.54
Pb	0.00	0.53	0.84	0.01	0.49	0.76
Sr	0.00	0.04	0.05	0.00	0.26	0.14
V	0.35	3.98	6.00	0.00	0.00	0.00
Zn	0.01	1.36	1.86	0.14	6.58	7.99

Table 2. Cations leached during acid treatment

The amount of Ca^{2+} , Mg^{2+} , Na^+ and K^+ removed by acid treatment increases as the acid concentration increase up to 4N. The amount of Ca^{2+} , Na^+ , K^+ removal by acid treatment corresponds to the exchangeable cations which are located out of the smectite lattice (between layers), so that they dissolve under mild condition. However, a considerable amount of these elements is still found in the activated clays due to the presence of impurities, mainly feldspar that contains calcium, sodium and potassium, and is resistant to acid attack (see Fig. 2). The amount of Al, Si and Fe removed during acid attack increases with acid concentration (Table 2) and no amount of Ti was determined in the filtrates. This correlates with the XRD patterns which show the presence of anatase, resistant during acid attack.

The variations of the CEC and pH values with the concentration of H_2SO_4 in clay-acid mixture are given in Table 3. The CEC values of the activated materials display similar trends in both materials. It decreases continuously with increasing degree of activation in the two clay samples. This progressive decrease in CEC values upon treatment with sulphuric acid can be understood in terms of the depopulation of the octahedral sheet. In fact, it is well established by [Breen et al., 1995; Falaras et al., 1999](#) that leaching of the octahedral cations (Mg^{2+} , Fe^{2+}) results in reduction of the negative layer charge and therefore of the CEC) [30,

[31\]. Finally, the pH values measured on activated clays are low compared to initial clays, these obtained values are due to the leaching and exchanging divalent or monovalent cations of the interlayer of natural clays by protons \(\$H^+\$ \) during the treatment, these values are in agreement with those of the industrial adsorbents and activated clays measured by Nguetnkam and coworkers \[9\].](#)

Sample	CEC (UV)	CEC (Chem)	Exchange cations measured by atomic absorption (mg/L)							pH
			Na	K	Ca	Mg	Fe	Al	Si	
BN	56	60	0.2	1.5	4.1	2.6	0.04	83.8	2.3	4.2
BN-0.5	53	49	0.5	1.5	0.9	2.7	0.17	62.2	7.2	3.4
BN-0.7	52	50	0.05	0.9	0.89	3.2	0.13	62.2	7.8	3.2
BN-1.0	52	46	0.45	1.2	0.90	3.1	0.13	57.5	7.6	3.2
BN-4.0	46	28	0.10	0.6	0.60	4.6	0.42	31.9	5.4	3.6
S	38	36	0.40	4.5	32.5	15.7	0.00	3.3	1.9	5.8
S-0.5	27	15	0.34	2.71	9.20	4.74	0.13	11.10	2.46	3.9
S-0.7	26	14	0.30	2.43	7.53	3.90	0.09	11.70	2.49	3.7
S-1.0	25	12	0.31	2.32	6.10	3.14	0.06	9.93	2.41	3.6
S-4.0	25	12	0.32	1.73	1.95	1.08	0.07	13.2	2.45	3.2

Table 3. Cation-exchange capacity and pH of natural and activated samples.

3.3. Textural properties, particle size distribution and microstructure

The two natural clays present specific surface areas (SSA) of 65 and 74 m²/g respectively for BN and S. Those values are within the typical surface area values for smectites (50-120 m²/g) [\[32, 33\]](#) and confirm that these two clays consist mainly of very small particles of smectites [\[8\]](#). However it can be observed that the surface area of the both clays increases continuously with acid concentration during the treatment (Table 4). This specific surface increase indicates that the maximum values of this parameter are not reached. The surface area depends on the acid strength. The Bana clay develops great surface area faster than the Sabga clay over the acid treatment. The 4N acid concentration, Sabga and Bana clays display the surface area values of 84 and 134 m²/g, respectively. This is about two times higher than that of the Bana natural clays. We note that the effect of treatment with sulfuric acid is a little stronger on the BN samples, which results in the decrease of microporosity and increase of non-micropores surfaces.

Sample	Specific Surface BET SSA (m^2/g)	Micropores Surface	Non-micropores
		(m^2/g)	Surface (m^2/g)
BET Method		t-plot Method (Boer et al., 1951)	
BN	64.8	28.2	40.8
BN-0.5	76.0	29.5	51.0
BN-0.7	82.6	30.4	56.0
BN-1.0	92.4	32.2	64.3
BN-4.0	134.3	27.6	110.1
S	74.0	18.0	58.7
S-0.5	77.7	19.6	60.7
S-0.7	78.8	19.7	61.6
S-1.0	79.2	21.1	60.9
S-4.0	83.7	26.3	60.6

Table 4. Textural properties resulting from the analysis of N_2 adsorption isotherms of activated clays.

Changes are relatively less evident on sample from Sabga. It was also noted that changes in specific surface areas depending on the concentration are greater for samples BN than samples S. Generally, stronger acid enhances the destruction of the clay improving the specific surface area. However, this destruction also taking into account the impurities that can be vulnerable (e.g. iron oxyhydroxides $\text{Fe OOH}/\text{Fe}_2\text{O}_3$) or acid resistant (e.g. quartz or cristobalite, feldspars, anatase). These impurities may increase or decrease the specific surface area of activated products.

The N_2 adsorption/desorption isotherms at the temperature $\sim 77 \text{ K}$ for natural and acid-treated clay samples are shown in Fig.7. From the results, the adsorption capacity (Q_{ads}) continuously increases with increasing H_2SO_4 content. Such observation can be explained in terms of increasing numbers of pores in the samples. However, no decrease in the adsorption capacity is observed, suggesting that we can extend continue treatment with sulfuric acid concentration higher than 4.0 N. According to the classification described by [Brunauer et al. 1940](#), all the isotherms are similar to Type II, characteristic of mesoporous solids but also contain some micropores [34]. The overlapping of the adsorption-desorption isotherms over the interval $0.35 < P/P^0 < 0$ shows that the multimolecular and monomolecular adsorptions are reversible.

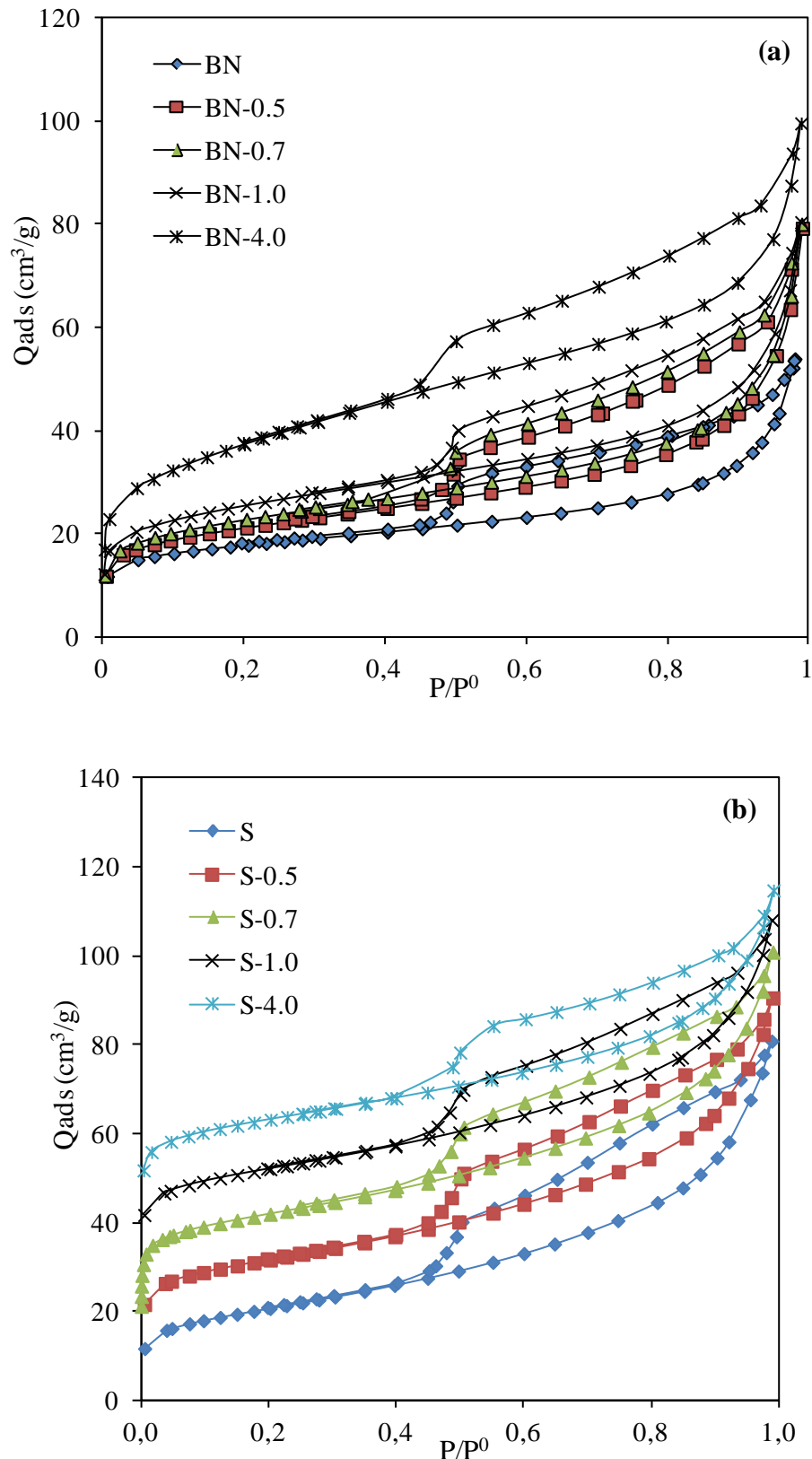


Fig 7. Adsorption/desorption isotherms of nitrogen at 77 K on the treated and untreated clays: (a) Bana samples; (a) Sabga samples

The particle size distribution of the samples is shown in Fig. 8. The BN sample activated with 4.0 N H₂SO₄ exhibits an increased proportion of particles size between 2.2 µm and 45 µm (Fig. 8a). The change is not as important in the sample S as observed in BN (Fig. 8b), suggesting no significant grain size modification during the treatment. The increase of the specific surface of the treated samples with acid can be linked also to increased proportions of grain sizes dissolved during the acid attack. This result is consistent with the specific surface values presented in Table 3.

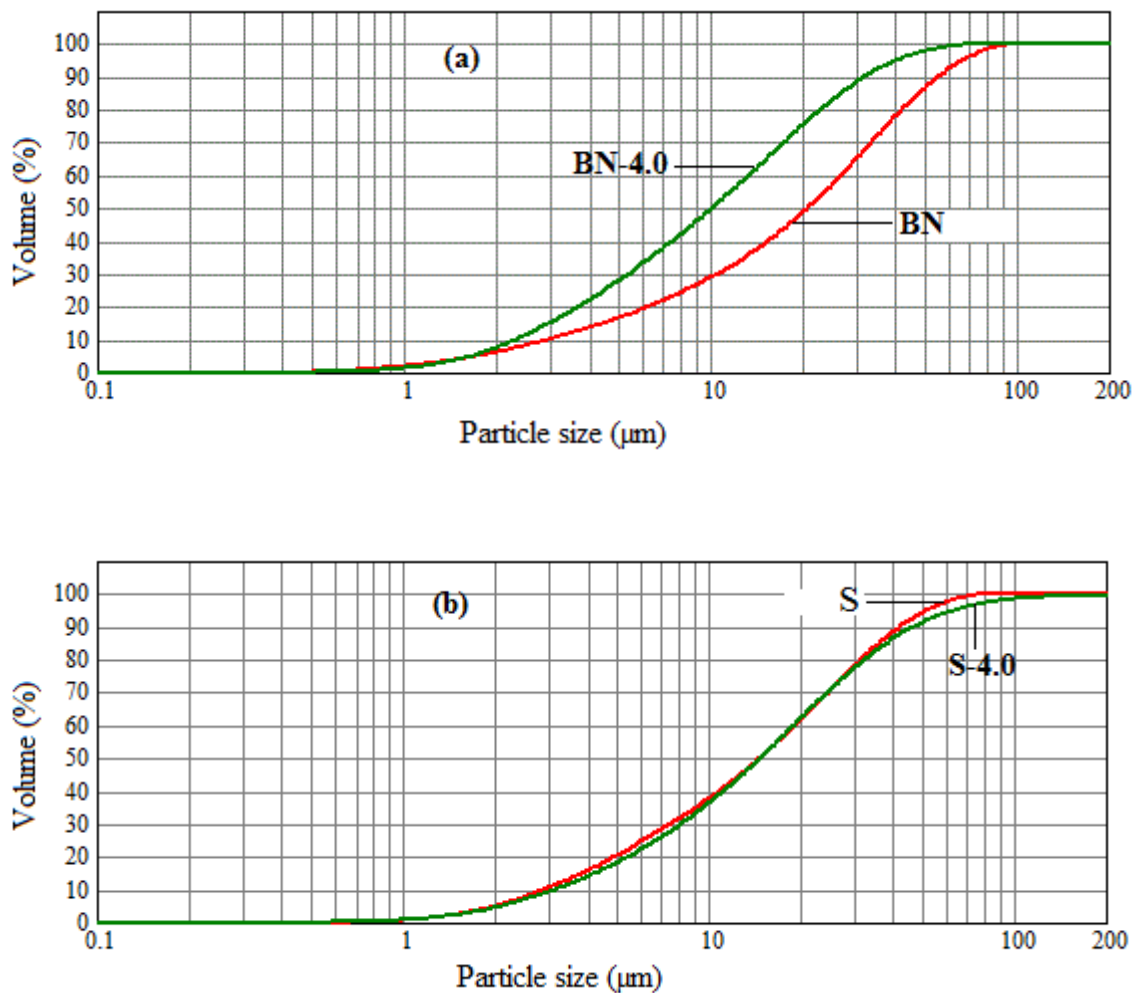


Fig.8. Particle size distribution of the untreated and acid-treated samples

- (a) Untreated (BN) and treated (BN-4.0) samples from Bana
- (b) Untreated (S) and treated (S-4.0) samples from Sabga

In order to confirm the morphological changes between natural and activated clays, scanning electron microscope was used. Fig. 9 shows the wavy subhedral and honeycomb texture of smectite in the untreated samples (N-BN and N-S). After the sulfuric acid treatment to 4.0 N, the wavy subhedral and honeycomb texture of smectites have been replaced by flat flakes (see A-BN and A-S in Fig. 8). These observations are coherent with the results given by XRD analysis on the structural changes of smectite. The black flat flakes observed on treated BN samples (A-BN) are probably the amorphous materials (SiO_2) produced during acid activation and revealed by the relative increase observed for the percentages of SiO_2 oxides in both samples

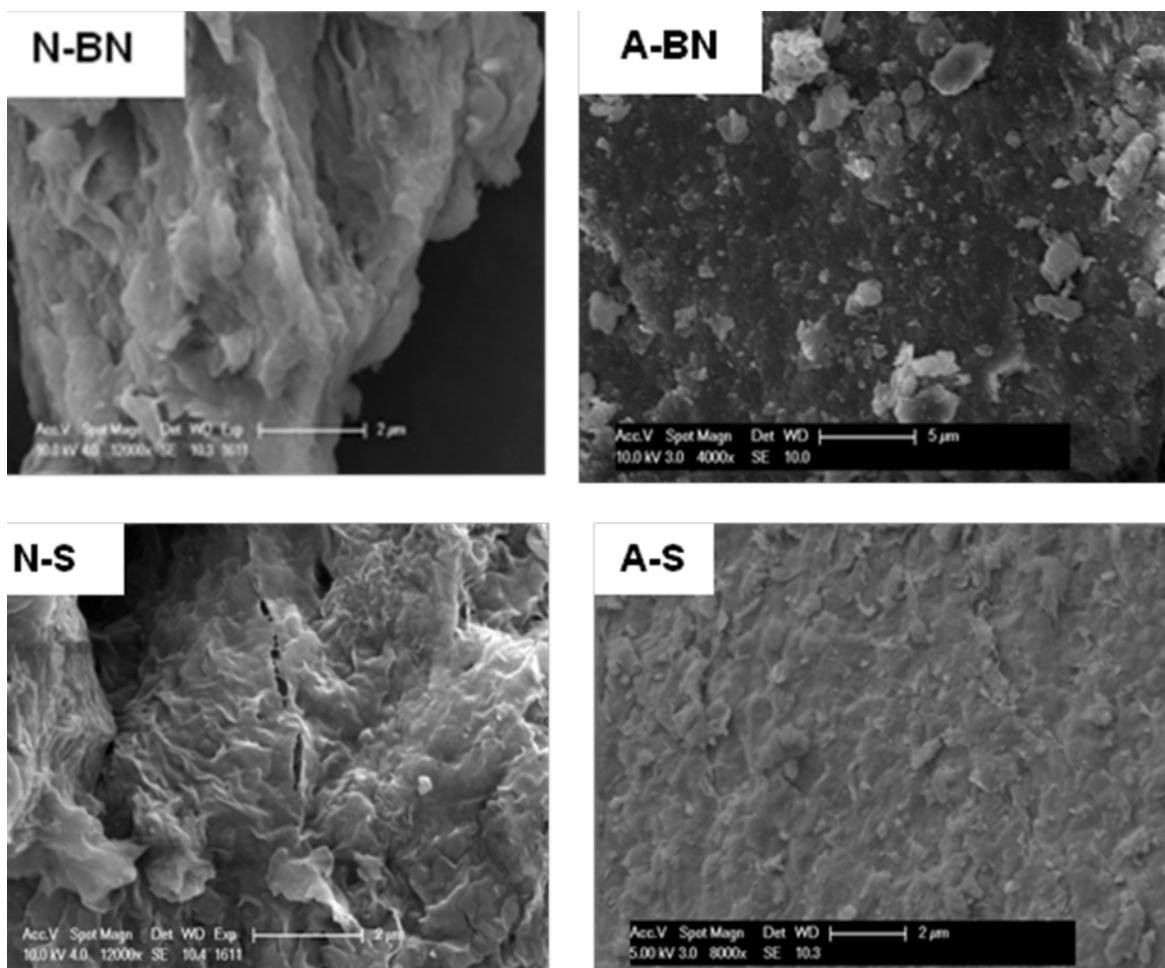


Fig.9. SEM micrographs of the natural and products of acid activation using 4.0 N H_2SO_4 : N-BN and N-S (micrographs of untreated samples from Bana and Sabga, respectively); A-BN and A-S (micrographs of acid-activated samples from Bana and Sabga, respectively)

CONCLUSION

The effect of the acid activation on the physicochemical and mineralogical properties of smectites was evaluated on natural clays from Cameroon. Acid treatment on these clays containing accessory minerals such as quartz, cristobalite, anatase and feldspars led to the following conclusion:

- i) - The X-ray diffraction and Thermal analysis (DTA/TG) showed a progressive decrease in intensity and partial disappearance of basal plane (001) and (020) reflections of smectite. The basal reflection of non-clay minerals remains essentially unchanged; however the intensity of quartz increases. FTIR confirmed that a small amount of smectite survived during the acid treatment, but this treatment degraded the 2:1 layer structure, particularly the octahedral sheets.
- ii) Increase of H_2SO_4 concentration up to 4 N causes increase of cation dissolution (Ca, K, Mg, Na, Al, Fe and Si). No amount of titanium is dissolved during acid treatment, indicating that anatase is not destroyed. In the 2:1 clay minerals, the tetrahedral cations are generally the most resistant to acid attack, followed by the octahedral cations, and the exchangeable cations are the most vulnerable.
- iii)- The specific surface area of acid-activated samples increased with the acid concentration, such that acid activation at 4 N gave rise to a specific surface area $134 \text{ m}^2/\text{g}$ and $84 \text{ m}^2/\text{g}$, respectively for BN and S clay samples; whereas in the untreated samples it was $65 \text{ m}^2/\text{g}$ and $74 \text{ m}^2/\text{g}$. The changes in surface area are associated with changes in the smectite structure over the treatment. This method can be useful for manufacturing a surface active, porous and high surface area materials which can be used for refining oil as well as an adsorbent.

Acknowledgements

This work was carried out under the credit No. O.ACRDGEN 01-17-F-0060- Federal grant for research - research stay abroad in the “Laboratoire Environnement et Minéralurgie” (Nancy, France), financed by the University of Liege. The authors thank the University of Liege for this grant and also Thomas Fabien for instrumental analytical support.

REFERENCES

- [1] M.Ç. Karakaya, N. Karakaya, Ş. Küpeli, Mineralogical and geochemical properties of the Na-and Ca-bentonite of Ordu (Ne Turkey), *Clays Clay Miner.* **59** (2011) 75-94.
- [2] H.H. Murray, Applied clay mineralogy today and tomorrow, *Clay Miner.* **34** (1999) 39-49.
- [3] M. Önal, Y. Sarikaya, Preparation and characterization of acid-activated bentonite powders, *Powder Technol.* **172** (2007) 14-18.
- [4] S. Korichi, A. Elias, A. Mefti, Charaterization of smectite after acid activation with microwave irradiation, *Appl. Clay Sci.* **42** (2009) 432-438.
- [5] G.A. Ikhtiyarova, A.S. Özcan, Ö. Gök, A. Özcan, Characterization of natural- and organo-bentonite by XRD, SEM, FT-IR and thermal analysis techniques and its adsorption behavior in aqueous solutions, *Clay Miner.* **47** (2012) 31-44.
- [6] F. Hussin, M.K. Aroua, W.M.A. Wan Daud, Textural characteristic, surface chemistry and activation of bleaching earth: A review, *Chemical Engineering Journal.* **170** (2011) 90-106.
- [7] A. Steudel, L.F. Batenburg, H.R. Fischer, P.G. Weidler, K. Emmerich, Alteration of swelling clay minerals by acid activation, *Appl. Clay Sci.* **44** (2009) 105-115.
- [8] G.E. Christidis, P.W. Scott, A.C. Dunham, Acid activation and bleaching capacity of bentonites from the Island of Milos and Chios, Aegean, Greece, *Appl. Clay Sci.* **12** (1997) 329-347.
- [9] J.P. Nguetnkam, R. Kamga, F. Villiéras, G.E. Ekodeck, A. Razafitianamaharavo, J. Yvon, Alteration of cameroonian clays under acid treatment. Comparison with industrial adsorbents, *Appl. Clay Sci.* **52** (2011) 122-132.
- [10] J.M. Adams, Synthetic organic chemistry using pillared, cation-exchanged and acid-treated montmorillonite catalysts-a review, *Appl. Clay Sci.* **2** (1987) 309-342.
- [11] C. Breen, Thermogravimetric study of the desorption of cyclohexylamine and pyridine from an acid-treated Wyoming bentonite, *Clay Miner.* **26** (1991) 473-486.
- [12] C.N. Rhodes, M. Franks, G.M.B. Parkes, D.R. Brown, The effect of acid treatment on the activity of clay supports for $ZnCl_2$ alkylation catalysts, *J. Chem Soc. Comm.* (1991) 804-807.
- [13] C.N. Rhodes, D.R. Brown, Structural characterisation and optimisation of acid-treated montmorillonite and high porosity silica supports for $ZnCl_2$ alkylation catalysts, *J. Chem Soc. Faraday Trans.* **88** (1992) 2269–2274.

- [14] C.N. Rhodes, D.R. Brown, Surface properties and porosities of silica and acid-treated montmorillonite catalyst supports: influence on activities of supported ZnCl₂ catalysts, *J. Chem Soc. Faraday Trans.* **89** (1993) 1387-1391.
- [15] C.N. Rhodes, D.R. Brown, Catalytic activity of acid-treated montmorillonite in polar and non-polar reaction media, *Catalysis Letters*. **24** (1994) 285-291.
- [16] P. Komadel, M. Janek, J. Madejová, A. Weekes, C. Breen, Acidity and catalytic activity of mildly acid-treated Mg-rich montmorillonite and hectorite, *J. Chem. Soc. Faraday Trans.* **93** (1997) 4207-4210.
- [17] S. Mahmoud, S. Saleh, Effect of acid activation on the detert-butylations activity of some Jordanian clays, *Clays Clay Miner.* **47** (1999) 481-486.
- [18] R. Fahn, K. Fenderl, Reaction products of organic dye molecules with acid-treated montmorillonites, *Clay Miner.* **18** (1983), 447-458.
- [19] A.J.C. Anderson, P.N. Williams, Refining of oils and fats for edible purposes, Pergamon, New York, 1962.
- [20] M.K.H. Siddiqui, Bleaching Earths. Pergamon, Oxford, 1968, pp.32.
- [21] W.P. Gates, J.S. Anderson, M.D. Raven, G.J. Churchman, Mineralogy of a bentonite from Miles, Queensland, Australia and characterization of its acid activation products, *Appl. Clay Sci.* **20** (2002) 189–197.
- [22] J.Temuujin, Ts. Jadambaa, G. Burmaa, Sh. Erdenechimeg, J. Amarsanaa, K.J.D. MacKenzie, Characterisation of acid activated montmorillonite clay from Tuulant (Mongolia), *Ceram. Int.* **30** (2004) 251-255.
- [23] J.H. De Boer, B.C. Lippens, B.G. Linsen, J.C.P. Brokhoff, A. Van DerHeuvel, T.J. Osinga, The t-cuve of multimolecular N₂ adsorption, *J. Colloid Interface Sci.* **21** (1966), 405-414.
- [24] E.P. Barrett, L.G. Joyner, P.P. Halenda, The determination of pore volume and area distributions in porous substances. I. Computation from nitrogen isotherms, *J. Am. Chem. Soc.* **73** (1951) 373–380.
- [25] E. Srasra, F. Bergaya, H. Van Damme, N.K. Ariguib, Surface properties of activated bentonite: decolorization of rape seed oil, *Appl. Clay Sci.* **4** (1989) 411-421.
- [26] J.Madejová, P. Komdel, B. Cicel, Infrared study of octahedral site populations in smectites, *Clay Miner.* **29** (1994) 319-326.

- [27] B. Tyagi, C.D. Chudasama, R.V. Jasra, Determination of structural modification in acid activated montmorillonite clay by FT-IR spectroscopy, *Spectrochim. Acta A.* **64** (2006) 273-278.
- [28] J. Madejová, FTIR techniques in clay mineral studies, *Vib Spectrosc.* **31** (2003) 1–10.
- [29] A. Amari, M. Chlendi, A. Gannouni, A. Bellagi, Optimised activation of bentonite for toluene adsorption, *Appl. Clay Sci.* **47** (2010) 457-461.
- [30] C. Breen, J. Madejová, P. Komadel, Characterization of moderately acid-treated, size fractionated montmorillonites using IR and MASNMR spectroscopy and thermal analysis, *J. Mat. Chem.* **5** (1995) 469-474.
- [31] P. Falaras, I. Kovanis, F. Lezou, G. Seiragakis, Cotton oil bleaching by acid-activated montmorillonite, *Clay Miner.* **34** (1999) 221-232.
- [32] D.A. Morgan, D.B. Shaw, M.J. Sidebottom, T.C. Soon, R.S. Taylor, The function of bleaching earths in the processing of palm, palm kernel and coconut oils, *J. Am. Oil Chem. Soc.* **62** (1985) 292-299.
- [33] H. Van Olphen, J.J. Fripiat, *Data Handbook for Clay Materials and Other Non-Metallic Minerals*, Pergamon Press, 1979.
- [34] S. Brunauer, L.S. Deming, D.M. Deming, E. Teller, On a theory of the van der Waals adsorption on gases. *J. Am. Chem. Soc.* **62** (1940) 1723-1732.

CHAPITRE IV

EVALUATION DU POUVOIR DECOLORANT DES ARGILES MODIFIEES

Introduction

Ce chapitre présente l'évaluation du pouvoir décolorant des argiles modifiées par activation à l'acide sulfurique tel que rapporté au précédent chapitre. Pour parvenir à cette étude, il a été procédé à la décoloration de l'huile de palme brute par l'emploi des argiles traitées. Ce test de décoloration s'appuie sur les paramètres contrôlables tels que : la température, la masse d'adsorbant utilisée et le temps de traitement. La méthode spectrophotométrique U.V-visible a permis de déterminer l'absorbance des huiles brutes et traitées afin de calculer le pouvoir décolorant de nos adsorbants et d'en apprécier leur efficacité. Enfin, nous avons procédé à un contrôle de la qualité de huiles ainsi traitées par deux méthodes d'analyses couramment utilisées en contrôle de qualité à savoir : la spectroscopie infrarouge à transformée de Fourier et la chromatographie gazeuse couplée à la spectroscopie de masse (CG-MS). Les résultats de cette étude sont présentés à la section (§IV.2) ci-dessous sous la forme d'un article en préparation.

IV.1. Résumé de l'article

Une argile riche en smectite dioctaédrique activé avec de l'acide sulfurique a été étudiée afin d'évaluer son pouvoir décolorant vis-à-vis de l'huile de palme. L'effet des paramètres tels que la masse d'argile, le temps de traitement et de la température sur l'efficacité des argiles activées à décolorer l'huile de palme a été suivi. Les résultats ont montré que la concentration en acide utilisé pour l'activation de l'argile présente un effet remarquable, par rapport aux autres paramètres. Il a été constaté que le pouvoir décolorant des matériaux activés augmente avec la masse de l'adsorbant, la durée et la température de traitement. Dans les conditions optimales de l'activation dudit matériau (c-à-d concentration en acide sulfurique 4.0 N), sa capacité de décoloration est de 87% lorsque la durée de traitement, la température et le pourcentage en masse d'argile utilisée étaient de 120 min, 97°C et 5 %, respectivement. Le pouvoir décolorant naturel de ce matériau est faible comparé aux matériaux traités avec de l'acide sulfurique. Ceci est dû au fait que la structure protonée de l'argile activée par un acide sert de site de fixation du bêta-carotène, tandis que la structure non protonée présente moins

de site actif donc peu efficace pour la décoloration de l'huile de palme. Les analyses par spectroscopie FT-IR et chromatographie en phase gazeuse couplée à la spectrométrie de masse (GC-MS) révèlent que les échantillons d'huiles de palme traitées ne sont pas détériorés au cours du processus de décoloration.

IV.2. Bleaching Performance of acid-activated smectite clays from Bana (West Region of Cameroon)

Mache J.R^{1,2,3,*}, Signing P², Mbey J.A⁴, Barres Odile⁵, Faure Pierre⁵, Thomas F⁴, Njopwouo D², Fagel N¹

¹ UR AGES Argiles, Géochimie et Environnements sédimentaires, Département de Géologie, Université de Liège, B18, Allée du 6 Août, B-4000 Liège, Belgique

² Laboratoire de Physico-chimie des Matériaux Minéraux, Département de Chimie Inorganique, Université de Yaoundé 1, B.P. 812 Yaoundé, Cameroun

³ Mission de Promotion des Matériaux Locaux, B.P 2396 Yaoundé, Cameroun

⁴ Laboratoire Interdisciplinaire des Environnements Continentaux, UMR 7360 CNRS-Université de Lorraine, 15 Avenue du Charmois, B.P. 40. F-54501, Vandoeuvre-lès-Nancy Cedex, France

⁵GéoRessources, UMR 7359 CNRS-Université de Lorraine - Faculté des Sciences et Technologies - BP 70239 - 54506 Vandoeuvre, France

ABSTRACT

Clay-rich smectite from Bana in the West region of Cameroon was activated with sulphuric acid solutions of 0.5 to 4.0 N at 80 °C for 2 hours. In this present study, we investigated the bleaching capacity of these acid-activated clay materials to bleach palm oil. The effect of parameters such as dosage, contact time and temperature upon the acid-activated clays effectiveness in the bleaching of palm oil was investigated. Acid concentration used for clay sample activation has the strongest effect, in or by comparison to the others parameters. Bleaching power of activated clays increased with increase in dosage, time and temperature of treatment. At the optimal conditions of activation (4.0 N H₂SO₄), the bleaching power was found to be 87 % when the bleaching time, temperature and dosage were 120 min, 97°C and 5%, respectively. The bleaching capacity of natural clay sample is significantly lower than acid-activated clays. The protonated structure of acid-activated clays develops many active sites for bonding beta-carotene, while the structure unprotonated of the natural clay presents less active site therefore low efficiency in bleaching palm oil. FT-IR spectroscopy and Gas Chromatography coupled with Mass Spectrometry (GC-MS) analyses indicate that the bleached palm oils are not deteriorated during the bleaching process.

Keywords: smectite clays, palm oil, bleaching power, adsorption kinetic

1. INTRODUCTION

Palm oil is one of the major oils consumed not only in African continent regions, but also in Asian region and in numerous countries in the worldwide under various forms (Salawudeen et al., 2007). The color of the crude palm oil is naturally red-yellow mainly due to beta-carotene. It contains free fatty acids, triglyceride and minor components such as carotenoids, phospholipids, tocopherols, sterols, metals at trace concentrations, and other pigments like chlorophyll (Goh et al., 1985; Puah et al., 2004). These substances degrade the quality of the oil by alteration of its taste and color. They also affect the color attraction and reduce the market value. The purity characteristics (acidity, color, etc.) desirable in edible oil can be obtained by removing pigments such as β -carotene and other undesirable substances during the refining processing (Rossi et al., 2001, 2003). Bleaching process is performed in order to prepare a sufficiently light-coloured product of enhanced appearance and improved stability. However, bleaching process requires the uses of materials with a strong adsorption power (Falaras et al., 199). The principle of bleaching is based on several adsorption mechanisms including physical adsorption through van der Waals' forces, chemical bonding via covalent or ionic bonds, ion exchange, molecular trapping and chemical decomposition (Pritchard, 1994). During the bleaching process, colouring pigments (primarily carotenoids and chlorophylls), peroxides and other color bodies are removed from the palm oil by decreasing the levels, they can also remove traces of metals (such as Cu^{2+} , Fe^{3+}), phospholipids, soap, oxidation products and to minimize the increasing of free fatty acid during bleaching (Falaras et al., 199; Zhansheng et al., 2006; Didi et al., 2009). The materials used in the bleaching processing or "bleaching earths" are usually smectites activated with sulfuric or chlorhydric acids (Christidis et al., 1997; Kirali and Lacin, 2006; Makhoukhi et al., 2009; Taha et al., 2011). In fact, the efficiency of the acid-activated montmorillonite as bleaching earth in the processing of vegetable oils has been demonstrated by several studies (Morgan et al., 1985), which exhibit a wide range of chemical and physical properties depending on the degree of activation.

Edible vegetable oil refining factories in Cameroon represent the main industries, which consume the bleaching earth satisfied by import. Since most bleaching earths or clays are imported from China, South-Africa, Germany and England, it is imperative to find the clay materials locally to reduce the importation of bleaching earth.

In a previous work, we reported an acid activation procedure of dioctahedral smectite mainly consist of montmorillonite from Bana with various H_2SO_4 concentrations and

evaluated the effect of this treatment on the mineralogical and physico-chemical properties. Important physical changes were clearly visible in acid-activated clays, such as the increase of specific surface area and surface micropores, depending on acid concentration. The purpose of this present study was to evaluate the bleaching performance of these acid-activated clays in the bleaching process of palm oil.

2. MATERIALS AND METHODS

A dioctahedral smectite consists mainly of montmorillonite named BN used in this present study was collected from Bana (west Region of Cameroon). The crude palm oil (designated as CPO) was bought from local market provided by SOCAPALM Co (Cameroon). All chemical used were analytical reagent grade, obtained from Merck Company.

2.1. Pretreatment of adsorbents

The < 63 µm fractions of sample BN were separated by wet sieving, decantation and subsequently dried at 110°C; after drying, the clay sample was reduced by gentle grinding in an agate mortar. Adsorbents were prepared from the < 63 µm fraction samples with sulfuric acid concentration of 0.5, 0.7, 1.0 and 4.0 N at 80°C for 2 hours. The acid-activated samples were characterized in the previous study ([Mache et al. submitted](#)). The resulting solids obtained were designated as BN-0.5, BN-0.7, BN-1.0 and BN-4.0. The natural sample was named as BN. Table 1 shows the physico-chemical properties of natural and activated clays.

Parameters	BN	BN-0.5	BN-0.7	BN-1.0	BN-4.0
BET SSA (m ² /g)	64.8	76.0	82.6	92.4	134.3
Micropores Surface (m ² /g)	28.2	29.5	30.4	32.2	27.6
Non-micropores Surface (m ² /g)	40.8	51.0	56.0	64.3	110.1
CEC (U.V) ¹	56	53	52	52	46
CEC(Chem) ²	60	49	50	46	28
pH	4.2	3.4	3.2	3.2	3.6

Table 1. Physico-chemical properties of natural and activated clays

¹ : CEC (U.V): derived from the measurement of cobaltihexamine concentrations by U.V-visible spectroscopy

² : CEC (Chem): derived from analysis of displaced cations

2.2. Bleaching process

For the bleaching experiment, 10 g of CPO was placed in 300 mL jacketed glass reactor equipped with water circulation thermostated at the predetermined temperature (80°C, 90°C and 97°C). When the reactor had reached the required temperature (20 minutes) a known amount of adsorbent (% by mass of the palm oil) previously dried at 110°C for 4h was added to the reactor. The mixing was continuously stirred during 5 to 120 minutes. After the oil treatment, the bleaching earth (acid-activated samples) is removed by filtration through Whatman no.1 filter paper.

2.3. Analyses of bleaching performance

2.3.1. Bleaching capacity

Bleaching of crude palm oil removes some pigments by adsorption. β -carotene is the main predominant pigment responsible of red/yellow color in the palm oil and other color is caused probably by chlorophyll. The maximum absorbance wavelength and absorbance of β -carotene values were determined by using a SHIMAZU UV PC 2100 spectrophotometer. About 50 mg of oil was dissolved in 5 mL acetone and the absorbance was measured between 350 to 700 nm (Fig.1). The bleaching capacity (BC) percentage of the adsorbents was determined by applying the following equation ([Falaras et al., 1999](#)):

$$\text{BC (\%)} = ((A_0 - A) / A_0) \times 100$$

Where A_0 and A are the absorbance of the crude and bleached palm oil, respectively, at the maximum absorbance wavelength of the crude oil (449 nm).

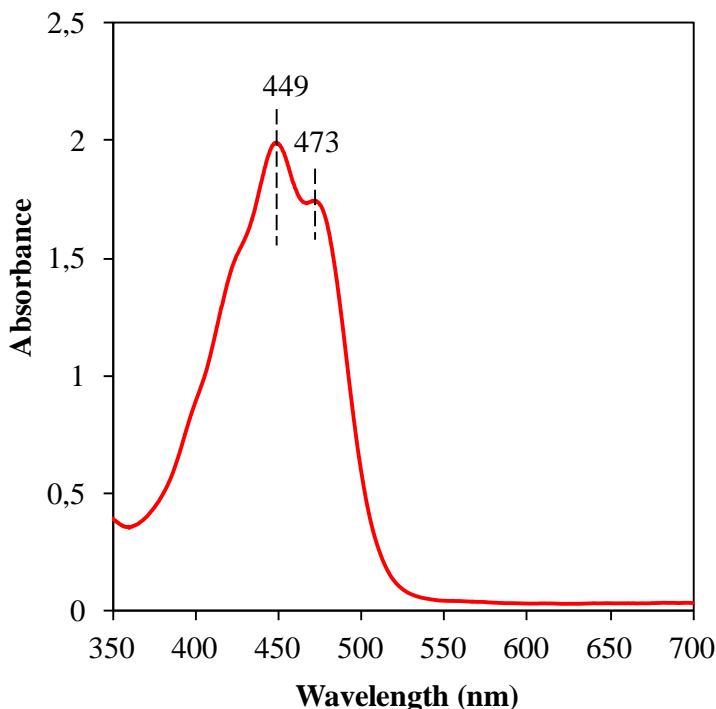


Fig. 1. Maximum absorbance wavelength of crude palm oil (CPO).

2.4. Fourier Transform Infra Red (FTIR) Spectroscopy

Transmission infra-red spectra were recorded on the crude and bleached palm oil using a Fourier Transform Infrared Spectrometer Bruker IFS 55 equipped with a DTGS detector (Laboratoire Environnement et Minéralurgie, Nancy, France). The samples were prepared by depositing and spreading one drop of oil with a dropper on a ZnSe window. The spectra were recorded from 4000 cm^{-1} to 450 cm^{-1} with a resolution of 2 cm^{-1} by accumulating 64 scans (around 1 min).

2.5. Gas Chromatography-Mass Spectrometry (GC-MS)

Organic compounds were analyzed by Gas Chromatography-Mass Spectrometry (Agilent technologies 6890 GC coupled to an Agilent technologies 5973 Inert mass spectrometer) equipped with a split-splitless injector and a 60 m DB-5 J&W, 0.25 mm i.d, 0.1 m film fused silica column (Géologie et Gestion des Ressources Minérales et Energétiques, Nancy, France). The temperature program was 60 to $300\text{ }^{\circ}\text{C}$ at $3\text{ }^{\circ}\text{C}.\text{min}^{-1}$ followed by an isothermal stage at $315\text{ }^{\circ}\text{C}$ for 15 min (constant helium flow of $1,4\text{ mL}.\text{min}^{-1}$).

Because of the presence of carboxylic acids, silylation using BSTFA + TMCS 99/1 (v/v) was carried out to improve chromatographic resolution (Wenclawiak et al., 1993). A small aliquot of sample was dissolved with the derivative solution at 4 mg mL⁻¹ and treated during 15 minutes at 50 °C. Then, 1 µL solution was directly injected into the gas chromatograph. Compounds were identified according to their mass spectra and retention time with reference to the Wiley and U.S. National Bureau of Standards computerized mass spectral libraries.

3. RESULTS AND DISCUSSION

3.1. Effect of acid concentration on the bleaching of crude palm oil

Figure 2 shows that the bleaching capacity increases with sulphuric acid (0; 0.5; 0.7; 1.0 and 4.0 N) concentration at constant temperature (80 °C), when the same mass of clay samples (5 % by mass of oil) were used and during 75 minutes. The increase in bleaching power with H₂SO₄ acid concentration is a result of the number of active sites or acidic centers of the clays which increase during activation. The active sites or acidic centers play an important role in bleaching performance of clays. Hussin et al. (2011) stated that adsorption of β-carotene is catalysed by the Bronsted and Lewis acidity over the bleaching process.

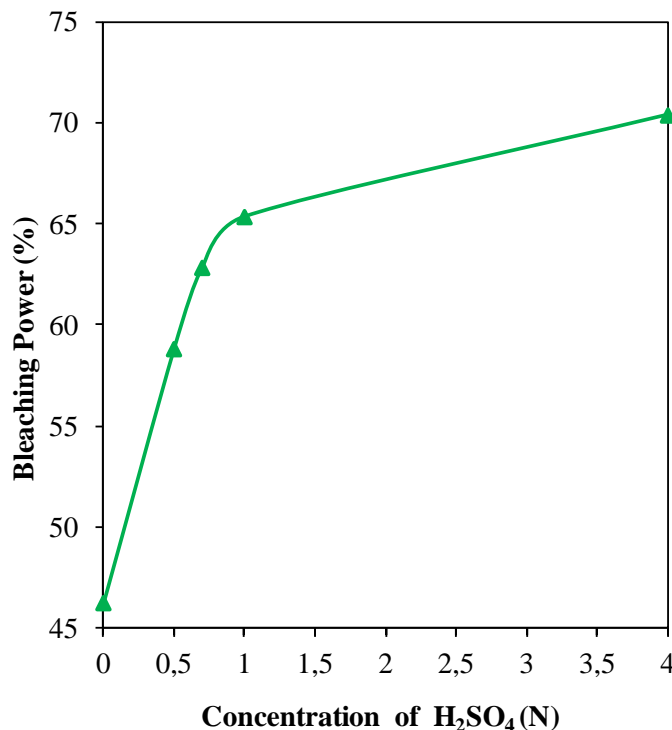


Fig. 2. Effect of acid concentration on the bleaching of crude palm oil

Falaras et al. (1999) were indicated that such behaviour is not unexpected, and Morgan et al. (1985) suggested that pigments such as β -carotene can either be adsorbed directly onto a cation to form a chemisorbed complex. This complex reacts directly with the protonic centres present on the clay surface. In a similar way, one could suppose that the protonated clay framework, highly hydrophilic in character, probably attracts the polar pigments. Our results indicate that enhanced Brønsted surface acidity and surface area (see Table 1) are the main factors in bleaching efficiency of clay-rich montmorillonite.

The acid-activated samples are more efficient bleaching agent than natural sample. The sample treated at 4.0 N presented the highest bleaching power, in relation to a significant increase of the specific surface area. These results are in agreement with those obtained by Didi et al. (2009). The bleaching power of the untreated clay is 47 %. It increases in parallel with the acid concentration from 58 % for 0.5 N to 72 % for 4.0 N.

3.2. Effect of dosage on the bleaching of crude palm oil

The bleaching power of the natural and treated clays as a function of adsorbent mass percentage for decolourization crude palm oil is represented in Fig. 3. The clay dosage was varied from 0.1 g to 1.5 g (1 % - 15 % by mass of palm oil). The bleaching power increases with increase in mass percentage of adsorbent. For those experiments the temperature was fixed at 80°C over contact times of 75 minutes. The experiment was reported with different acid concentration. The changes in bleaching capacity are attributed to the occurrence of more and more active sites created by the exchange of interlayer cation by proton (Komadel, 2003). The protonated structure of acid-activated clays serves as an effective binding site for β -carotene. The unprotonated structure presents less effective active site. The results clearly indicate that the bleaching efficiency increases with the value at adsorbent dosage and acid concentration. This could be explained by the fact that adsorption equilibrium has not been reaching between the adsorbent/oil mixtures, thereby, the active sites are also present for further pigment removal by the excess adsorbent dosage.

Our experiments allow identifying the optimal conditions for the application of Bana clays in bleaching process i.e. activated clay with 4.0 N H₂SO₄ has the best decolouration

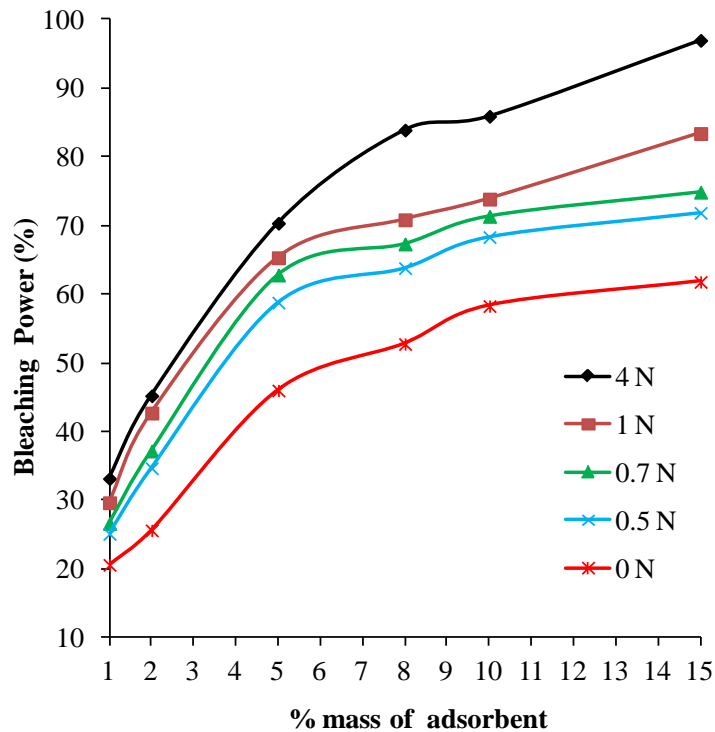


Fig. 3. Effect of dosage on the bleaching of crude palm oil

3.3. Adsorption kinetic of crude palm oil

The kinetic adsorption curves of β -carotene from crude palm oil were carried out at 80 °C, 90 °C and 97 °C with a clay/oil ratio of 5 %. The sample used for this kinetic is the most efficient activated clay (4.0 N sulphuric acid solutions). The adsorption curves (Fig. 4) obtained during the kinetics studies are different for each temperature. The bleaching power of the treated clay varies in parallel with the temperature. The decolorization of the crude palm oil is faster in the first 20 minutes and progresses slower after. After 15 minutes, activated clay shows similar bleaching power (~ 60%) for the lower temperatures (80 °C and 90 °C). At the same time, the bleaching power reaches 73 % at 97 °C. The increase in the bleaching power with temperature is high. The gap value of bleaching power was clearly observed and progresses after the first 15 minutes between the temperature 80 and 90 °C. This gap value of bleaching power measured between 80 and 97 °C temperatures is about 20 %. For all selected temperature, the decolorization efficiency was stabilized after about 90 minutes of bleaching time. The bleaching power calculated from the selected temperature (see Fig. 4) can be ranked in the order: 87 % (97 °C) > 78 % (90 °C) > 70 % (80 °C).

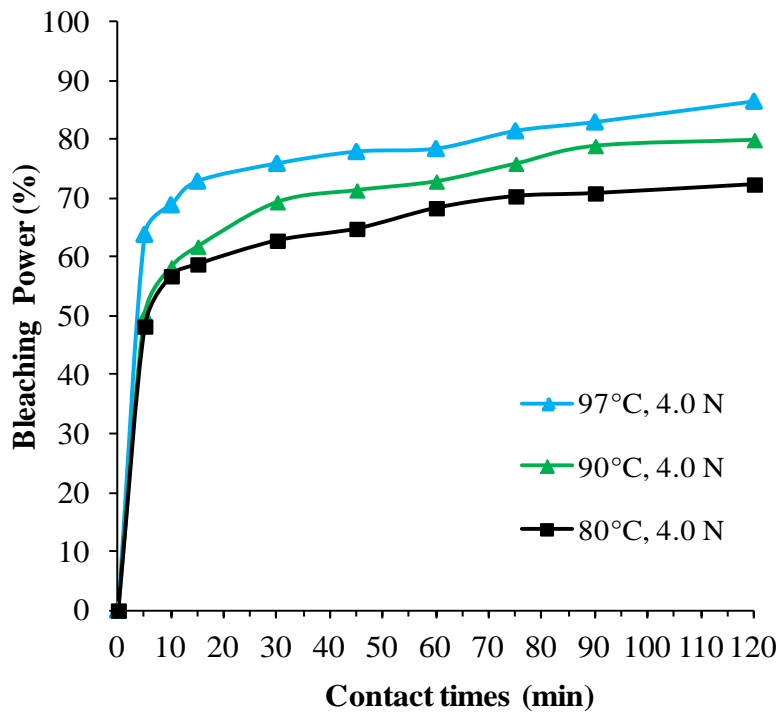


Fig.4. Kinetics of crude palm oil bleaching at 97 °C, 90 °C and 80 °C by acid-activated BN clays at 4.0 sulphuric acid.

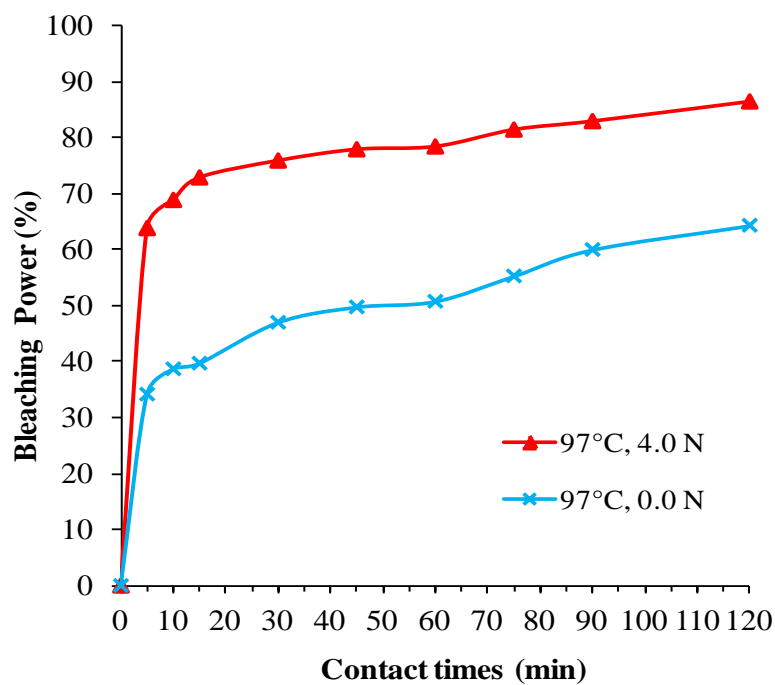


Fig.5. Kinetics of crude palm oil bleaching at 97°C with natural and acid-activated BN clays

The sulphuric acid activation affects the bleaching efficiency of clay sample (Fig. 5). The gap value observes between the bleaching capacity of natural and activated clay reached up to 40 %.

Visible spectra of the crude palm oil and oil samples bleached with acid-activated clay (BN-4.0) at various temperatures are presented in Fig. 6. These absorption spectra were performed in the wavelength domain between 350 nm and 700 nm. The spectrum of crude palm oil (CPO) is characterized by two absorption maxima at 449 nm and 473 nm for beta-carotene, respectively. These absorption bands decrease in bleached palm oil spectra. The intensity is less and less with temperature increases, the peak almost disappear after bleaching crude oil sample at 97 °C. The effects of the temperature on the performance of the acid-activated clay in the absorption spectra increase in parallel with bleaching temperature. The absorbance of crude and bleached palm oil obtained at various temperatures can be ranked in the order: $A_{\text{CPO}} > A_{\text{BPO} (80 \text{ }^{\circ}\text{C})} > A_{\text{BPO} (90 \text{ }^{\circ}\text{C})} > A_{\text{BPO} (97 \text{ }^{\circ}\text{C})}$. The removal of the β -carotene pigment increases with increasing bleaching temperature.

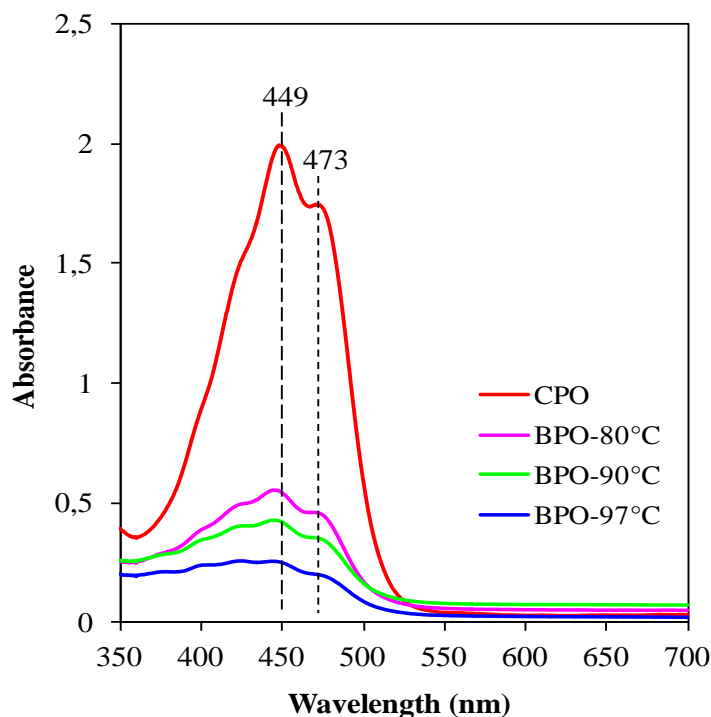


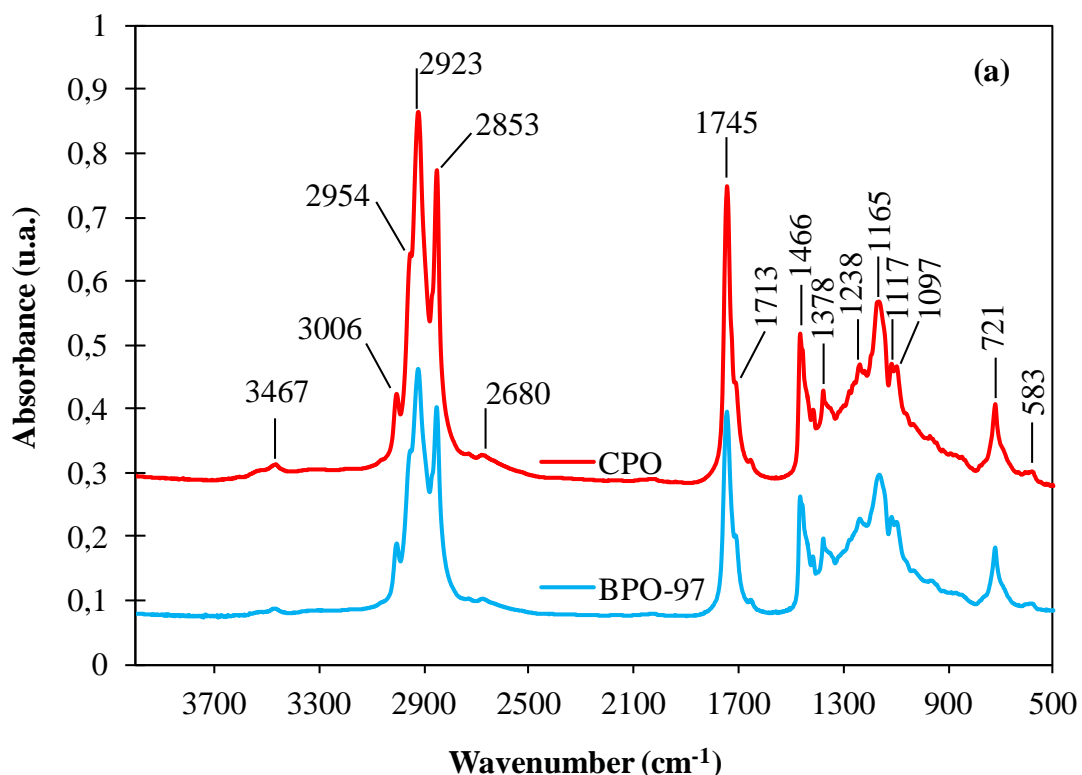
Fig.6. Absorbance spectra of crude palm oil (CPO) and palm oil bleached (BPO) at 97 °C, 90 °C and 80 °C with activated sample at 4.0N (BN-4.0).

Based on the kinetic curves of decolouration (Fig. 4), the temperature and the contact time were the parameters affecting the performance of adsorbents. These kinetic curves allow to determine the optimal temperature and the contact time for decolouration of crude palm oil. The natural clay from Bana has a low bleaching power compared to those activated with sulphuric acid. This study confirms that acid-activated clays play an important role in bleaching crude palm oil procedure. However, it is very important to check if the use of activated clays affects the quality of the bleached oil.

3.4. Analysis of oils

In order to evaluate the effect of bleaching process on the quality of palm oil, we investigate the spectral features of palm oil before and after treatment using FT-IR transmission spectra (Fig. 7).

Each infrared absorption band corresponds to a functional in the studied oil samples



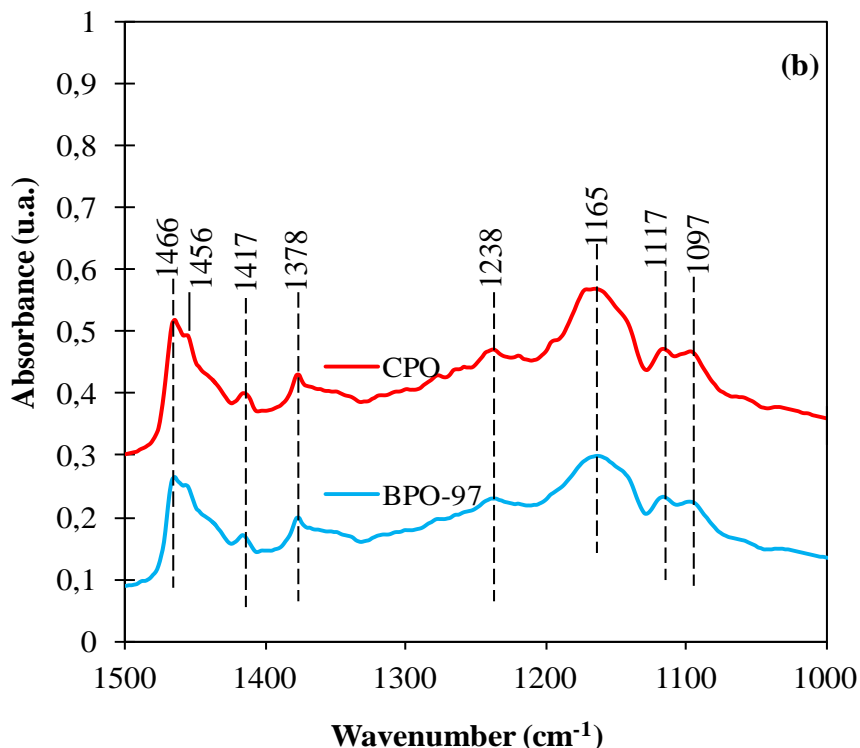


Fig. 7. FT-IR transmission spectra of crude palm oil (CPO) and bleached palm oil (BPO) with activated clay (BN-4.0) at 97 °C: (a) complete spectra; (b) Region at 1500-1000 cm⁻¹

The vibration at 3467 cm⁻¹ observed in both spectra is assigned as the OH stretching ([Albuquerque et al., 2003](#)).

The vibration band at 3006 cm⁻¹ in the spectrum of crude palm oil is attributed as the CH stretching related to =C-H bonding. Similar vibration with increased intensity was also observed for the bleached oil, this vibration is in agreement with CH stretching related to =C-H in the molecule of oleic acid.

The weak band at 2954 cm⁻¹ is assigned to the asymmetric stretching vibration of CH₃ group. In both oil samples, it can be seen the two intense bands at 2923 or 2924 cm⁻¹ and 2853 cm⁻¹ attributed to CH₂ asymmetric and symmetric stretching vibrations, respectively. However, the intensity of these bands is higher in the crude palm oil than the bleached oil.

The absorbance peak at 1745 cm⁻¹ assigned to the double bond stretching vibration C=O of the carboxylic groups. It appears around the same absorbance for methyl ester and triglycerides. Hence, the observation of this band in the spectra of the crude and bleached palm oils indicates the presence of the ester function.

The weak band at 1653 cm^{-1} is assigned to a C=C stretching vibration (present in both spectra). The 1466 cm^{-1} band is attributed to CH₂ scissors deformation vibration. The peak at 1378 cm^{-1} in the spectrum of crude palm oil attributed to C-H bond in methyl (-CH₃) group is higher than the same peak in the spectrum of bleached palm oil. The band between 1300 and 1200 cm is ascribed to the CH₂ wagging band progression resulting from the wagging vibrations of all-trans conformers. A broad 1165 cm^{-1} band is attributed for the ester CO-O single bond stretching vibration. However, the intensity of this band is higher in the spectrum of crude palm oil than the spectrum of bleached oil. It probably indicated that there was decreasing amount of ester group during the bleaching.

The bands at 1117 cm^{-1} and 1098 cm^{-1} are probably due to the stretching vibrations of ether linkage in triacylglycerols ([Guillen and Cabo, 1997](#)). These peak heights were shown to be inversely related with proportion of saturated acyl groups and oleic acyl groups, respectively ([Jaswir et al., 2003](#)). Crude palm oil displays approximately equal proportion of saturated acyl groups and oleic acyl groups which was reflected in the spectrum, in which peaks of 1117 and 1098 cm^{-1} appeared as having the same height. In the bleached oil spectrum, the same equal heights of peaks are also observed, suggesting that the studied oils were similar in terms of proportion of saturated acyl groups and oleic acyl groups.

Finally the band at 721 cm^{-1} (present in both spectra) is probably due to the presence of fatty acids and triglycerides; it is assigned to the CH₂ rocking mode.

Both spectra appear very similar but they revealed slight differences in bands intensities and the exact frequencies at which the maximum absorbance were generated in each oils, due to the proportion of different molecules content of studied oils ([Guillen and Cabo, 1997](#)), especially at wavenumber regions of 2923 , 2853 , 1745 , 1466 and 1165 cm^{-1} .

In crude and bleached palm oil, GC-MS analysis was performed to identify the components. The results of the analysis of studied oils before and after bleaching process with natural and activated clay sample (BN-4.0) are shown in table 4 and 5, respectively. Major fatty acid molecules were identified in the crude palm oil such as palmitic acids (C16:0) that have no double bond; oleic acids (C18:0) that have one double bond (C18:1) and two double bonds (C18:2). The identified fatty acids in the crude palm oil are clearly observed in the bleached oils, suggesting that the treated oils still contain the same constituents in terms of fatty acid molecules.

Components	Retention time (min)	Relative abundance (%)
Palmitic acid methyl ester, C16:0	31.89	41.1
Linoleic acid methyl ester, C18:2	36.80	11.6
Oleic acid methyl ester, C18:1	37.26	41.0
Stearic acid methyl ester, C18:0	37.79	6.4

Table 4: Result of GC-MS analysis of crude palm oil

Components	Relative abundance (%)		
	Oil bleached with natural clay (BN)	Oil bleached with activated clay (BN-4.0)	Standards CODEX
Palmitic acid methyl ester, C16:0	42.8	42.8	38.0 - 43.5 ⁴
Linoleic acid methyl ester, C18:2	10.0	9.8	10.0 - 13.5 ⁴
Oleic acid methyl ester, C18:1	40.4	40.9	39.8 - 46.0 ⁴
Stearic acid methyl ester, C18:0	6.7	6.5	3.5 - 6.0 ³

Table 5: Result of GC-MS analysis of palm oil after decolorization with natural and activated clay samples

Compared to the crude palm oil, bleached oils by natural or activated clay samples present slight variation in terms of proportion. However the proportions of the various constituents of the treated oils in Table 5 remain in the range of fatty acids by ([CODEX STAN 210-1999⁴ amended in 2011](#)). The calculation of various indices of oils (Table 6) shows that these values

³ : www.alimentation-sante.org/wp-content/.../Presentation_Hd-P_1112.pdf (consulté le 13/05/2013)
 État des lieux - L'huile de palme : aspects nutritionnels, sociaux et environnementaux - novembre 2012
 Fonds Français pour l'Alimentation et la Santé

⁴ : www.codexalimentarius.org/input/download/standards/CXS_210f.pdf (consulté le 13/05/2013)

don't vary significantly. These results are coherent with those obtained by FTIR, which indicate the lower decreasing of the intensity band of some functional groups.

Indices			
	Crude palm oil	Oil bleached with natural clay (BN)	Oil bleached with activated clay (BN-4.0)
C18/C16	1.4	1.3	1.3
(C18//) / (C18/)	0.3	0.2	0.2
(C18//+C18)/(C18)	8.2	7.5	7.8

Table 6: Result of GC-MS analysis of palm oil before and after decolourization with natural and activated clays

The slightly indices variation in treated oils compared to the crude oil confirms the lower variation in terms of proportion of fatty acids in the treated oils.

Finally, the bleaching process by activated and natural clays does not degrade the nature of palm oil.

CONCLUSION

Our experiment evaluates the bleaching capacity of clay-rich smectite from Bana (West Region of Cameroon). The bleaching capacities of clays attack with H_2SO_4 solutions were higher than the natural clay (BN). An increase of acid concentration improves the bleaching capacity of clay samples. The most efficient bleaching capability of these clay-rich smectite was obtained by activating the clays with 4.0 N of sulphuric acid. Activation allows to increase effective bleaching agent in palm oil treatment.

FTIR spectroscopy and Gas chromatography-mass spectroscopy (CG-MS) attest the stability of bleached oil compared to the crude palm oil. The bleached oil with activated clay (BN-4.0) does not undergo degradation during processing.

The dioctahedral smectite clay collected from Bana in the western region of Cameroon can be converted into efficient potential agent for bleaching palm oil, and thus can represent an alternative solution to the importation of bleaching earths for our local refining palm oil industries.

REFERENCES

- Albuquerque, M.L.S., Guedes,I., Alcantara Jr. P., Moreira, S.G.C., 2003. Infrared absorption spectra of Buriti (*Mauritia flexuosa* L.) oil. *Vibrational Spectroscopy*, **33**, 127-131.
- Christidis, G.E., Scott, P.W., Dunham, A.C., 1997. Acid activation and bleaching capacity of bentonite from the Islands of Milos and Chios, Aegean, Greece. *Applied Clay Science*, **12**, 329–347.
- Didi, M., Makhoukhi, B., Azzouz, A., Villemin, D., 2009. Colza oil bleaching through optimized acid activation of bentonite: A comparative study. *Applied Clay Science*, **42**, 336-344.
- Falaras, P., Kovanis, I., Lezou, F., Seiragakis, G., 1999. Cottonseed oil bleaching by acid-activated montmorillonite. *Clay Minerals*, **34**, 221-232.
- Guillen, M.D., Cabo, N., 1997. Characterization of edible oils and lard by Fourier transform infrared spectroscopy: Relationships between composition and frequency of concrete bands in the fingerprint region. *Journal of the American Oil Chemists' Society*, **74**, 1281-1286.
- Goh, S.H., Choo, Y.M., Ong, S.H., 1985. Mineral constituents of palm oils. *Journal of the American Oil Chemists' Society*, **62**, 237-240.
- Hussin, F., Aroua, M.K., Wan Daud, W.M.A., 2011. Textural characteristic, surface chemistry and activation of bleaching earth: A review. *Chemical Engineering Journal*, **170**, 90-106.
- Jaswir, I., Mirghani, M.E.S., Hassan, T.H., and Said, M.Z. 2003. Determination of lard in mixture of body fats of mutton and cow by Fourier transform infrared spectroscopy. *Journal of Oleo Science*, **52**, 633-638.
- Kirali, E., Lacin, O., 2006. Statistical modeling of acid activation on cotton oil bleaching by Turkish bentonite. *Journal of Food Engineering*, **75**, 137-141.
- Komadel, P., 2003. Chemically modified smectites. *Clay Minerals*, **38**, 127-138.
- Mache, J.R., Signing, P., Mbey, J.A., Razafitianamaharavo, A., Njopwouo, D., Fagel, N. (Submitted). Acid activation of smectite clays from Cameroon: Effect on mineralogical and physico-chemical properties.
- Makhoukhi, B., Didi, M. A., Villemin, D., Azzouz, A. 2009. Acid activation of bentonite for use as a vegetable oil bleaching agent. *Grasasy Aceites*, **60** (4), 343-349.

- Morgan, D.A., Shaw, D.B., Sidebottom, M.J., Soon, T.C., Taylor, R.S., 1985. The function of bleaching earths in the processing of palm, palm kernel and coconut oils. *Journal of the American Oil Chemists' Society*, **62**, 292-299.
- Pritchard, J.L.R., 1994. *Analysis of Oilseeds, Fats and Fatty Foods*. (D. Rossell, editor) Elsevier, Amsterdam.
- Puah, C. W., Choo, Y. M., Ma, A. N., Chuah, C., 2004. Degumming and Bleaching: Effect on selected Constituents of palm oil. *Journal of Oil Palm Research*, **16** (2), 57-63.
- Rossi, M., Gianazza, M., Alamprese, C., Stanga, F., 2001. The Effect of Bleaching and Physical Refining on Color and Minor Components of Palm Oil. *Journal of the American Oil Chemists' Society*, **78**(10), 1051-1055.
- Rossi, M., Gia Naza, M., Alan Presc., Stanga, F., 2003. The Role of Bleaching clays and synthetic silica in palm oil physical Refining. *Food Chemistry*, **82**, 291 – 296.
- Salawudeen, T.O., Dada, E.O., Alagbe, S.O., 2007. Performance Evaluation of Acid Treated Clays for palm Oil Bleaching. *Journal of Engineering and Applied Sciences*, **2**(11), 1677-1680.
- Taha, K.K., Suleiman, T.M., Musa, M.A., 2011. Performance of Sudanese activated bentonite in bleaching cotton seed oil, *J. Bangladesh Chem. Soc*, **24** (2), 191–201.
- Wenclawiak BW, Jensen TE, Richert JFO. (1993) GC/MS-FID analysis of BSTFA derivatized polar components of diesel particulate matter (NBS SRM-1650) extract. *Fresenius Journal of Analytical Chemistry*, **346**, 808-812.
- Zhansheng, W., Chun, L., Xifang, S., Xiaolin, X., Bin, D., Jin'e, L., Hongsheng, Z., 2006. Characterization, Acid Activation and Bleaching Performance of Bentonite from Xinjiang. *Chinese Journal of Chemical Engineering*, **14**, (2), 253-258.

CONCLUSIONS GENERALES ET PERSPECTIVES

Cette thèse avait pour objectif global de contribuer au projet de valorisation des matériaux argileux du Cameroun. L'approche suivie comporte quatre objectifs spécifiques: Le premier consistait à identifier et collecter les échantillons dans les zones potentiellement riches en argiles. Le deuxième portait sur la caractérisation de ces matériaux sur le plan minéralogique et physico-chimique. Le troisième objectif spécifique était de procéder à un traitement de ces argiles par l'acide sulfurique à diverses concentrations et de caractériser les produits dérivés. Enfin, dans le quatrième objectif spécifique, évaluer le pouvoir décolorant de ces matériaux à l'état naturel et activé dans la décoloration de l'huile de palme.

Les localités de Bana et Sabga, respectivement dans les régions de l'Ouest et Nord-ouest Cameroun ont fait l'objet de prospection et de collectes des échantillons. Elles se situent sur la ligne volcanique du Cameroun, zones potentiellement riches en matériaux argileux. La caractérisation minéralogique des matériaux argileux collectés dans les zones d'études par des méthodes classiques (diffraction de rayon X, spectroscopie infrarouge et analyse thermique) a permis d'identifier les minéraux argileux et non-argileux. Les matériaux de Bana sont constitués de quartz, d'anatase et de feldspath potassique comme impuretés. Ceux collectés à Sabga sont constitués en termes de minéraux non-argileux de cristobalite, feldspath potassique, ilménite et d'heulandite. Les fractions argileuses des échantillons de Bana sont constituées de la smectite dioctaédrique comme minéral argileux dominant qu'accompagnent la kaolinite et le mica. Un test de saturation au lithium a permis d'identifier la nature montmorillonitique de la smectite dioctaédrique. Dans les fractions argileuses de Sabga le principal minéral argileux est une montmorillonite avec de la kaolinite comme minéral associé dans certains échantillons. La composition chimique, déterminée par spectrométrie d'émission atomique (ICP-AES), montre que les principaux oxydes sont SiO_2 , Al_2O_3 et Fe_2O_3 . Dans les argiles de Bana, les proportions en oxydes majeurs sont dans l'ordre (49-53 %) SiO_2 ; (22-24 %) Al_2O_3 et (6-9 %) Fe_2O_3 avec un rapport $\text{SiO}_2/\text{Al}_2\text{O}_3$ de 2,3. Les teneurs faibles en MgO varient entre 1,5 % et 2,8 %, tandis que les teneurs en TiO_2 (2,2 %) restent constantes dans tous les échantillons. Les argiles de Sabga comportent une teneur élevée en SiO_2 (66-70 %), Al_2O_3 (13-16 %) et Fe_2O_3 (3-7 %). Le rapport $\text{SiO}_2/\text{Al}_2\text{O}_3$ de l'ordre de 4 à 5 indique le caractère plus sableux de celles-ci par rapport aux argiles de Bana. Les capacités d'échanges cationiques des matériaux varient de 50 à 62 méq/100 g pour

les argiles de Bana et de 38 à 46 méq/100 g pour celles de Sabga. Les valeurs de pH des matériaux argileux des deux zones d'études sont quasi identiques ($\text{pH} \sim 5,0 \pm 0,1$). Les surfaces spécifiques déterminées à partir des isothermes d'adsorption-désorption d'azote à 77 K par la méthode de BET donnent des valeurs de l'ordre de 50 à 62 m^2/g pour les argiles de Bana et 33 à 90 m^2/g pour celles de Sabga.

L'activation par diverses concentrations d'acide sulfurique a provoqué au sein des matériaux argileux des modifications structurales observées sur les diffractogrammes de rayons X. Une diminution progressive d'intensité de la réfection (001) de la montmorillonite et un déplacement de leur distance basale ont été observées sur les argiles traitées avec de l'acide sulfurique. L'observation morphologique des argiles activées par la microscopie électronique à balayage (MEB) montre que la texture en nid d'abeilles et la forme ondulée de la montmorillonite ont été remplacée par des flocons plats suite à l'activation acide. Le traitement acide a également entraîné une diminution de la capacité d'échange cationique (CEC) des argiles au fur et à mesure que la concentration en acide utilisée augmente. La surface spécifique de l'argile activée augmente jusqu'à doubler pour l'argile de Bana traitée avec 4,0 N H_2SO_4 . Cette augmentation de surface spécifique est peu marquée dans l'échantillon d'argile de Sabga. L'activation acide qui procède par un remplacement des cations interfoliaires par le proton H^+ , a favorisé une augmentation de la teneur en silice et de la surface spécifique des argiles étudiées.

L'efficacité de l'argile de Bana à l'état naturel à décolorer l'huile de palme a été effectuée à 97 °C, avec un pourcentage de 5% par rapport à la masse d'huile et pendant une durée de 90 minutes. Le pouvoir décolorant de ce matériau sur l'huile de palme est de 55 %, cette capacité de décoloration est faible comparée aux adsorbants industriels couramment utilisés dans le processus de raffinage d'huile de palme comestible. C'est pour cette raison que l'étude cinétique de décoloration a été réalisée à différentes températures (80°, 90° et 97° C), avec 5 % d'argile activée et pour un temps de contact variant entre 5 et 120 minutes. Il ressort de cette étude que le pouvoir décolorant de l'argile de Bana augmente avec la concentration en acide pour atteindre une valeur maximale à 4,0N, cette augmentation est d'autant plus marquée que la température de traitement augmente. L'étude cinétique a permis de déterminer les conditions optimales de décoloration. L'argile de Bana activée à une concentration de 4,0 N H_2SO_4 exhibe une capacité de décoloration de 87 % lorsque le pourcentage d'argile utilisée est de 5 % par rapport à la masse d'huile à 97 °C pendant 120 minutes.

Riche en smectite dioctaédrique (montmorillonite) et possédant une performance dans la décoloration de l'huile de palme, cette argile pourra être un matériau de rechange aux adsorbants industriels importés, d'autant plus qu'elle ne fait pas subir à l'huile de palme une détérioration dans sa composition.

A l'issue de cette étude, quelques axes qui mériteraient des approfondissements apparaissent. A titre d'illustration, il serait intéressant, pour une meilleure compréhension des smectites de Bana et Sabga, de procéder à la détermination de la formule structurale de la montmorillonite par des analyses chimiques ponctuées sur la fraction argileuse (analyse à la microsonde électronique). La prospection des argiles dans d'autres localités des régions de l'Ouest et Nord-ouest devrait être envisagée, afin d'enrichir la base des données des matériaux argileux du Cameroun. De même, la réalisation d'études sur le traitement acide pour davantage optimiser le pouvoir décolorant de ces argiles en jouant sur les paramètres tels que la température et le temps d'activation seraient d'un apport décisif. Le suivi de la diffusion de certains métaux au cours de la décoloration reste une piste que l'on pourrait également prospectée dans le suivi du contrôle de la qualité des huiles traitées. L'approche de recyclage des matériaux utilisés lors de la décoloration de l'huile de palme mérite une attention particulière afin de limiter la pollution. L'étude sur l'évaluation du pouvoir décolorant de l'argile de Sabga devrait être menée en vue d'une comparaison avec celle de Bana. Enfin, il serait intéressant, pour la mise en valeur de ces matériaux argileux dans d'autres applications industrielles (cosmétique, pharmaceutique, traitement des eaux, boue de forage, charges minérales) de tenir compte des exigences spécifiques de chaque domaine d'application. Des procédés de purification par des coupures granulométriques pourraient être envisagés.

